

# TECHNISCHE UNIVERSITÄT MÜNCHEN

Lehrstuhl für Biochemische Pflanzenpathologie

## Characterization of tissue-resident CD8+ T cell memory formation upon skin infection with the viral vector MVA

Andreas Muschaweckh

Vollständiger Abdruck der von der Fakultät Wissenschaftszentrum Weihenstephan für Ernährung, Landnutzung und Umwelt der Technischen Universität München zu Erlangung des akademischen Grades eines

Doktors der Naturwissenschaften

genehmigten Dissertation.

Vorsitzender: Univ.-Prof. Dr. P. A. Knolle

Prüfer der Dissertation:

1. Univ.-Prof. Dr. J. Durner
2. Univ.-Prof. Dr. I. Drexler
3. Univ.-Prof. Dr. D. Haller

Die Dissertation wurde am 16.06.2015 bei der Technischen Universität München eingereicht und durch die Fakultät Wissenschaftszentrum Weihenstephan für Ernährung, Landnutzung und Umwelt am 24.03.2016 angenommen.



**Index**

<b>1</b>	<b>Abstract .....</b>	<b>1</b>
<b>2</b>	<b>Zusammenfassung .....</b>	<b>3</b>
<b>3</b>	<b>Introduction .....</b>	<b>6</b>
3.1	Vaccinia virus and MVA.....	6
3.1.1	Vaccinia virus.....	6
3.1.2	Modified vaccinia virus Ankara (MVA) .....	7
3.2	The skin as an immune-competent organ.....	9
3.3	The CD8+ T cell response to acute infection .....	12
3.4	Memory CD8+ T cell subsets.....	16
3.5	Tissue-resident memory CD8+ T cells (TRM cells) .....	18
3.6	TRM cells as vaccine targets.....	21
3.7	Aim of the study .....	24
<b>4</b>	<b>Materials and Methods .....</b>	<b>25</b>
4.1	Materials.....	25
4.1.1	Antibodies .....	25
4.1.2	Fluorescent dyes .....	26
4.1.3	Biochemicals/Chemicals .....	26
4.1.4	Enzymes .....	28
4.1.5	MHC class I tetramers.....	28
4.1.6	Buffers and Solutions .....	29
4.1.7	Synthetic Peptides .....	30
4.1.8	Cell lines .....	31
4.1.9	Kits .....	31
4.1.10	Viruses .....	31
4.1.11	Mice .....	32
4.1.12	Software .....	33
4.1.13	Consumables .....	33
4.1.14	Laboratory Equipment.....	34
4.2	Methods.....	36
4.2.1	Mammalian cell culture.....	36
4.2.2	Preparation of cryo sections from mouse skin .....	36
4.2.3	X-Gal staining of frozen skin tissue sections .....	36
4.2.4	Immunohistochemistry.....	37
4.2.5	Immunizations and viral challenges .....	38
4.2.6	Intravital imaging of luciferase activity .....	39
4.2.7	Collection of sera from immunized mice .....	39
4.2.8	Anti-Vaccinia virus ELISA.....	39

## Index

4.2.9	Preparation of splenocytes .....	40
4.2.10	Preparation of peripheral blood mononuclear cells (PBMCs) .....	40
4.2.11	Preparation of cell suspensions from skin tissue.....	40
4.2.12	Peptide re-stimulation of lymphocytes .....	41
4.2.13	Live-dead dye staining and Fc receptor blockade.....	41
4.2.14	Staining of surface markers .....	42
4.2.15	Intracellular cytokine staining.....	42
4.2.16	MHC class I tetramer staining .....	42
4.2.17	Sorting and adoptive transfer of OT-I cells.....	42
<b>5</b>	<b>Results.....</b>	<b>44</b>
5.1	MVA skin inoculation by tattooing.....	44
5.2	Viral tattooing induces CD8+ T cell responses of similar quality and magnitude as the conventional intramuscular route .....	46
5.3	MVA tattooing confers protective immunity against infection with replication-competent VV.....	49
5.4	MVA tattooing promotes effector CD8+ T cell recruitment to the skin .....	50
5.5	Virus-specific CD8+ T cells persist in MVA-tattooed skin .....	52
5.6	Virus-specific memory CD8+ T cells generated in MVA-tattooed skin predominantly reside within the epidermis and express markers of tissue residence.....	57
5.7	Formation of endogenous virus-specific TRM cells .....	59
5.8	Skin TRM provide enhanced protection against a local VV reinfection.....	61
5.9	Role of Foxp3+ CD4+ regulatory T cells in TRM formation in the skin.....	63
5.10	Skin injury alone promotes local effector CD8+ T cell accumulation .....	66
5.11	Local skin injury alone poorly supports the establishment of CD8+ TRM cells .....	70
5.12	Homing of effector CD8+ T cells to inflamed skin does not depend on the presence of their cognate antigen <i>in situ</i> .....	71
5.13	Local antigen recognition drives TRM development in MVA-infected skin.....	74
5.14	Local competition between different antiviral CD8+ T cells influences the composition of the TRM pool in MVA-infected skin.....	77
5.15	TRM cells generated in MVA-tattooed skin are non-recirculating cells.....	81
5.16	TRM cell formation upon MVA delivery by intradermal injection .....	84
5.17	MVA tattooing is superior to i.d. injection of MVA in generating CD103 <sup>hi</sup> skin TRM cells.....	87
<b>6</b>	<b>Discussion .....</b>	<b>90</b>
<b>7</b>	<b>Reference list.....</b>	<b>107</b>
<b>8</b>	<b>Danksagung.....</b>	<b>119</b>

## Abbreviations

### Abbreviation List

aa	amino acid
Ag	antigen
AP	alkaline phosphatase
APC	antigen presenting cell
APC	allophycocyanine
BAC	bacterial artificial chromosome
Bcl-2	B cell lymphoma 2
CCR	chemokine receptor
CD	cluster of differentiation
CEF	chicken embryo fibroblasts
CNS	central nervous system
CTL	cytotoxic T lymphocyte
CVA	Choriallantois vaccinia virus Ankara
CXCL	chemokine (C-X-C motif) ligand
CXCR3	chemokine (C-X-C motif) receptor 3
d	day(s)
DC	dendritic cell
DEREG	Depletion of REGulatory T cells
DETC	dendritic epidermal T cell
DMSO	dimethylsulfoxide
DNA	deoxyribonucleic acid
DTR	diphtheria toxin receptor
DTX	diphtheria toxin
EDTA	ethylenediaminetetraacetic acid
ELISA	enzyme-linked immunosorbent assay
EMA	ethidium monoazide
Eomes	Eomesodermin
FACS	fluorescence-activated cell sorting
FCS	fetal calf serum
FITC	fluorescein isothiocyanate
g	gram(s)
GFP	green fluorescence protein
h	hour(s)
HIV	human immunodeficiency virus
HRP	horseradish peroxidase
HSV	herpes simplex virus
ICS	intracellular cytokine staining
ICOS	inducible co-stimulatory molecule

## Abbreviations

i.d.	intradermal
IFN	interferon
Ig	immunoglobulin
IHC	immunohistochemistry
IL	interleukin
i.m.	intramuscular
i.n.	intranasal
i.p.	intraperitoneal
IU	infectious units
i.v.	intravenous
k	kilo
kb	kilobase
KLF2	Kruppel-like factor 2
KLRG1	killer cell lectin-like receptor subfamily G, member 1
l	liter
LC	Langerhans cell
LN	lymph node
LCMV	lymphocytic choriomeningitis virus
m	meter
m	milli
M	molar
μ	micro
MACS	magnetic-activated cell sorting
min	minute(s)
MHC	major histocompatibility complex
MPEC	memory precursor effector cell
MVA	modified vaccinia virus Ankara
NK	natural killer
NKG2D	natural-killer group 2, member D
NLR	Nod-like receptor
OVA	ovalbumin
PBS	phosphate buffered saline
PE	phycoerythrin
PerCP	peridinin chlorophyll
PFA	paraformaldehyde
PFU	plaque forming units
p.i.	post infection
PI	propidium iodide
PRR	pattern recognition receptor
RAG	recombination activating gene
RIG	retinoic acid inducible gene

## Abbreviations

RK	pabbit kidney
RNA	ribonucleic acid
rpm	revolutions per minute
RPMI	Roswell Park Memorial Institute
s	second(s)
S1P	sphingosine 1-phosphate
S1P1	sphingosine 1-phosphate receptor
s.c.	subcutaneous
SEM	standard error of the mean
SLEC	short-lived effector cell
SLO	secondary lymphoid organ
TAC	Tris ammonium chloride
T-bet	T-box protein expressed in T cells
TCM	central memory T cell
TCR	T cell receptor
TEM	effector memory T cell
TGF	transforming growth factor
TLR	Toll-like receptor
TNF	tumor necrosis factor
Treg	regulatory T cell
TRM	tissue-resident memory T cell
VARV	variola virus
VGf	vaccinia growth factor
VLA	very late antigen
VSV	vesicular stomatitis virus
VV	vaccinia virus
v/v	volume per volume
WHO	World Health Organization
WR	Western Reserve
w/v	weight per volume





# 1 Abstract

Tissue-resident memory CD8<sup>+</sup> T cells (TRM cells) are a recently identified subset of cytotoxic memory T cells which permanently reside within epithelial barriers of non-lymphoid tissues, including skin, gut, lung and the mucosa of female reproductive tract, and form a critical first line of defense against local reinfection. Once reactivated in these tissues, TRM cells critically contribute to local pathogen clearance through an immediate killing of infected host cells *in situ* and also by an almost instant secretion of effector cytokines which can act directly on infected cells, but in addition promote the local recruitment of other immune cells from the circulation. Recent evidence suggests that the rapid local cytokine response by specifically reactivated TRM cells can induce an organ-wide state of pathogen alert that can protect the tissue even from infection with an antigenically unrelated pathogen. Despite the well-described role of TRM cells in mediating protective immunity upon localized infection, little is known about the mechanisms that govern the formation and maintenance of TRM cells within non-lymphoid barriers. A thorough understanding of these mechanisms however might be critical for the development of novel vaccines or vaccination strategies to target infectious diseases in which rapid local pathogen control might be essential.

In this study, it was investigated whether TRM cells could be established in the skin of mice upon local infection with the modified vaccinia virus Ankara (MVA), a highly attenuated, non-replicating vaccinia virus which is now widely tested as recombinant vaccine in clinical trials. It could be shown that a single cutaneous application of MVA by tattooing, a method that predominantly delivers the virus into the skin epidermis, promoted the formation of mostly epidermis-resident CD69<sup>+</sup> CD103<sup>hi</sup> CD49a<sup>+</sup> TRM cells, which preferentially accumulated in previously infected skin and persisted locally for several months after viral application. Consistent with the marked accumulation of TRM cells in MVA-tattooed skin, previously inoculated skin regions rapidly cleared a secondary local infection with replication-competent vaccinia virus, whereas skin regions distant from the original MVA application site were only incompletely protected from a local rechallenge. TRM formation could also be achieved by an intradermal injection of MVA, but proved to be considerably weaker than after tattoo application of the virus, suggesting that skin immunization through barrier disrupted skin is more suitable for the induction of long-lived skin-resident CD8<sup>+</sup> T cell memory.

Based on the recent suggestion that TRM formation in the skin can be instructed by local inflammation alone, an adoptive transfer model was established which allowed to discriminate between the contribution of skin inflammation (associated with either mechanical epidermal injury alone or the viral infection) and local specific antigen recognition to the acute recruitment and persistence of antiviral CD8<sup>+</sup> T cells in MVA-tattooed skin. The experimental data revealed that cognate antigen production during the local viral infection was not required for the local recruitment of effector CD8<sup>+</sup> T cells, indicating that CD8<sup>+</sup> T cell infiltration into MVA-infected skin is solely mediated by the cutaneous inflammatory response. However, the presence of cognate antigen in MVA-tattooed skin was indispensable for an efficient local establishment of TRM cells. The data thus reveal a critical role of local antigen recognition in instructing TRM formation in virus-infected skin and offer an explanation as to why TRM cells are preferentially generated at the site of prior virus inoculation.

This study further demonstrates that the access of CD8<sup>+</sup> T cells to the TRM cell niche of MVA-infected skin is restricted and regulated by a local competition between antiviral CD8<sup>+</sup> T cells of different specificities ('cross-competition'), most likely for local antigenic signals. This was indicated by the finding that in MVA-OVA-infected skin, adoptively transferred OT-I cells expressing a high affinity T cell receptor specific for the model antigen OVA almost completely abrogated the local formation of endogenous MVA-specific TRM cells, which dominate the local TRM cell pool in the absence of competing OT-I cells.

In conclusion, the data from this study suggest that recognition of antigen within MVA-infected skin not only plays an important role in instructing tissue-infiltrating CD8<sup>+</sup> T cells to become TRM cells but also determines the composition of the repertoire of antiviral CD8<sup>+</sup> T cells that will develop into TRM cells at the site of prior infection. These findings contribute to our mechanistic understanding of the establishment of immunological CD8<sup>+</sup> T cell memory in non-lymphoid tissues and have important implications for the development of vaccines that aim for a potent induction of protective TRM cells at sites of pathogen entry.

## 2 Zusammenfassung

Gewebeständige CD8<sup>+</sup> Gedächtnis T Zellen (TRM Zellen; engl. „tissue-resident memory“) sind ein neu identifiziertes Subset zytotoxischer Gedächtnis T Zellen, die sich permanent in epithelialen Barrieren nicht-lymphoider Organe wie z.B. der Haut, dem Darm, der Lunge oder der Schleimhaut des weiblichen Geschlechtstraktes aufhalten und dort eine effiziente erste Verteidigungslinie gegen erneute lokale Infektion bilden. TRM Zellen tragen maßgeblich zur lokalen Pathogenkontrolle im Gewebe bei, da sie in der Lage sind, unmittelbar nach ihrer spezifischen Reaktivierung infizierte Zellen vor Ort zu töten und Effektor-Zytokine auszuschütten, welche nicht nur direkt auf infizierte Zellen wirken, sondern auch eine schnelle Rekrutierung anderer Immunzellen aus der Zirkulation vermitteln. Aktuelle Studien haben belegt, dass die unmittelbare lokale Zytokinausschüttung durch spezifisch reaktivierte TRM Zellen einen gewebeumfassenden Alarmzustand hervorruft, der sogar lokalen Schutz gegen eine Infektion mit einem nicht-verwandten Pathogen bietet.

Trotz der gut charakterisierten Rolle von TRM Zellen in der Immunprotektion nach lokalisierter Infektion ist bislang wenig über die Mechanismen bekannt, die die Entstehung und Aufrechterhaltung dieser T-Zell-Subpopulation in Geweben regulieren. Ein detailliertes Verständnis dieser Mechanismen ist aber von entscheidender Bedeutung für die Entwicklung neuer Impfstoffe oder Impfstrategien gegen Infektionskrankheiten, bei denen eine schnelle Eliminierung von Pathogenen im Gewebe essentiell ist.

Im Rahmen dieser Arbeit wurde im Mausmodell untersucht, ob TRM Zellen nach lokaler Hautinfektion mit dem modifizierten Vacciniavirus Ankara (MVA), einem hoch attenuierten und nicht-replizierenden Vacciniavirusstamm, der bereits als rekombinante Vakzine in klinischen Studien Verwendung findet, induziert werden können.

Es konnte gezeigt werden, dass eine einzelne kutane Applikation von MVA mittels lokaler Tätowierung - einer Methode, bei der das Virus in erster Linie in die Epidermis verabreicht wird - zur Entstehung von überwiegend Epidermis-residenten CD69<sup>+</sup> CD103<sup>hi</sup> CD49a<sup>+</sup> TRM Zellen führte, die sich preferentiell an der Applikationsstelle ansiedelten und dort für mehrere Monate nach Infektion persistierten. Übereinstimmend mit der bevorzugten Akkumulation von TRM Zellen in der MVA-infizierten Hautregion konnte gezeigt werden, dass diese Region nahezu vollständig geschützt war gegen eine erneute lokale Reinfektion mit replikations-kompetentem Vacciniavirus, wohingegen Hautregionen, die entfernt von der initialen MVA Applikationsstelle liegen, nur unzureichend geschützt waren. TRM Zellen konnten auch mittels intradermaler Injektion von MVA generiert

werden, jedoch war deren Induktion deutlich schwächer als nach MVA Tätowierung, was darauf hindeutet, dass eine Hautimmunisierung in Gegenwart einer leichten Verletzung der Hautbarriere für die Etablierung von langlebigem Haut-residenten CD8+ T Zell-Gedächtnis eher geeignet ist.

Basierend auf neueren Daten, die zeigen, dass die Bildung von TRM Zellen in der Haut sogar durch eine lokale Entzündung alleine vermittelt werden kann, wurde ein adoptives Transfermodell etabliert, welches erlaubt den individuellen Beitrag von Hautinflammation (hervorgerufen entweder durch eine ausschließlich mechanische Verletzung der Epidermis oder zusätzlich durch eine virale Infektion) und lokaler spezifischer Antigenerkennung zur akuten Rekrutierung sowie zur Langzeitpersistenz antiviraler CD8+ T Zellen in MVA-tätowierter Haut zu untersuchen. Die experimentellen Daten konnten zeigen, dass die Produktion von Antigen während der lokalen Hautinfektion für die Rekrutierung virus-spezifischer Zellen während der akuten Phase nicht benötigt wird, was darauf hindeutet, dass die Infiltration von Effektor CD8+ T Zellen in MVA-tätowierte Haut ausschließlich durch die lokale Inflammation gesteuert wird. Es stellte sich jedoch heraus, dass die Anwesenheit von Antigen in MVA-tätowierter Haut absolut unerlässlich für eine effiziente lokale Entwicklung von TRM Zellen war. Die Daten offenbaren somit, dass Antigenerkennung in der Haut eine entscheidende instruktive Rolle bei der Entstehung von TRM Zellpopulationen einnimmt und liefern einen Erklärungsansatz für die deutliche lokale Anreicherung von TRM Zellen an der ursprünglichen Virusinokulationsstelle.

Des Weiteren konnte in der vorliegenden Arbeit gezeigt werden, dass die Kapazität der Gedächtnis-T-Zellnische in MVA-infizierter Haut begrenzt ist und dass die Aufnahme von CD8+ T Zellen in dieselbe durch lokale Konkurrenz zwischen antiviralen CD8+ T Zellen von unterschiedlicher Antigenspezifität („Kreuz-Konkurrenz“) reguliert wird. Diese lokale T-Zellkonkurrenz beruht höchstwahrscheinlich auf dem Zugang zu Antigenen im Gewebe. Dies zeigte sich in dem hier etablierten Modellsystem dadurch, dass adoptiv transferierte OT-I Zellen, welche einen hochaffinen T-Zellrezeptor spezifisch für das Modellantigen OVA exprimieren, in MVA-OVA-infizierter Haut nahezu vollständig die Bildung anderer virus-spezifischer TRM Zellen unterdrückten, die in Abwesenheit konkurrierender OT-I Zellen den lokalen TRM Zell-Pool dominieren.

Zusammenfassend konnte im Verlauf dieser Forschungsarbeit gezeigt werden, dass Antigenerkennung in MVA-infizierter Haut nicht nur eine wichtige Rolle bei der lokalen Entwicklung von Haut-infiltrierenden CD8+ T Zellen zu langlebigen TRM Zellen spielt,

sondern zudem auch die Zusammensetzung des lokalen TRM Zell-Repertoires in der Haut reguliert. Die hier gewonnenen Erkenntnisse tragen zu unserem mechanistischen Verständnis der Entstehung von CD8+ T-Zell-Gedächtnis in nicht-lymphoiden Geweben bei und haben wichtige Implikationen für die Entwicklung von Vakzinen, die auf eine robuste Induktion protektiver TRM Zellen an möglichen Eintrittspforten für Pathogene abzielen.

## 3 Introduction

### 3.1 Vaccinia virus and MVA

#### 3.1.1 Vaccinia virus

Vaccinia virus (VV) is a large double stranded DNA virus (around 200 kb) which belongs to the genus *Orthopoxviridae* of the family of *Poxviridae* (Moss, 2001). Poxviruses are unique among DNA viruses in that they possess the ability to replicate entirely in the cytoplasm of the host cell. VV served as the live vaccine in the WHO-led global campaign to eradicate variola virus (VARV), another member of the *Orthopoxviridae* and the causative agent of smallpox. For smallpox vaccination, VV was delivered via the cutaneous route using a method called skin scarification. Thereby, a small droplet of VV was inoculated into a small area of skin (about 5 mm in diameter) by multiple perpendicular punctures with a bifurcated needle, through which the virus was targeted beneath the cornified layer of the epidermis. The vaccination was considered successful if as result of the localized VV infection a small local skin lesion appeared that eventually left behind a characteristic scar or pock mark (Fenner et al., 1988). Mass immunization of nearly the entire human population with VV induced potent cross-protective immunity to infection with VARV and eventually led to the worldwide eradication of smallpox in 1980 (Fenner et al., 1988). Notably, later studies have revealed that vaccinia-specific antibody and T cell responses persisted for several decades in the majority of vaccinees, suggesting that long-lasting immunity had been established by the vaccination (Combadiere et al., 2004; Hammarlund et al., 2003). Despite the global eradication of smallpox and the discontinuation of routine smallpox vaccination, interest in VV continued in particular with regards to their development as vectors for the expression of foreign genes and as candidate live recombinant vaccines against infectious diseases or cancer (Pastoret & Vanderplasschen, 2003). There is still a need for a smallpox vaccine that would be suitable for a widespread use in humans in case of emergency, such as an intentional release of VARV as biological weapon (Whitley, 2003) or outbreaks of human monkeypox (Di Giulio & Eckburg, 2004). However, safety concerns have been raised regarding the use of vaccines based on live VV, as severe (albeit infrequent) complications had been documented in smallpox vaccinated individuals, such as eczema vaccinatum (in subjects suffering from eczema or atopic dermatitis), postvaccinal encephalitis in infants or progressive and disseminated vaccinia in adults suffering from immune deficiencies

(Pastoret & Vanderplasschen, 2003; Roos & Eckerman, 2002). Therefore, approaches were undertaken to improve the safety of poxvirus vectors, leading to the development of genetically attenuated vaccinia virus strains.

### **3.1.2 Modified vaccinia virus Ankara (MVA)**

One of these strains is the highly attenuated and non-replicating vaccinia virus strain modified vaccinia virus Ankara (MVA). MVA has been developed from the CVA (chorioallantois vaccinia virus Ankara) strain of vaccinia virus during the late phase of the global smallpox eradication efforts (Mayr et al., 1978). Attenuation of MVA was achieved by a series of more than 570 passages of the parental virus CVA on primary chicken embryo fibroblasts (CEF) cultures, during which the virus has lost around 15% of the parental genomic information including a number of genes involved in viral host range or immune evasion (Antoine et al., 1998; Blanchard et al., 1998). Although MVA is capable of infecting mammalian cells, it is unable to productively replicate in human and most other mammalian cells due to a blockade in viral assembly during the late phase of the viral life cycle (Sutter & Moss, 1992). Despite the inability of MVA to produce infectious viral progeny in mammalian cells, the virus is still able to carry out the full cascade-like course of transcription of early, intermediate and late viral genes and shows no overt impairment in viral and recombinant protein synthesis compared to the parental wild-type virus (Sutter & Moss, 1992).

MVA has been shown to grow productively in CEF and the Syrian hamster cell line BHK-21 (Carroll & Moss, 1997; Drexler et al., 1998), which can be used for virus amplification (Carroll & Moss, 1997). In addition to its severely restricted host range, MVA proved completely non-pathogenic when administered to newborn, irradiated or immunodeficient (SCID) mice or immune suppressed macaques (Meyer et al., 1991; Stittelaar et al., 2001; Wyatt et al., 2004) (Meyer et al., 1991; Stittelaar et al., 2001; Wyatt et al., 2004). Importantly, MVA has also tested completely avirulent when used as a smallpox vaccine in more than 120,000 humans, including high-risk patients in which regular smallpox vaccination was contraindicated due to advanced age, immune suppressive therapy or atopic skin diseases (Mayr et al., 1978; Stickl et al., 1974). Adding to the safety aspect of MVA is the extremely unlikely event that viral DNA may be integrated into the host genome, as all poxvirus-encoded genes are transcribed within the cytoplasm of the host cell (Drexler et al., 2004).

Studies in mice have shown that MVA elicits both humoral and cellular immune responses that are protective against pathogenic orthopoxvirus challenge (Belyakov et al., 2003; Drexler et al., 2003; Wyatt et al., 2004). Notably, the protective capacity of MVA was similar to that provided by conventional VV vaccines (e.g. the licensed Dryvax smallpox vaccine), although equivalent protection required slightly higher inoculation doses of MVA (Drexler et al., 2004). Further evidence for the high immunogenicity of MVA has been derived from studies in non-human primates which demonstrated that MVA vaccination conferred significant protection against a lethal monkeypox virus challenge (Earl et al., 2004).

Another important feature of MVA is the large packaging capacity of its genome for foreign DNA (allowing for integration of up to 50 kb foreign DNA without compromising its infectivity), which makes the virus an ideal vector for the expression of full-length or multivalent antigens or even the co-expression of antigen and co-stimulatory molecules (e.g. CD40L) (Lauterbach et al., 2013; Sutter & Staib, 2003).

Due to its outstanding safety record and immunogenicity, MVA is not only evaluated as a candidate smallpox vaccine but is currently also extensively tested as a recombinant vaccine vector in numerous human clinical trials targeting infectious diseases, including HIV (MVA-HIV-1-nef (Cosma et al., 2003)), malaria (MVA-METRAP (McConkey et al., 2003; Moorthy et al., 2003)), tuberculosis (MVA 85A (McShane et al., 2004)) or cancer (Gilbert, 2013). Recombinant MVA vectors are commonly used in heterologous immunization regimens to boost pre-existing CD8<sup>+</sup> T cell responses to a given antigen that had been primed e.g. by DNA vaccination (McConkey et al., 2003).



### 3.2 The skin as an immune-competent organ

The skin is one of the largest organs of the body and constitutes an important protective interface between the environment and the inner organs. Although long considered only as a passive physical barrier, the skin has now been accepted as a highly complex immune organ that plays an active role in immune defense (Heath & Carbone, 2013; Nestle et al., 2009). Anatomically, the skin can be divided into two main compartments, namely the epidermis and dermis, which are separated from one another by a basement membrane (Fig. A).

The epidermis is the outer compartment of the skin and is made up of different layers of keratinocytes, which represent the predominant cell type in the epidermis. The stratum corneum (or cornified layer) forms the outermost sheet of the epidermis and consists of terminally differentiated (dead) keratinocytes, followed by a layer called stratum granulosum whose intercellular space is sealed by tight junctions. This is followed by the stratum spinosum and finally by a basal layer of undifferentiated keratinocytes (stratum basale) which is attached to the basement membrane (Heath & Carbone, 2013; Nestle et al., 2009).

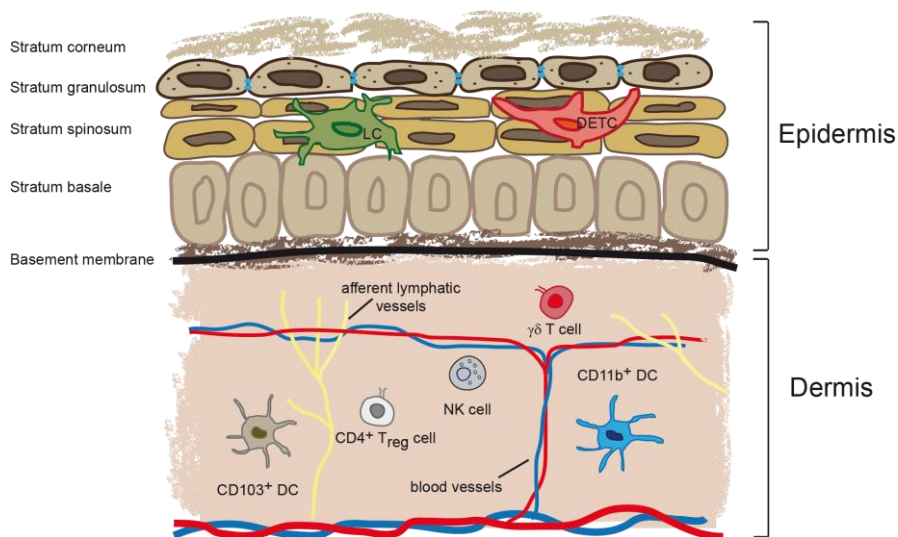


**Figure A: Schematic overview of the anatomical structure of murine skin and its associated immune cell repertoire (adapted from (Heath & Carbone, 2013)).**

Keratinocytes can act as frontline sensors of pathogen invasion or tissue injury since they express numerous pattern recognition receptors (PRRs), which allow them to respond to a wide spectrum of conserved bacterial or viral components and also self-constituents

(Gutowska-Owsiak & Ogg, 2012; Heath & Carbone, 2013). These include the Toll-like receptors (TLRs), the Nod-like receptors (NLRs) Nod1 and Nod2 (which recognize bacterial peptidoglycans), NLR pyrin domain-containing proteins (for detection of viral, fungal or damaged self-components), RIG-I like helicase receptors (recognition of viral RNA species) and C-type lectins (recognition of fungal infections, e.g. dectin-1). Detection of pathogens via these PRRs promotes the activation of the cell and the subsequent release of pro-inflammatory cytokines and chemokines, which contribute to inflammation and the recruitment of innate and adaptive effector cells from the circulation.

A recent study demonstrated that upon skin injury, RNA released from necrotic cells can stimulate keratinocytes via TLR3 to release pro-inflammatory cytokines (Lai et al., 2009).

The epidermis is also interspersed with different types of specialized immune cells, including a resident subset of dendritic cells (DCs) named Langerhans cells (LCs), as well as a subpopulation of gamma delta ( $\gamma\delta$ ) T cells that expresses the invariant V $\gamma$ 5 V $\delta$ 1 T cell receptor (TCR). The latter are unique to murine epidermis and are referred to as dendritic epidermal T cells (DETCs) due to their strict epidermal localization and dendritic cell-like morphology. DETCs make up the vast majority of all epidermal T cells (Di Meglio et al., 2011), are distributed throughout the epidermal layer in a network-like fashion and play a prominent role in promoting wound healing after tissue injury (Havran & Jameson, 2010; Macleod & Havran, 2011). Although the natural ligand for their invariant TCR is currently unknown, several other DETC molecules have been identified that respond to 'stress ligands' on damaged keratinocytes and contribute to DETC activation. These include the activating receptor NKG2D, which recognizes ligands such as Rae-1 (upregulated on virus-infected and malignant cells) (Girardi et al., 2001; Whang et al., 2009), the co-stimulatory molecule JAML (junctional adhesion molecule-like protein) which interacts with the coxsackie and adenovirus receptor (CAR) expressed on recently injured keratinocytes (Witherden et al., 2010), or semaphorin-4D (CD100) which binds to plexin B2 molecules on wounded keratinocytes (Witherden et al., 2012). In response to skin injury, activated DETC release various pro-inflammatory cytokines and chemokines, anti-microbial peptides as well as keratinocyte growth factors to facilitate the healing process (Di Meglio et al., 2011; Havran & Jameson, 2010).

Langerhans cells (LCs) represent the professional antigen-presenting cell population of the epidermis and are characterized by the expression of the type II C-type lectin receptor Langerin (CD207), which specifically binds to glycosylated residues (e.g. mannose) on the pathogen surface and mediates internalization. By projecting their long dendrites between

neighboring keratinocytes and DETC, LCs form a dense network throughout the epidermis which enables an efficient sampling of the local microenvironment for foreign antigen (Romani et al., 2012b).

Owing to their capacity to stimulate naïve CD8<sup>+</sup> T cells *in vitro* (Schuler & Steinman, 1985; Stoitzner et al., 2006), LCs have for a long time been regarded as the dominant DC subset involved in the priming of adaptive immune responses upon cutaneous infection. However, more recent findings have challenged this concept. For instance, Allan et al. described that following HSV-1 skin infection, virus-specific CD8<sup>+</sup> T cell responses were exclusively primed by the lymph node-resident CD8<sup>+</sup> DC subset, suggesting that LCs may rather play an indirect role in CD8<sup>+</sup> T cell priming, i.e. shuttling antigen to the draining lymph node for cross-presentation by the resident CD8<sup>+</sup> DC subset (Allan et al., 2003). Similar observations were made after cutaneous infection with other viruses, such as influenza or vaccinia virus (Belz et al., 2004; He et al., 2006). Interestingly, a recent study has revealed an important role of skin-derived DCs in the priming of CD8<sup>+</sup> T cell responses after intradermal infection with a non-cytolytic lentiviral vector (He et al., 2006). Conversely, the same study also found that after skin infection with vaccinia virus, a cytolytic virus that induces DC apoptosis, LCs were impaired in their ability to prime CD8<sup>+</sup> T cells after their migration to the LN (He et al., 2006). Thus, the contribution of LCs to the induction of adaptive immunity after skin infection is likely to differ between different types of pathogens (Merad et al., 2008). Interestingly, a recent study reported that selective depletion of LCs after intradermal immunization with MVA completely abrogated the priming of virus-specific CD8<sup>+</sup> T cells, but did not affect the induction of antiviral CD4<sup>+</sup> T cells (Liard et al., 2012). Although the study did not address whether in this infection model, MVA-specific CD8<sup>+</sup> T cells were primed directly by infected LCs or cross-presenting lymphoid tissue-resident CD8<sup>+</sup> DCs, these results nevertheless demonstrate an involvement of LC in the induction of antiviral immunity following skin infection (Liard et al., 2012).

The dermis is separated from the epidermis by a basement membrane and is composed of elastin fibers, collagen fibers and other extracellular matrix components produced by dermal fibroblasts (Heath & Carbone, 2013) (Fig. A). In contrast to the epidermis, the dermis is vascularized and contains a network of blood vessels and afferent lymphatic vessels. The dermal compartment is home to a variety of immune cells, including mast cells, macrophages, a subset of dermal  $\gamma\delta$  T cells,  $\alpha\beta$  T cells and at least two different subpopulations of dermal DC (Heath & Carbone, 2013). The two dermal DC subsets

include the classical dermal CD11b<sup>+</sup> DCs and the recently identified Langerin<sup>+</sup> CD103<sup>+</sup> dermal DCs (Bursch et al., 2007; Ginhoux et al., 2007; Poulin et al., 2007). Recent data suggest that the Langerin<sup>+</sup> CD103<sup>+</sup> dermal DC subset plays a critical role in promoting antiviral immunity in the skin. After HSV skin infection, Langerin<sup>+</sup> DCs were demonstrated to be the dominant migratory DC subset that efficiently cross-presented viral antigen to CD8<sup>+</sup> T cells (Bedoui et al., 2009). Furthermore, a recent study suggested that CD103<sup>+</sup> DCs may also be essential for an effective induction of CD8<sup>+</sup> T cell immunity upon skin scarification with vaccinia virus (Seneschal et al., 2013).

The presence of such a diverse network of specialized immune cells demonstrates that the skin is highly adept at responding to infection or external insults and therefore represents an ideal target organ for the delivery of vaccines. In fact, recent data suggest that for immunization using VV-based vaccines, including MVA, delivery through barrier disrupted skin via the traditional skin scarification method might even be the most potent way of inducing robust T cell-mediated responses (Liu et al., 2010). Nevertheless, vaccines in humans are still commonly applied by injection into the subcutaneous fat or the muscle (Romani et al., 2012a) and thus may not fully harness the immune stimulatory potential of the skin immune system.

### **3.3 The CD8<sup>+</sup> T cell response to acute infection**

CD8<sup>+</sup> T cells (also known as cytotoxic T lymphocytes or CTL) play a crucial role in host defense against infections with intracellular pathogens, such as bacteria or viruses (Williams & Bevan, 2007). CD8<sup>+</sup> T cells are specialized in killing infected host cells, which they can mediate either through the release of cytolytic molecules such as perforins and granzymes, or via Fas ligand-mediated induction of apoptosis (Schepers et al., 2005). In addition, upon recognition of infected targets CD8<sup>+</sup> T cells are able to release pro-inflammatory cytokines such as interferon- $\gamma$  (IFN- $\gamma$ ) or tumor necrosis factor- $\alpha$  (TNF- $\alpha$ ) that can interfere with pathogen replication within the cell (Schepers et al., 2005).

The interaction of CD8<sup>+</sup> T cells with infected cells is mediated by the TCR, which recognizes its cognate antigen in the form of a complex consisting of a short peptide (8-11 amino acids) bound to an major histocompatibility (MHC) class I molecule on the host cell surface (Schepers et al., 2005). In the naïve CD8<sup>+</sup> T cell repertoire, the precursor frequency of CD8<sup>+</sup> T cells specific for a given peptide/MHC class I complex is extremely

low. Studies in mice have estimated that, prior to an antigen encounter, the total number of precursor cells specific for a given epitope ranges between 50-200 cells (corresponding to a frequency of 1 antigen-specific CD8<sup>+</sup> T cell per 10,000 total CD8<sup>+</sup> T cells) (Blattman et al., 2002). These rare antigen-specific CD8<sup>+</sup> T cells still lack effector characteristics and recirculate between the blood stream and secondary lymphoid organs (lymph nodes and spleen) in continuous search for their cognate antigen. In order to expand in number and to become fully functional cytotoxic cells, naïve CD8<sup>+</sup> T cells must first be primed for their cognate antigen by a professional antigen-presenting cell (APC) (Schepers et al., 2005; Williams & Bevan, 2007).

Following acute viral infection, CD8<sup>+</sup> T cell responses commonly proceed through three distinct phases: Expansion, Contraction and Memory (Fig. B).

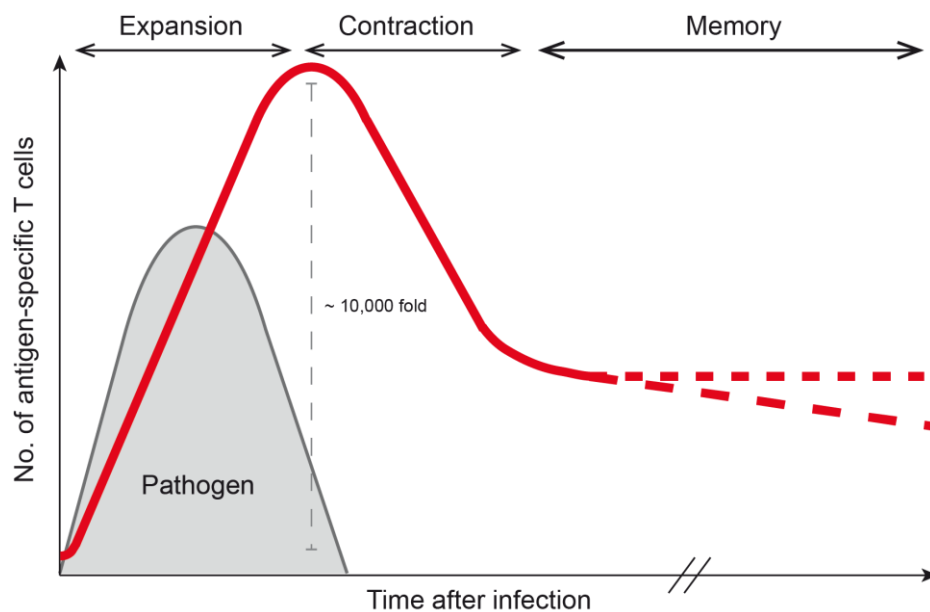


**Figure B: Schematic overview of the different phases of an antigen-specific CD8<sup>+</sup> T cell response after acute infection.** Red curve depicts the change in absolute number of CD8<sup>+</sup> T cells specific for a given antigen over time. Grey shaded curve depicts the pathogen load (adapted from (Williams & Bevan, 2007)).

The expansion phase is initiated in secondary lymphoid organs (SLOs), where naïve CD8<sup>+</sup> T cells encounter mature professional antigen-presenting cells (such as DCs) which display their cognate antigen on the surface MHC class I molecules. In order to mount an effective immune response, naïve CD8<sup>+</sup> T cells require at least three signals: TCR stimulation (signal 1), co-stimulation via surface receptors such as CD28, CD40, 4-1BB, CD27, OX40 or ICOS (signal 2) and the presence of inflammatory cytokines, e.g. IL-12 or type I IFNs (signal 3). If these signals are provided, naïve CD8<sup>+</sup> T cells are able to undergo multiple

rounds of cell division which give rise to a vast number of antigen-specific effector CD8<sup>+</sup> T cell progeny. As activated CD8<sup>+</sup> T cells clonally expand, they undergo functional differentiation into cytotoxic T cells with the capacity to secrete effector cytokines and cytolytic molecules. Concomitantly, the cells also dramatically change their pattern of adhesion molecule expression and thus acquire the ability to exit the SLOs and to migrate to the tissues in order to participate in pathogen clearance (Kaech et al., 2002; Williams & Bevan, 2007).

Recent studies have indicated that the location of T cell priming can have an influence on the resulting homing patterns of stimulated T cells. For example, activation in lymph nodes (LNs) draining the skin preferentially instructs T cells to upregulate the expression of P- and E-selectin ligands or the chemokine receptors CCR4 and CCR10, which are important for homing to inflamed skin (Campbell & Butcher, 2002; Mora et al., 2005). Similarly, priming in gut-associated lymphoid tissue (e.g. mesenteric LN) has been shown to preferentially induce expression of  $\alpha 4\beta 7$  integrin and CCR9, which facilitate T cell homing to the small intestine (Campbell & Butcher, 2002; Mora et al., 2003). Although such ‘migrational imprinting’ of T cells in regional LNs can generate a bias in T cell trafficking towards the respective LN-associated non-lymphoid tissue, it should be noted that this process is not absolute, since even in the context of a localized peripheral infection, considerable numbers of effector CD8<sup>+</sup> T cells can be found in non-lymphoid organs that are not associated with the site of T cell priming (Masopust et al., 2004).

Clonal expansion of antigen-specific CD8<sup>+</sup> T cells typically peaks within one week after their initial stimulation. Thereafter, the pool of effector CD8<sup>+</sup> T cells undergoes a contraction phase, during which the vast majority of antigen-specific effector CD8<sup>+</sup> T cells (90-95%) die by apoptosis. A small portion of effector CD8<sup>+</sup> T cells (5-10%) however survives this contraction and populates the early memory T cell pool. With time, this pool of antigen-specific memory CD8<sup>+</sup> T cells further differentiates and progressively acquires memory cell qualities which provide the basis for a protective immunity to a renewed infection with the same pathogen. These include the capacity to persist long-term in the absence of antigen through constant self-renewal in response to the homeostatic cytokines IL-15- and IL-7 (homeostatic proliferation), the ability to undergo rapid recall expansion to generate a new wave of secondary effector cells as well as the capacity to quickly reacquire of effector function upon antigen reencounter. These key attributes of memory CD8<sup>+</sup> T cells, together with their elevated number and more widespread tissue distribution in comparison to naïve antigen-specific precursor cells, enable the host to mount a more

rapid and vigorous response to a secondary encounter with the same pathogen (Kaech et al., 2002; Williams & Bevan, 2007).

Recent studies have shown that the precursors to long-lived memory CD8<sup>+</sup> T cells can already be identified within the early pool of effector cells. Kaech and colleagues have observed that at the peak of response after acute viral infection two distinct subpopulations of effector CD8<sup>+</sup> T cells emerge that differ in their expression of the IL-7R $\alpha$  chain (CD127) (Kaech et al., 2003). While the fraction of Ag-specific CD8<sup>+</sup> effector T cells expressing IL-7R (around 5-20%) preferentially gives rise to long-lived memory T cells, IL-7R<sup>lo</sup> effector cells exhibit a rather poor memory potential and are destined to undergo apoptosis during the contraction phase (Huster et al., 2004; Kaech et al., 2003).

Closer characterization of these two effector CD8<sup>+</sup> T cell subsets revealed that the IL-7R<sup>lo</sup> subpopulation of effector cells (termed short-lived effector cells or SLECs) expresses high levels of the receptor KLRG1 (killer cell lectin-like receptor subfamily G, member 1), a marker of terminal differentiation or senescence, whereas their IL-7R<sup>hi</sup> counterparts (termed memory precursor effector cells or MPECs) exhibit only low levels of this molecule (Joshi et al., 2007). Although KLRG1<sup>hi</sup> IL-7R<sup>lo</sup> SLECs and KLRG1<sup>lo</sup> IL-7R<sup>hi</sup> MPECs exhibited similar cytotoxic activity and IFN- $\gamma$  expression, KLRG1<sup>lo</sup> IL-7R<sup>hi</sup> MPECs cells were more potent in producing IL-2 upon re-stimulation *ex vivo* and demonstrated better survival *in vivo* after adoptive transfer (Sarkar et al., 2008), consistent with a higher intracellular expression of the anti-apoptotic protein Bcl-2 (Kaech et al., 2003). Further studies have revealed that already at early time points post infection the pool of MPECs segregates in two subpopulations with high or low expression of the LN-homing receptor CD62L, which likely represent the precursors of CD62L<sup>hi</sup> central memory (TCM) and CD62L<sup>lo</sup> effector memory (TEM) CD8<sup>+</sup> T cells found after contraction of the response (Obar & Lefrancois, 2010).

Interestingly, Stemberger et al. could demonstrate that a single antigen-specific precursor cell has the potential to give rise to all the described heterogeneous effector and memory CD8<sup>+</sup> T cell populations (Stemberger et al., 2007). Thus, it appears that the fate of each individual naïve CD8<sup>+</sup> T cell precursors is not fixed but rather determined by the sum of signals it receives throughout the course of the infection.

Several factors have been described that influence the commitment of responding CD8<sup>+</sup> T cells towards either SLEC or MPEC fate. These include for instance the duration and intensity of stimulatory signals delivered via the TCR or co-stimulatory receptors, CD4<sup>+</sup> T cell help, transcriptional regulation (most notably through the T-box family members T-bet

and Eomes) and also the degree and duration of exposure to pro-inflammatory (e.g. IL-12, type I and type II IFNs) or anti-inflammatory cytokines (e.g. IL-10) (for detailed review see (Kaech & Cui, 2012))

### **3.4 Memory CD8+ T cell subsets**

Early studies by Sallusto et al. have grouped the memory T cell populations in human peripheral blood into two functionally distinct subsets based on a differential expression of the lymph node homing receptors CD62L (L-selectin) and CCR7 (chemokine receptor 7). The two subsets were defined as central memory (TCM) and effector memory (TEM) cells (Sallusto et al., 1999).

CD8+ TCM cells constitutively express the homing receptors CD62L and CCR7, which are required for entry into SLOs via high endothelial venules (HEVs) and the subsequent migration to the paracortical T cell zone. Thus, similar to naïve cells (which also express high levels of CD62L and CCR7), CD8+ TCM cells predominantly recirculate between the blood and SLOs and are largely excluded from non-lymphoid tissues. Upon reencountering their antigen, CD8+ TCM cells are able to secrete high amounts of IL-2 and mount a vigorous proliferative response to generate large amounts of secondary effector CD8+ T cells. CD8+ TEM cells on the other hand lack CD62L and CCR7 expression, but instead express homing receptors that can mediate their migration into non-lymphoid tissues (Sallusto et al., 2004). In contrast to CD8+ TCM cells, CD8+ TEM cells have a limited capacity to produce IL-2 and to proliferate in response to Ag stimulation. Importantly, however, similar to recently activated effector CD8+ T cells, TEM cells are able to immediately acquire effector functions (e.g. cytotoxicity of infected cells) upon antigen recognition (Sallusto et al., 2004). Based on these functional and phenotypical differences, it was proposed that these two memory CD8+ T cell subsets carry out distinct roles in immune surveillance. While CD8+ TEM cells, by continuously recirculating between blood and non-lymphoid tissues, provide a first line of defense at the site of pathogen invasion, CD8+ TCM cells contribute to pathogen control by generating a second wave of effector cells capable of infiltrating infected tissues after a short period of proliferation within the SLOs (Masopust & Schenkel, 2013; von Andrian & Mackay, 2000). In agreement with this concept, subsequent studies in mice showed that upon infection or immunization, memory CD8+ T cells with enhanced effector capabilities were present in



various non-lymphoid tissues (Masopust et al., 2001; Reinhardt et al., 2001), and it was assumed that these memory cells were the equivalents to TEM cells found in the systemic circulation.

However, several observations were made that could not be reconciled with the concept that all memory CD8<sup>+</sup> T cells in non-lymphoid tissues represented recirculating memory CD8<sup>+</sup> T cells. For example, in order to exit non-lymphoid tissues and to be transported back into the blood stream, T cells must gain access to local afferent lymphatic vessels. However, studies have found that expression of CCR7 on T cells was critically required for an efficient T cell entry into the afferent lymph (Bromley et al., 2005; Debes et al., 2005). Since lack of CCR7 expression was considered a defining characteristic of the TEM subset, it was thus unclear how TEM cells could continuously traffic between the blood and the tissues. Also, several studies have noted that CD62L<sup>-</sup> virus-specific memory CD8<sup>+</sup> T cells isolated from the intestinal mucosa upon clearance of systemic LCMV (lymphocytic choriomeningitis virus) or VSV (vesicular stomatitis virus) infection, displayed markedly different functional and phenotypic characteristics as CD62L<sup>-</sup> TEM cells in the blood or the spleen (Kim et al., 1999; Masopust et al., 2001; Masopust et al., 2006b), which suggested that mucosal and systemic memory CD8<sup>+</sup> T cells might not be part of a common memory pool. Further evidence for this has been provided by studies utilizing parabiosis, which describes a procedure in which two mice are joined by surgery in order to share a common blood circulation. These studies found that when two VSV-immune mice (each containing virus-specific memory CD8<sup>+</sup> T cells with traceable and distinguishable congenic markers) were joined, virus-specific memory CD8<sup>+</sup> T cells readily exchanged between the two parabionts and established equilibrium in the blood and spleen within approximately two weeks. However, even after a prolonged time of shared circulation, VSV-specific memory CD8<sup>+</sup> T cells did not reach equilibrium in the small intestinal mucosa, i.e. the mucosal pool of VSV-specific CD8<sup>+</sup> T cells in either parabiont remained skewed towards the endogenous population (Klonowski et al., 2004). These findings thus indicated that the entry of circulating memory CD8<sup>+</sup> T cells into the small intestine is restricted during steady-state memory and further implied that the mucosa of the small intestine must contain populations of memory CD8<sup>+</sup> T cells that are permanently residing within the tissue.

### 3.5 Tissue-resident memory CD8<sup>+</sup> T cells (TRM cells)

Numerous studies have now provided evidence that such non-recirculating memory CD8<sup>+</sup> T cells not only exist in the small intestine (Masopust et al., 2010), but are also found in various other non-lymphoid organs, including the skin, CNS, sensory ganglia, female reproductive tract, salivary glands and lung airways (Cuburu et al., 2012; Gebhardt et al., 2009; Hofmann & Pircher, 2011; Jiang et al., 2012; Shin & Iwasaki, 2012; Wakim et al., 2013; Wakim et al., 2010).

These non-recirculating memory CD8<sup>+</sup> T cells, which are now collectively referred to as tissue-resident memory CD8<sup>+</sup> T cells (or TRM cells), are typically found in high numbers in regions of cleared localized infection or inflammation and have been demonstrated to play a critical role in the host defense against local reinfection (Gebhardt & Mackay, 2012; Schenkel & Masopust, 2014). Tissue-resident memory CD8<sup>+</sup> T cells have also been identified in humans, for example in vaginal skin at sites of recurrent infection with herpes simplex virus (HSV)-2 and have been suggested to play an important role in the initial containment of HSV-2 within the tissue during episodes of spontaneous reactivation (Zhu et al., 2013).

TRM cells are phenotypically distinct from recirculating TEM and TCM cells and possess a unique repertoire of surface receptors which support their retention and/or survival in the non-lymphoid tissue microenvironment. In most non-lymphoid tissues (including the skin), TRM cells are characterized by high expression of the  $\alpha E$  subunit (CD103) of  $\alpha E\beta 7$  integrin. Integrin  $\alpha E\beta 7$  is known to bind to E-cadherin, a cell adhesion molecule expressed on most epithelial cells (e.g. keratinocytes in the skin or vaginal mucosa or enterocytes in the small intestine) (Cepek et al., 1993; Cepek et al., 1994). Interestingly, TRM cells are most often found within epithelial barriers of non-lymphoid tissues and it has therefore been suggested that CD103 plays a role in the retention and/or survival of TRM cells within these compartments, for instance by mediating anchoring to neighboring epithelial cells (Gebhardt & Mackay, 2012). In fact, epidermis-resident  $\gamma\delta$  T cells (DETCs, dendritic epidermal T cells) express high levels of CD103 and it has been observed that this population is substantially diminished in CD103<sup>-/-</sup> mice (Schon et al., 2002). Consistent with this, adoptively transferred CD103<sup>-/-</sup> CD8<sup>+</sup> T cells were found to be strongly impaired in their ability to persist within the small intestinal epithelium after systemic LCMV infection (Casey et al., 2012). Furthermore, CD8<sup>+</sup> T cells in which CD103 was suppressed by retroviral knockdown demonstrated poor retention and survival in the brain after

intranasal infection with vesicular stomatitis virus (Wakim et al., 2010). Interestingly, using adoptive co-transfer of wild-type and CD103<sup>-/-</sup> T cells, Mackay et al. recently demonstrated that CD103 expression was not required for entry into herpes simplex virus 1 (HSV-1)-infected epidermis, but was critical for the long-term survival of recruited virus-specific CD8<sup>+</sup> T cells within this anatomical niche (Mackay et al., 2013). It has been suggested, that in addition to physically retaining T cells within their tissue of residence, CD103 could also directly transmit survival signals. In line with this, Wakim et al. showed that CD103<sup>+</sup> CD8<sup>+</sup> T cells in the brain contained higher levels of the anti-apoptotic protein Bcl-2 compared to CD103<sup>-</sup> CD8<sup>+</sup> T cells from the same location (Wakim et al., 2010).

Another signature marker of CD8<sup>+</sup> TRM cells is the surface molecule CD69, a C-type lectin that is also transiently expressed on recently activated T cells. CD69 is known to antagonize the sphingosine-1-phosphate receptor 1 (S1P1), which mediates the exit of T cells from the LNs by directing their migration along a gradient of sphingosine-1-phosphate (S1P) (Shiow et al., 2006). Transient upregulation of CD69 on recently stimulated T cells therefore leads to a temporary retention of the cells within the lymph node (Shiow et al., 2006), which likely serves as a mechanism to allow for more efficient interactions with local APCs. Recent data indicate that CD69 also plays an important role during TRM cell formation, presumably by mediating an early local retention of CD8<sup>+</sup> T cells upon their arrival in the tissue (Mackay et al., 2013; Skon et al., 2013).

In the skin and salivary glands, CD8<sup>+</sup> TRM cells have been found to express high levels of the surface molecule CD49a, the  $\alpha 1$  chain of  $\alpha 1\beta 1$  integrin (also known as VLA-1, very late antigen 1). VLA-1 has been described to bind to a number of extracellular matrix proteins, including collagen type IV (the major component of basement membranes), collagen type I and laminin (Ben-Horin & Bank, 2004), and is therefore likely also involved in the local retention of CD8<sup>+</sup> TRM cells in these non-lymphoid compartments. Furthermore, VLA-1 also seems to play role in CD8<sup>+</sup> T cell persistence in the lung following influenza infection (Ray et al., 2004).

Although TRM cells do not take part in recirculation, they are not completely sessile. Studies of TRM cells in murine epidermis have shown that these cells steadily migrate through the local network of keratinocytes, DETCs and LCs and thereby actively scan surrounding cells for antigen (Ariotti et al., 2012; Gebhardt et al., 2011). Skin TRM cells have been described to migrate through the epidermal compartment in random directions at a rather slow rate (around 1  $\mu\text{m}/\text{min}$ ) (Ariotti et al., 2012; Gebhardt et al., 2011; Zaid et al.,

2014). Long-term computational simulations have revealed that it is because of this slow and random mode of migration that TRM cells remain largely within the region in which they had initially formed, i.e. the site of prior infection (Zaid et al., 2014).

Much effort has been made in identifying the mechanisms that lead to the development and permanent lodgment of TRM cells in non-lymphoid tissues.

Accumulating data suggest that peripheral pools of TRM cells are formed already during the effector phase of the CD8<sup>+</sup> T cell response, when the tissue-homing properties of CD8<sup>+</sup> T cells are highest (Klonowski et al., 2004; Mackay et al., 2012; Masopust et al., 2010; Shin & Iwasaki, 2012). Mackay et al. have found that TRM cells which populate the epidermis upon localized HSV infection originate from the KLRG1<sup>lo</sup> subset of effector CD8<sup>+</sup> T cells (memory precursor effector cells or MPECs) (Mackay et al., 2013). Upon arrival in the tissue, these KLRG1<sup>lo</sup> precursors undergo a local differentiation into CD103<sup>+</sup> CD69<sup>+</sup> TRM cells in response to certain tissue-specific signals. The local signals that instruct the development of TRM cells within the tissues are still poorly understood and there appear to be some differences in the requirements for TRM cell formation between different non-lymphoid tissues. For example, in neuronal compartments such as the CNS or the dorsal root ganglia (DRG), tissue-immigrating CD8<sup>+</sup> T cells need to receive local antigenic signals in order to acquire CD103 expression and to become long-term residents within these compartments (Wakim et al., 2010). In most other non-lymphoid tissues (including skin or mucosal epithelia of gut and vagina) on the other hand, *in situ* antigen recognition seems to be dispensable for the acquisition of TRM signatures and local T cell persistence. For example, it was shown that in the skin or the vaginal mucosa, local inflammation alone (induced by topical treatment with skin irritant or a spermicidal agent) can be sufficient to promote the recruitment of circulating effector CD8<sup>+</sup> T cells to the tissue and to instruct their local development into CD103<sup>+</sup> TRM cells (Mackay et al., 2012). Similarly, Casey et al. found that upon adoptive transfer into RAG-deficient mice, naïve CD8<sup>+</sup> T cells underwent lymphopenia-driven homeostatic expansion, settled into the small intestinal epithelium and adopted a characteristic TRM phenotype even in the absence of inflammation or local antigen stimulation (Casey et al., 2012).

These studies indicate that the local cytokine milieu within non-lymphoid tissues has an important role in instructing TRM differentiation of infiltrating effector CD8<sup>+</sup> T cells. Accumulating data suggest that transforming growth factor- $\beta$  (TGF- $\beta$ ) might be critically involved in this process. TGF- $\beta$  is constitutively expressed in many epithelial barriers, including the skin epidermis and the small intestinal epithelium (Kane et al., 1990;

Koyama & Podolsky, 1989), and has been demonstrated to be a potent driver of CD103 expression in activated T cells *in vitro* (Casey et al., 2012; Cepek et al., 1993). Consistent with this, CD8<sup>+</sup> T cells with a deficiency in TGF- $\beta$ R expression failed to upregulate CD103 upon migration into the skin, small intestine and lung and showed poor long-term retention in these organs (Casey et al., 2012; El-Asady et al., 2005; Lee et al., 2011; Mackay et al., 2013; Sheridan et al., 2014; Zhang & Bevan, 2013). Recent studies have also revealed a functional role of the homeostatic cytokine IL-15 as well as aryl hydrocarbon receptor ligands in the development and/or maintenance of TRM cells in the skin (Mackay et al., 2013; Zaid et al., 2014).

### **3.6 TRM cells as vaccine targets**

As TRM cells permanently occupy the front-line barriers of non-lymphoid tissues, they are positioned to immediately respond to renewed local tissue infection. Several studies in mice have already documented that TRM cells make a critical contribution to protective immunity against localized infections (Ariotti et al., 2012; Gebhardt et al., 2009; Gebhardt et al., 2011; Hofmann & Pircher, 2011; Jiang et al., 2012; Mackay et al., 2012; Shin & Iwasaki, 2012). For example, Gebhardt et al. showed that skin regions which had previously undergone infection with HSV and therefore contained high numbers of virus-specific TRM cells were far more resistant to a secondary local HSV skin infection than previously uninfected skin regions, as indicated by a substantial decrease in viral load at the site of HSV challenge (Gebhardt et al., 2009). Notably, Mackay et al. found that TRM cells embedded at the site of HSV challenge could greatly limit the extent of latent infection in skin-innervating dorsal root ganglia, which suggests that these cells controlled the viral replication in the skin in a highly rapid fashion (Mackay et al., 2012). In an attempt to directly compare the protective roles of TRM cells versus recirculating memory CD8<sup>+</sup> T cells, Jiang et al. generated parabiotic pairs between naïve mice and previously VV-infected mice which contained both skin TRM cells and recirculating memory CD8<sup>+</sup> T cells (~90% of which were of TCM phenotype) (Jiang et al., 2012). After the systemic TCM cell compartment had equilibrated, conjoined partners were separated and cutaneously challenged with VV. The study showed that the previously VV-infected partner controlled the secondary VV skin infection around 10<sup>4</sup> times more efficiently as the previously non-infected partner that contained only recirculating memory CD8<sup>+</sup> T cells.

Notably, previously VV-infected parabionts almost completely cleared the virus from the tissue within 6 days post challenge, whereas in non-immunized parabionts complete viral clearance was not observed until 3 weeks post infection. Strikingly, previously VV-infected parabionts showed a similarly efficient local viral control even when the recruitment of TCM cells and newly generated secondary effector CD8<sup>+</sup> T cells was inhibited through treatment with FTY720, a S1P1 antagonist that prevents lymphocyte egress from SLOs (Jiang et al., 2012). These findings demonstrate that the rapid viral control at the site of VV reinfection was mediated solely by local TRM cells and further suggest that recirculating memory CD8<sup>+</sup> T cells are highly limited in their ability to protect against infections encountered within non-lymphoid tissues.

Given that the elimination of infected host cells by CD8<sup>+</sup> T cells requires direct cell-to-cell contact (Russell & Ley, 2002), it is likely that the accelerated protection offered by TRM cells can be attributed to their localization in immediate proximity to the site of pathogen invasion. Interestingly, recent studies have elucidated that in addition to mediating cellular cytotoxicity, TRM can contribute to local pathogen control also through non-cytolytic means (Ariotti et al., 2014; Schenkel et al., 2014; Schenkel et al., 2013). For instance, when reactivated by their cognate peptide *in situ*, TRM cells residing in the female reproductive tract have been shown to almost instantly secrete the effector cytokine IFN- $\gamma$ . This immediate IFN- $\gamma$  production by reactivated TRM cells promoted a robust local expression of inflammatory chemokines and upregulation of adhesion molecule expression on the local vascular endothelium that enabled a rapid recruitment of circulating memory CD8<sup>+</sup> T cells to the site of TRM cell reactivation. Moreover, cytokine secretion by reactivated TRM cells was further shown to cause a rapid activation and licensing of NK cells as well as maturation of DC within the tissue (Schenkel et al., 2014). Interestingly, another study has shown that IFN- $\gamma$  released by reactivated TRM cells in the skin can also act directly on the surrounding tissue and thereby induce the expression of proteins that facilitate local pathogen control. For instance, it was found that within hours post TRM cell triggering, both epidermal and dermal cells upregulated expression of IFITM3 (interferon-induced transmembrane protein 3), a protein with broad-spectrum antiviral functions (Ariotti et al., 2014). Evidence suggests that this tissue-wide response by locally reactivated TRM cells can create a local state of pathogen alert that can even confer resistance to infection with an unrelated pathogen (Ariotti et al., 2014; Schenkel et al., 2014).

Collectively, these data show that TRM cells are a potent first line of defense against pathogens that invade via the body surfaces. Therefore, establishing TRM cells at common sites of pathogen entry might be an appealing goal for novel vaccines that aim for a rapid containment of pathogens at the site of first exposure. Such instant tissue-based CD8<sup>+</sup> T cell memory responses might be particularly relevant for the control of pathogens like HIV or HSV, which are known to rapidly establish latent or chronic reservoirs in the host upon transmission and initial replication within non-lymphoid tissues.

Importantly, there is mounting evidence that the long-term maintenance of TRM cells within tissues does not require persisting antigen stimulation (Casey et al., 2012; Mackay et al., 2012). Therefore, generation of TRM cells might also be efficiently achieved using vaccines based on non-replicating viral vectors.

### **3.7 Aim of the study**

Tissue-resident memory CD8<sup>+</sup> T cells (TRM cells) are now widely accepted as key players in local immune protection against infections originating within non-lymphoid barrier tissues, such as the skin or mucosa and thus represent promising targets for novel vaccines against pathogens that invade via these peripheral body surfaces. However, despite their well-documented role in local protective immune responses, little is still known about the mechanisms that control the development and long-term retention of TRM cells in non-lymphoid locations.

The aim of this thesis was to study the formation of TRM cells after acute skin infection with the viral vector MVA (modified vaccinia virus Ankara), a highly attenuated and non-replicating vaccinia virus that is currently being tested as recombinant vaccine in clinical studies. For this purpose, skin tattooing of MVA should be established as a means to generate a localized skin infection in C57BL/6 mice.

In the first part of this study, MVA tattooing should be characterized with regard to its efficacy to deliver virus into the skin, its immunogenicity in comparison to the conventional intramuscular route of MVA immunization as well as its capacity to promote effector CD8<sup>+</sup> T cell recruitment and subsequent TRM cell formation in the tissue.

Based on the finding that long-lived populations of virus-specific memory CD8<sup>+</sup> T cells were readily formed in MVA-tattooed skin, subsequent analyses should be undertaken to characterize the local virus-specific memory cell pool in terms of phenotype, tissue localization and protective capacity against secondary local VV challenge infection.

In the second part of this study, the MVA skin infection model should further be used to identify the relevant local factors that mediate TRM cell formation in MVA-infected skin (e.g. inflammation, local antigen, site of viral antigen expression), with the goal to define how MVA can best be used for the establishment of CD8<sup>+</sup> TRM cells in non-lymphoid tissues.



## 4 Materials and Methods

### 4.1 Materials

#### 4.1.1 Antibodies

Specificity	Clone	Species/Isotype	Conjugate	Manufacturer
Anti-mouse CD4	RM4-5	Rat IgG2a	FITC, eFluor450	eBioscience (Frankfurt/Main)
Anti-mouse CD8a	53-6.7	Rat IgG2a	PerCP-Cy5.5, eFluor450	eBioscience (Frankfurt/Main)
Anti-mouse CD8a	53-6.7	Rat IgG2a	-	BD Pharmingen (Hamburg)
Anti-mouse CD8a	5H10	Rat IgG2b	APC	Caltag/Invitrogen (Karlsruhe)
Anti-mouse CD16/CD32	2.4G2	Rat IgG2b	-	BD Pharmingen (Hamburg)
Anti-mouse CD45.1	A20	Mouse IgG2a	FITC, eFluor450, APC-eFluor780	eBioscience (Frankfurt/Main)
Anti-mouse CD45.2	104	Mouse IgG2a	FITC, PE	eBioscience (Frankfurt/Main)
Anti-human/mouse CD45RA (B220)	RA3-6B2	Rat IgG2a	FITC	eBioscience (Frankfurt/Main)
Anti-rat/mouse CD49a	Ha31/8	Armenian Hamster IgG2	-, AlexaFluor647	BD Pharmingen (Hamburg)
Anti-mouse CD62L	MEL-14	Rat IgG2a	PE, PE-Cy7	eBioscience (Frankfurt/Main)
Anti-mouse CD69	H1.2F3	Armenian Hamster IgG	PerCP-Cy5.5	eBioscience (Frankfurt/Main)
Anti-mouse CD103	2E7	Armenian Hamster IgG	PE, APC	eBioscience (Frankfurt/Main)
Anti-mouse CD127	A7R34	Rat IgG2a	APC	eBioscience (Frankfurt/Main)
Anti-mouse CXCR3	CXCR3-173	Armenian Hamster IgG	APC	eBioscience (Frankfurt/Main)
Anti-mouse IFN- $\gamma$	XMG1.2	Rat IgG1	FITC, APC	BD Pharmingen (Hamburg)
Anti-mouse MHC II (I-A/I-E)	M5/114.15.2	Rat IgG2b	FITC	eBioscience (Frankfurt/Main)
Anti-mouse NK1.1	PK136	Mouse IgG2a	FITC	eBioscience (Frankfurt/Main)
Anti-mouse KLRG1	2F1	Golden Syrian Hamster IgG	PE-Cy7, APC, FITC	eBioscience (Frankfurt/Main)
Anti-mouse V alpha 2 TCR	B20.1	Rat IgG2a	FITC	eBioscience (Frankfurt/Main)
Anti-FITC	polyclonal	Rabbit	-	Invitrogen (Camarillo, CA, USA)

Anti-mouse IgG1	A85-1	Rat IgG1	Biotin	BD Pharmingen (Hamburg)
Anti-mouse IgG2a	R19-15	Rat IgG1	Biotin	BD Pharmingen (Hamburg)
Anti-mouse IgG2b	R12-3	Rat IgG2a	Biotin	BD Pharmingen (Hamburg)
Anti-mouse IgG3	R40-82	Rat IgG2a	Biotin	BD Pharmingen (Hamburg)
Anti-mouse IgM	R6-60.2	Rat IgG2a	Biotin	BD Pharmingen (Hamburg)
Anti-rabbit IgG (H+L)	polyclonal	Goat IgG	HRP	Jackson ImmunoResearch Laboratories, Inc. (West Grove, PA, USA)
Anti-rat IgG (H+L)	polyclonal	Goat IgG	AP	Jackson ImmunoResearch Laboratories, Inc. (West Grove, PA, USA)

#### 4.1.2 Fluorescent dyes

Name	Stock concentration	Final concentration	Manufacturer
Ethidium monoazide bromide (EMA)	2 mg/ml in DMF	1 µg/ml	Molecular Probes (Eugene, OR, USA)
Propidium iodide (PI)	10 mg/ml in water	1µg/ml	Molecular Probes (Eugene, OR, USA)

#### 4.1.3 Biochemicals/Chemicals

Name	Manufacturer
Acetone	Pharmacy, Klinikum rechts der Isar (Munich)
Aluminum sulfate octadecahydrate $\text{Al}_2(\text{SO}_4)_3 \cdot 18 \text{H}_2\text{O}$	Sigma (Munich)
Ammonium chloride ( $\text{NH}_4\text{Cl}$ )	Sigma (Munich)
Bovine serum albumin (BSA)	Sigma (Munich)
Brefeldin A (Golgi-Stop)	Sigma (Munich)
Calcium chloride ( $\text{CaCl}_2$ )	Sigma (Munich)
Dimethyl sulfoxide (DMSO)	Merck (Darmstadt)

Diphtheria toxin (DTX)	Calbiochem ( <i>San Diego, CA, USA</i> )
EDTA	Sigma ( <i>Munich</i> )
Ethanol (99%, 70%)	Pharmacy, Klinikum rechts der Isar ( <i>Munich</i> )
Eukitt mounting medium	Sigma ( <i>Munich</i> )
Fetal calf serum (FCS)	Biochrom KG ( <i>Berlin</i> )
Fetal bovine serum (FBS)	GibcoBRL ( <i>Karlsruhe</i> )
Heparin-Natrium-25000-ratiopharm	Pharmacy, Klinikum rechts der Isar ( <i>Munich</i> )
Hydrochloric acid (HCl)	Pharmacy, Klinikum rechts der Isar ( <i>Munich</i> )
Isofluran	CP-Pharma ( <i>Burgdorf</i> )
Kernechtrot Certistain (nuclear fast red)	Merck ( <i>Darmstadt</i> )
Ketamin Inresa 10 ml (50 mg/ml)	Inresa Arzneimittelwerk GmbH ( <i>Freiburg</i> )
D-Luciferin - K <sup>+</sup> Salt Bioluminescent Substrate	PerkinElmer ( <i>Waltham, MA, USA</i> )
Magnesium chloride (MgCl <sub>2</sub> )	Sigma ( <i>Munich</i> )
Paraformaldehyde (PFA)	Sigma ( <i>Munich</i> )
Phosphate buffered saline (PBS)	Lonza ( <i>Verviers, Belgium</i> )
Potassium chloride (KCl)	Sigma ( <i>Munich</i> )
Potassium ferricyanide(III)	Sigma ( <i>Munich</i> )
Potassium hexacyanoferrat(II) trihydrate (Potassium ferrocyanide(II))	Sigma ( <i>Munich</i> )
Potassium phosphate monobasic (KH <sub>2</sub> PO <sub>4</sub> )	Sigma ( <i>Munich</i> )
Pen-Strep 100x (10,000 U/ml penicillin, 10 mg/ml streptomycin)	Sigma ( <i>Munich</i> )
RPMI 1640 medium	Lonza ( <i>Verviers, Belgium</i> )
Sodium bicarbonate (NaHCO <sub>3</sub> )	Roth ( <i>Karlsruhe</i> )
Sodium carbonate (Na <sub>2</sub> CO <sub>3</sub> )	Sigma ( <i>Munich</i> )
Sodium chloride (NaCl)	Merck ( <i>Darmstadt</i> )
Sodium hydroxide (NaOH) (0.2N, 10N)	Pharmacy, Klinikum rechts der Isar ( <i>Munich</i> )
Sodium phosphate dibasic (Na <sub>2</sub> HPO <sub>4</sub> )	Sigma ( <i>Munich</i> )
Streptavidin-HRP	Sigma ( <i>Munich</i> )
Sulfuric acid (H <sub>2</sub> SO <sub>4</sub> ) 2N	Merck ( <i>Darmstadt</i> )
Tissue Tek (O.C.T)	A. Hartenstein GmbH ( <i>Würzburg</i> )
Tris Base	Merck ( <i>Darmstadt</i> )
Trypan Blue	Biochrom KG ( <i>Berlin</i> )

Tween-20	Sigma ( <i>Munich</i> )
X-Gal (5-bromo-4-chloro-3-indolyl- $\beta$ -D-galactopyranoside)	Promega ( <i>Madison, WI, USA</i> )
Xylazine (Rompun 2% 25 ml, 20 mg/ml)	Bayer HealthCare AG ( <i>Leverkusen</i> )
Xylol	Roth ( <i>Karlsruhe</i> )

#### 4.1.4 Enzymes

Name	Manufacturer
Collagenase type III (CLS- 3)	Worthington Biochemical Corp. ( <i>Lakewood, NJ, USA</i> )
DNase I	Sigma ( <i>Munich</i> )
Trypsin-EDTA	Invitrogen ( <i>Karlsruhe</i> )

#### 4.1.5 MHC class I tetramers

Name	Manufacturer
H-2K <sup>b</sup> /B8R <sub>20</sub> tetramer (PE-conjugated)	Kindly provided by Prof. D.H. Busch ( <i>Munich</i> )
H-2K <sup>b</sup> /OVA <sub>257</sub> tetramer (PE-conjugated)	Kindly provided by Prof. D.H. Busch ( <i>Munich</i> )

#### 4.1.6 Buffers and Solutions

Name	Composition
PBS pH7.4 (1x)	0.14 M NaCl 2.7 mM KCl 3.2 mM Na <sub>2</sub> HPO <sub>4</sub> 1.5 mM KH <sub>2</sub> PO <sub>4</sub>
FACS buffer pH 7.4	1% BSA (w/v) 0.02 % NaN <sub>3</sub> from 20% stock (w/v) in 1x PBS
Paraformaldehyde (PFA) (2%, 4%)	2% (w/v) PFA or 4% (w/v) PFA in 1x PBS
TAC buffer	90 % (v/v) NH <sub>4</sub> Cl from 0.16 M stock 10 % (v/v) Tris pH 7.65 from 0.17 M stock
RPMI medium (1%, 10%)	RPMI 1640 supplemented with: 1% or 10% (v/v) heat-inactivated FCS 1% (v/v) Pen-Strep
Freezing medium	90% (v/v) heat-inactivated FCS 10% (v/v) DMSO
Collagenase/DNase medium	RPMI 10% medium supplemented with: 3 mg/ml collagenase type III 5 µg/ml DNase I 1 mM CaCl <sub>2</sub> 1 mM MgCl <sub>2</sub>
Nuclear Fast Red (Kernechtrot) Solution 1l	5% aluminum sulfate octadecahydrate ad 1l dH <sub>2</sub> O (boil in microwave 5-10 min, cool down) + 1 g Kernechtrot Certistain ( final c= 0.1% (w/v))
Trypan blue solution	0.2% (w/v) Trypan blue in 1x PBS
ELISA coating buffer pH9.6	70 mM NaHCO <sub>3</sub> 20 mM Na <sub>2</sub> CO <sub>3</sub>
ELISA blocking buffer	0.05% (v/v) Tween 20 10% (v/v) FCS in 1x PBS

ELISA washing buffer	0.05% (v/v) Tween 20 in 1x PBS
X-Gal solution 50 ml (1 mg/ml)	0.5 ml potassium ferricyanide(III) (from 500 mM stock) 0.5 ml potassium ferrocyanide (from 500 mM stock) 0.1 ml MgCl <sub>2</sub> (from 1 M stock) 2 ml X-Gal (from 25 mg/ml stock in DMF) ad 50 ml 1xPBS

Unless stated otherwise, buffers were prepared in ultrapure Milli-Q water. The pH was adjusted with HCl or NaOH.

#### 4.1.7 Synthetic Peptides

All synthetic peptides were purchased from Biosyntan (Berlin). Peptides were provided as lyophilisates containing an N-terminal NH<sub>2</sub>- and a C-terminal –COOH group and were dissolved in DMSO (stock concentration: 1 mg/ml) and stored at -80°C.

Peptide	MHC restriction	Sequence (aa)	Origin	Reference
B8R <sub>20</sub>	H-2K <sup>b</sup>	TSYKFESV	176R-B8R	(Tschärke et al., 2005)
A3L <sub>270</sub>	H-2K <sup>b</sup>	KSYNYMLL	122L-A3L	(Moutaftsi et al., 2006)
K3L <sub>6</sub>	H2-D <sup>b</sup>	YSLPNAGDVI	024-K3L	(Tschärke et al., 2005)
OVA <sub>257</sub>	H-2K <sup>b</sup>	SIINFEKL	Chicken ovalbumin	(Rotzschke et al., 1991)
β-Gal <sub>96</sub>	H-2K <sup>b</sup>	DAPIYTNV	β-galactosidase	(Overwijk et al., 1997)

#### 4.1.8 Cell lines

Name	Description	ATCC number
RK13	Rabbit kidney cell line	CCL-37

RK-13 cells were cultured in RPMI 1640 medium containing 10% FCS and 1% Pen-Strep in a 37°C incubator providing a 5% CO<sub>2</sub> atmosphere and 95% humidity.

#### 4.1.9 Kits

Name	Manufacturer
Anti-FITC MicroBeads	Miltenyi Biotec GmbH ( <i>Bergisch Gladbach</i> )
BD Cytotfix/Cytoperm	BD Pharmingen ( <i>Hamburg</i> )
Bond Polymer Refine Detection	Leica Biosystems ( <i>Wetzlar</i> )
Bond Polymer Refine Red Detection	Leica Biosystems ( <i>Wetzlar</i> )
TMB Microwell Peroxidase Substrate System	KPL ( <i>Gaithersburg, MD, USA</i> )

#### 4.1.10 Viruses

Purified stocks of the following viruses (in 1 mM Tris) were already present in the laboratory and were kindly provided by Ronny Ljapoci and Prof. Dr. Ingo Drexler. Virus stocks were kept at -80°C and were prepared and titrated as previously described. Before use, virus stocks were thawed and sonicated for 45 seconds in a cup sonicator on ice to singularize viral particles. For immunizations or viral challenges, virus stocks were diluted in sterile PBS (Lonza, Verviers, Belgium).

Virus	Full name	Reference
MVA wild-type	MVA IInew	(Staib et al., 2003)
MVA-OVA	MVA-OVA PH5	Obtained from Prof. Ingo Drexler
MVA-Luc	MVA-Luciferase PK1L	Obtained from Prof. Ingo Drexler
MVA-lacZ	MVA-lacZ PK1L	Obtained from Prof. Ingo Drexler
VV-WR wild-type	VV Western Reserve strain	Kind gift from Prof. Bernard Moss ( <i>NIH, Bethesda, MD, USA</i> )
VV-OVA	rVV-WR-OVA	Kind gift from Profs. Jonathan W. Yewdell and Jack R. Bennink ( <i>NIH, Bethesda, MD USA</i> )

## 4.1.11 Mice

Name	Description	Reference
C57BL/6N	Wild-type mice, MHC I alleles (H-2K <sup>b</sup> , H-2D <sup>b</sup> ) MHC II alleles (I-A <sup>b</sup> ), pan leukocyte marker <i>Ptprc</i> <sup>b</sup> (CD45.2)	<a href="http://jaxmice.jax.org">http://jaxmice.jax.org</a>
DEREG	BAC transgenic mouse line (C57BL/6 background) that expresses the simian diphtheria toxin receptor fused to enhanced GFP under the control of an additional Foxp3 promoter, allowing for specific <i>in vivo</i> depletion of Foxp3 <sup>+</sup> CD4 <sup>+</sup> regulatory T cells by diphtheria toxin application	(Lahl et al., 2007) <a href="http://jaxmice.jax.org">http://jaxmice.jax.org</a> C57BL/6-Tg(Foxp3-DTR/EGFP)23.2Spar/Mmjax
IFN- $\gamma$ R <sup>-/-</sup>	Mice (C57BL/6 background) deficient in IFN- $\gamma$ receptor expression	<a href="http://jaxmice.jax.org">http://jaxmice.jax.org</a> B6.129S7-Ifngr1tm1Agt/J
OT-I	Mice (C57BL/6 background) express a transgenic TCR recognizing the ovalbumin (OVA)-derived peptide OVA <sub>257-264</sub> (SIINFEKL) in the context of H-2Kb; homozygous or heterozygous for <i>Ptprc</i> <sup>a</sup> (CD45.1)	<a href="http://jaxmice.jax.org">http://jaxmice.jax.org</a> C57BL/6-Tg(TcraTcrb)1100Mjb/J

Wild-type C57BL/6N mice were purchased from Charles River (Sulzfeld, Germany) and kept at the mouse facility at the AVM Helmholtz Center Munich (Neuherberg) under specific pathogen-free conditions according to institutional guidelines.

OT-I transgenic mice were kindly provided by Prof. Dirk H. Busch (Munich) and bred at the Institute of Medical Microbiology, Immunology and Hygiene (TU Munich, Trogerstr. 30). DEREK mice were kindly provided by Prof. Tim Sparwasser and were bred the AVM Helmholtz Center Munich (Neuherberg) under specific pathogen-free conditions according to institutional guidelines. IFN- $\gamma$ R<sup>-/-</sup> mice were kindly provided by Prof. Thomas Korn (Experimentelle Neuroimmunologie, Klinikum rechts der Isar, TU Munich) and bred at the Zentrum für Präklinische Forschung (ZPF) (TU Munich, Trogerstr. 4a).



**4.1.12 Software**

Name	Manufacturer
Adobe Illustrator CS6	Adobe Systems Incorporated ( <i>San José, CA, USA</i> )
Adobe Photoshop CS6	Adobe Systems Incorporated ( <i>San José, CA, USA</i> )
cellSens 1.8	Olympus ( <i>Hamburg</i> )
Endnote	Thomson Reuters ( <i>New York, NY, USA</i> )
FACSDiva	BD Biosciences ( <i>Heidelberg</i> )
FlowJo 6.4.2	Tree Star ( <i>Ashland, OR, USA</i> )
GraphPad Prism 5	GraphPad Software, Inc. ( <i>San Diego, CA, USA</i> )
MS Office 2010	Microsoft ( <i>Redmond, WA, USA</i> )
Slide Path Digital Image Hub 4.0	Leica Microsystems ( <i>Wetzlar</i> )

**4.1.13 Consumables**

Name	Manufacturer
Blood lancets Supra	Megro ( <i>Wesel</i> )
Cell culture flasks (T25, T75, T185)	Greiner ( <i>Nürtingen</i> ) Corning ( <i>New York, NY, USA</i> ) Nunc ( <i>Wiesbaden</i> )
Cell culture plates 6-, 12-, 24-, 96-well	Corning ( <i>New York, USA</i> )
Cell strainer 100 µm	BD Pharmingen ( <i>Hamburg</i> )
Cell strainer cap 30 µm	BD Pharmingen ( <i>Hamburg</i> )
Cryo tubes	Nunc ( <i>Wiesbaden</i> )
Examination gloves	Kimberly-Clark ( <i>Mainz</i> )
FACS tubes	Bio-Rad ( <i>Munich</i> )
Falcon tubes (15 ml, 50 ml)	Greiner ( <i>Nürtingen</i> )
LS columns	Miltenyi Biotec GmbH ( <i>Bergisch Gladbach</i> )
Maxisorp plates for ELISA (96-well)	Nunc ( <i>Wiesbaden</i> )
Microscope slides Superfrost Plus	Thermo Scientific ( <i>Ulm</i> )
Mortar and Pestle	<i>Pharmacy, Klinikum rechts der Isar (Munich)</i>

Parafilm	Roth ( <i>Karlsruhe</i> )
Petri dishes	Nunc ( <i>Wiesbaden</i> )
Pipettes ‘Cellstar’ (5-25ml)	Greiner ( <i>Nürtingen</i> )
Pipet tips	Molecular Bioproducts ( <i>San Diego, CA, USA</i> )
Reaction tubes (1.5 ml, 2 ml)	Eppendorf ( <i>Hamburg</i> )
Sterile filters (Minisart 0.2-0.45 µm)	Sartorius AG ( <i>Göttingen</i> )
Syringes (Omnican 100)	Braun ( <i>Melsungen</i> )
Tattoo needles 15 Magnum (15M) 0.35 mm	DC-TC Europe GmbH ( <i>Neuburg am Rhein</i> )
Veet Crème Sensitive	Reckitt Benckiser ( <i>Mannheim</i> )

#### 4.1.14 Laboratory Equipment

Name	Type	Manufacturer
Centrifuge	Megafuge 1.0	Heraeus ( <i>Hanau</i> )
	Biofuge fresco	Heraeus ( <i>Hanau</i> )
CO <sub>2</sub> Incubator	Heracell 150	Heraeus ( <i>Hanau</i> )
Cryostat	CM1950	Leica Biosystems ( <i>Weztlar</i> )
Cup sonicator	Sonoplus HD200/UW200	Bandelin ( <i>Berlin</i> )
Flow cytometer	BD LSR II	BD Biosciences ( <i>Heidelberg</i> )
	Aria II (cell sorter)	BD Biosciences ( <i>Heidelberg</i> )
Freezer (-80°C)	Herafreeze Ult 2090	Heraeus ( <i>Hanau</i> )
Freezing Container	Mr. Frosty	Thermo Scientific ( <i>Ulm</i> )
Fridge (4°C)	UT6-K	Bauknecht ( <i>Stuttgart</i> )
Fridge (-20°C)	Excellence	Bauknecht ( <i>Stuttgart</i> )
Haematocytometer	Neubauer counting chamber	Karl Hecht KG ( <i>Sondheim</i> )
Ice machine	AF 200	Scotsman ( <i>Milan, Italy</i> )
Immunohistochemistry robot	BOND-MAX	Leica Biosystems ( <i>Wetzlar</i> )
Incubation shaker	Innova 4430	New Brunswick Scientific ( <i>Nürtingen</i> )
IVIS Imaging System	100 Series	PerkinElmer ( <i>Waltham, MA, USA</i> )
Laminar flow	HERAsafe HS 12	Heraeus ( <i>Hanau</i> )
MACS equipment	MidiMACS Separator	Miltenyi Biotec GmbH

	Multistand	<i>(Bergisch Gladbach)</i>
Magnetic stirrer	Ikamag Reo	IKA Werke <i>(Staufen)</i>
Micropipette	Pipetman P10-1000	Gilson <i>(Middleton, WI, USA)</i>
Microscope	Kolleg SHB 45 Axiovert 25 Olympus BX53	Eschenbach <i>(Nuremberg)</i> Carl Zeiss <i>(Oberkochen)</i> Olympus <i>(Hamburg)</i>
Multichannel pipette	Transferpipette-12 (20-200 µl) Calibra 852	Brand <i>(Wertheim)</i> Socorex <i>(Ecublens, Switzerland)</i>
Microplate reader	Infinite F200 PRO  Genios	Tecan <i>(Männedorf, Switzerland)</i>  Tecan <i>(Männedorf, Switzerland)</i>
Nitrogen container	Cryo 200	Forma Scientific <i>(Waltham, MA, USA)</i>
pH-Meter	InoLab pH Level 1	WTW GmbH <i>(Weilheim)</i>
Pipettor	Easypet Pipetman	Eppendorf <i>(Hamburg)</i> Gilson <i>(Middleton, WI, USA)</i>
Rotary tattoo device	W1	Cold skin, B. S. Trading BV <i>(Ljinden, Netherlands)</i>
Slide scanner	SCN400	Leica Microsystems <i>(Wetzlar)</i>
UV Lamp	UVT 2035	Hero Lab <i>(Wiesloch)</i>
Vortexer	Vortex Genie 2	Scientific Industries <i>(Bohemia, NY, USA)</i>
Water bath	Assistant VTE Var 3185	Hecht <i>(Sondheim)</i>

## **4.2 Methods**

### **4.2.1 Mammalian cell culture**

RK13 cells were cultured and handled under sterile conditions. Cultures were grown in RPMI 1640 medium supplemented with 10% FCS and 1% Pen-Strep (RPMI 10% medium) in a 37°C incubator providing a 5% CO<sub>2</sub> atmosphere and 95% humidity. When cells had reached approximately 90% confluency, monolayers were washed with sterile PBS and incubated with trypsin-EDTA at 37°C for 3 min. Detached cells were resuspended in fresh RPMI 10% medium and split at a ratio of 1:2 to 1:10 (depending on their growth kinetics and intended use).

For long-term cryopreservation, cells were trypsinized as described above, transferred into a 50 ml Falcon tube and pelleted for 5 min at 4°C and 1,400 rpm. The cell pellet was carefully resuspended in cold freezing medium and transferred into sterile cryo tubes in 1 ml aliquots. Cells were frozen slowly by storing them over night in a slow-cooling container at -80°C. After 24 h, the tubes were transferred to liquid nitrogen (-196°C) for long-term storage.

For recultivation of cryoconserved cells, aliquots were thawed in a 37°C water bath, washed with 10 ml of pre-heated RPMI 10% medium and pelleted for 5 min at room temperature and 1,400 rpm. Cells were then resuspended in pre-heated RPMI 10% medium and transferred into a fresh cell culture flask.

### **4.2.2 Preparation of cryo sections from mouse skin**

Skin from abdomen or ear was excised and after removal of residual subcutaneous fat (abdominal skin) or cartilage (from the base of the ear), tissue was embedded in Tissue Tek medium (with the cut surfaces facing down), immediately snap frozen in liquid nitrogen and stored at -80°C. Cross-sections were cut at 10 µm thickness using a Leica cryostat and placed on glass slides. Slides were air-dried at room temperature for 30 min and thereafter stored at -20°C until further use.

### **4.2.3 X-Gal staining of frozen skin tissue sections**

Frozen skin tissue sections were thawed and dried at room temperature and thereafter fixed for 10 min in 4% PFA. Sections were washed three times for 5 min with PBS and incubated for 24 hours at 37°C in X-Gal solution. X-Gal solution was washed off two

times for 5 min in PBS and sections were counterstained for 10 min using nuclear fast red (Kernechtrot Certistain) solution. Slides were rinsed shortly with dH<sub>2</sub>O, dehydrated in an ascending alcohol series (70%, 90%, 100%) and thereafter cleared in a xylol bath and mounted in Eukitt mounting medium. The nuclear fast red counterstain produces a distinct red staining of nuclei, while cytoplasm appear in light red color.

#### **4.2.4 Immunohistochemistry**

Frozen skin tissue sections (10 µm) were thawed and dried at room temperature. Slides were then fixed for 5 min in acetone, washed in PBS and blocked in FACS buffer containing anti-mouse CD16/CD32 antibodies (1:100) for 30 min at room temperature. Immunohistochemical stainings of the OT-I congenic marker CD45.1 were performed on an automated Leica BOND-MAX instrument according to standard protocol using anti-mouse CD45.1 FITC (1:200) as primary antibody and rabbit anti-FITC (1:500) as secondary antibody, followed by detection with Bond Polymer Refine Red Detection Solution (for AP).

Immunohistochemical co-staining of CD45.1 and CD8a was performed manually. After Fc receptor blockade (anti-mouse CD16/CD32; 1:100), slides were incubated in FACS buffer containing a mixture of anti-mouse CD45.1-FITC (1:200) and rat anti-mouse CD8a antibodies (clone 53-6.7 unconjugated; 1:200). Slides were thereafter incubated in FACS buffer containing rabbit anti-FITC antibodies (1:500), followed by incubation in FACS buffer containing AP-coupled goat anti-rat (secondary) antibody (1:100) and HRP-coupled goat anti-rabbit (tertiary) antibody (1:500). All antibody incubation steps were performed for 30 min at room temperature in the dark. Co-staining was developed by sequential incubation in Bond Polymer Refine Detection Solution (substrate for HRP) and Bond Polymer Refine Red Detection Solution.

All IHC stainings were counterstained in hematoxylin (contained in the Bond Polymer Refine Detection Solutions).

Images were acquired using the Leica SCN400 slide scanner analysis software (Slide Path Digital Image Hub 4.0) or were taken on an Olympus BX53 Microscope (DP72 digital camera) using the cellSens 1.8 digital imaging software (Olympus).

## 4.2.5 Immunizations and viral challenges

### 4.2.5.1 Immunizations

Only female mice between 8-12 weeks of age were used. Viruses used for immunizations or challenge experiments were diluted in sterile PBS. Unless stated otherwise, the standard dose of MVA used for immunizations was  $2 \times 10^6$  infectious units (IU).

For MVA tattooing on abdominal skin, abdominal hair was removed using Veet depilation crème and a droplet of 10  $\mu$ l virus suspension was tattooed into the skin for 20 s over a surface area of approximately 2 cm<sup>2</sup> using a sterile 15M needle bar mounted on a rotary tattoo machine. The tattoo needle depth was adjusted to a needle depth of 0.5 mm.

For MVA tattooing on the ear, a 5  $\mu$ l droplet of virus suspension was placed onto dorsal ear pinna (without prior depilation) and distributed with the rotating tattoo needle over the entire surface of the ear for 20 s.

For intradermal (i.d.) injection into the ear pinna, MVA was diluted in a 10  $\mu$ l volume and injected at the dorsal side using an Omnican 100 syringe.

For intravenous (i.v.) injections, MVA was injected in a total volume of 200  $\mu$ l into the tail vein. Before i.v. injection, tails were pre-heated with an infrared lamp to induce vasodilation of the lateral tail vein.

For intramuscular (i.m.) injection, hind legs were first depilated using Veet depilation crème and MVA was injected into the anterior tibial muscle in a volume of 50  $\mu$ l using an Omnican 100 syringe.

For mucosal application, MVA was diluted in 30  $\mu$ l volume and administered intranasally (i.n.) in a dropwise fashion into each nostril using a Gilson P20 micropipette.

Prior to cutaneous, i.m. or i.n. virus application, mice were anesthetized by intraperitoneal (i.p.) injection of ketamine/xylazine (100mg/10mg per kg body weight). Animals were kept under an infrared lamp until they recovered from anesthesia.

### 4.2.5.2 Viral challenges

For respiratory VV challenge,  $1 \times 10^6$  PFU VV-WR was administered i.n. as described above.

Weight of challenged mice was measured daily. Animals having lost more than 25% of their initial body weight due to severe systemic infection were euthanized.

For cutaneous VV challenge,  $2 \times 10^6$  PFU rVV-OVA was injected i.d. into the ear pinna as described above. Four days after challenge, VV-OVA-infected ears were harvested and homogenized using a mortar and pestle. Homogenized ear tissue was suspended in 1.5 ml

10% RPMI medium and stored at -80°C. For quantification of viral titers, ear homogenates were freeze/thawed three times (-80°C, 37°C), sonicated three times for 1 min on ice, and serial dilutions were titrated in duplicates on RK13 cells (6-well plates) by standard plaque assay.

#### **4.2.6 Intravital imaging of luciferase activity**

For imaging of luciferase activity *in vivo*, MVA-Luc-infected mice were injected i.p. with an aqueous solution of luciferin substrate (150 mg per kg body weight). Eighteen min later, mice were anesthetized using isoflurane and luciferase luminescence was acquired during 30s in an IVIS Imaging System (CCD camera). The luminescence signal intensity (expressed as total photon flux) was quantified as the sum of all detected light within the region of interest, after subtraction of background luminescence.

#### **4.2.7 Collection of sera from immunized mice**

Vaccinated animals were bled from the cheek pouch with the help of a lancet (submandibular bleeding method) and blood was collected in a 1.5 ml reaction tube. Blood samples were kept at room temperature for 4 hours and then centrifuged for 10 min at 4,000 rpm and 4°C. The supernatants were carefully pipetted off and transferred into a fresh 1.5 ml reaction tube. Sera were stored at -20°C until vaccinia virus-specific antibodies were measured by ELISA.

#### **4.2.8 Anti-Vaccinia virus ELISA**

4 µl of highly purified MVA stock ( $1 \times 10^{11}$  IU/ml) were diluted in 10 ml ELISA coating buffer and 100 µl of the solution was pipetted into each well of a 96-well Maxi Sorp immuno plate. Coating of the plates with viral MVA particles was performed for 3 hours at 37°C followed by incubation over night at 4°C. Plates were then washed four times with ELISA washing buffer and 200 µl blocking buffer was added to each well for 1 hour at 37°C to block non-specific binding. Plates were washed four times with ELISA washing buffer. Stepwise 1:3 dilutions (1:100 to 1:40,500) of mouse sera were prepared and 75 µl of each dilution was applied per well. Plates were incubated with the serum dilutions for 1 hour at 37°C and then washed four times with ELISA washing buffer. Then, 100 µl of a mixture of biotinylated anti-mouse antibodies (Ig isotypes IgG1, IgG2a IgG2b, IgG3, IgM;

1:1000 in ELISA washing buffer) was added to each well and incubated for 1 hour at room temperature. Plates were washed four times with ELISA washing buffer and then incubated in 75  $\mu$ l of streptavidin-HRP (1:3000 in ELISA washing buffer) for 45 min at room temperature. Plates were again washed four times with ELISA washing buffer and thereafter developed at room temperature by adding 75  $\mu$ l peroxidase substrate solution (TMB 2-Component Microwell Peroxidase Substrate System, prepared according to manufacturer's instructions). Color reaction was stopped by adding 75  $\mu$ l 2N H<sub>2</sub>SO<sub>4</sub> per well and absorbance was measured using a micropate reader at a wavelength of 450 nm.

#### **4.2.9 Preparation of splenocytes**

Spleens were excised and mashed through a wire mesh into 5 ml 1% RPMI medium using a syringe plunger. The resulting single-cell suspension was filtered through a 100  $\mu$ m cell strainer and centrifuged at 1,500 rpm for 5 min at 4°C. Pellets were resuspended with 3 ml TAC buffer and incubated for 2 min at 37°C to remove red blood cells. Lysis was stopped by addition of 40 ml RPMI 1% medium. Cells were then filtered through a 100  $\mu$ m cell strainer, centrifuged (1,500 rpm, 5 min, 4°C) and resuspended in 3 ml RPMI 10% medium. Living cells were then counted at a 1:40 dilution using a Neubauer hemocytometer in the presence of Trypan blue.

#### **4.2.10 Preparation of peripheral blood mononuclear cells (PBMCs)**

Mice were bled from the cheek pouch using a lancet and blood was collected into tubes containing 50  $\mu$ l of heparin (diluted 1:5 in PBS). Blood samples were transferred to a 96-well V-bottom plate, spun down at 1,400 rpm for 2 min. Pelleted cells were resuspended in 200  $\mu$ l TAC buffer and incubated for 15-20 min at room temperature to lyse red blood cells. Cells were washed twice with 200  $\mu$ l FACS buffer and stored on ice until surface antibody staining.

#### **4.2.11 Preparation of cell suspensions from skin tissue**

For the preparation of cell suspensions from skin, mice were euthanized and perfused with 20 ml PBS through the left heart ventricle. For abdominal skin preparations, mice were depilated beforehand using Veet crème and residual crème was thoroughly washed off under running water. Whole ear skin or 1.5 cm<sup>2</sup> of abdominal skin were excised and



transferred into a 1.5 ml tube containing 650  $\mu$ l RPMI 10% medium supplemented with 3 mg/ml collagenase (type III; Worthington) and 5  $\mu$ g/ml DNase I (Sigma) in the presence of 1  $\mu$ M  $\text{CaCl}_2$  and  $\text{MgCl}_2$ . Skin tissue was then chopped into small pieces with a scissor and incubated for 90 min at 37°C. Digested tissue was further incubated for 5 min at room temperature in the presence of 10 mM EDTA. Thereafter, tubes were vortexed for 10s, transferred into a 15 ml Falcon tube containing 5 ml fresh RPMI 10% medium and then vigorously pipetted up and down (10x) in order to maximize release of cells from tissue. The single-cell suspension was filtered through a 100  $\mu$ m cell strainer and washed with 10 ml RPMI 10% medium. After 6 min centrifugation at 1,500 rpm and 4°C, cells were resuspended in FACS buffer and transferred to a 96-well V-bottom plate and stored on ice until surface antibody staining.

#### **4.2.12 Peptide re-stimulation of lymphocytes**

For *ex vivo* peptide re-stimulation of lymphocytes, single-cell suspensions were transferred to a 96-well U-bottom plate in 200  $\mu$ l 10% RPMI medium ( $4 \times 10^6$  cells/well for re-stimulation of splenocytes). To each well 50  $\mu$ l 5x mastermix containing 5  $\mu$ g/ml peptide (1 mg/ml stock) and 5  $\mu$ g/ml brefeldin A (Golgi-plug; 1 mg/ml stock) was added to yield a final peptide and brefeldin A concentration of 1  $\mu$ g/ml. Plates were incubated for 5 hours at 37°C.

#### **4.2.13 Live-dead dye staining and Fc receptor blockade**

Cell suspensions were transferred to a 96-well V-bottom plate and spun down at 1,500 rpm for 2 min at 4°C. Pellets were resuspended in 100  $\mu$ l FACS buffer containing 2  $\mu$ g/ml EMA (ethidium monoazide bromide; 1 mg/ml stock) and 1  $\mu$ l anti-CD16/CD32 antibody. Cells were incubated on ice under constant illumination (for photo activation of EMA) for 15 min. Dead cells will incorporate EMA (excitation by 488 nm laser; emission peak at 625 nm) in their nucleic acid by a covalent link. Fc receptor blockade by anti-CD16/CD32 antibodies prevents unspecific binding of murine IgG antibodies to Fc receptors.

For experiments including only staining of surface markers, dead cells were stained by adding 10  $\mu$ l propidium iodide (1:10 diluted stock) to each sample directly before FACS analysis.

#### **4.2.14 Staining of surface markers**

Following EMA staining and Fc receptor blockade, cells were washed twice with FACS buffer and were then resuspended in 50  $\mu$ l FACS buffer containing a mix of cell surface antibodies. Cell surface marker staining was performed for 30 min on ice in the dark.

#### **4.2.15 Intracellular cytokine staining**

After staining of surface markers, cells were washed twice with 200  $\mu$ l FACS buffer, spun down at 1,400 rpm for 2 min at 4°C. Cells were permeabilized and fixed with 50  $\mu$ l BD Cytotfix/Cytoperm solution for 15 min on ice in the dark. Thereafter, cells were washed twice with 200  $\mu$ l BD 1x Perm/Wash buffer (in Milli-Q water) and stained with 50  $\mu$ l intracellular antibody mix in 1x Perm/Wash buffer for 30 min on ice in the dark. Stained cells were washed twice with 200  $\mu$ l 1x Perm/Wash, transferred to a FACS tube in 340  $\mu$ l FACS buffer and 70  $\mu$ l 2% PFA (0.4% PFA final concentration) was added for final fixation and samples were stored at 4°C until FACS analysis.

#### **4.2.16 MHC class I tetramer staining**

MHC class I tetramer staining of CD8<sup>+</sup> T lymphocytes was performed in a 96-well V-bottom plate. After Fc receptor blockade, cells were washed twice with 200  $\mu$ l FACS buffer and incubated for 15 min on ice in the dark with 40  $\mu$ l FACS buffer containing 1  $\mu$ l H2-K<sup>b</sup>/B8R<sub>20</sub> (1:40) or 10  $\mu$ l H-2K<sup>b</sup>/OVA<sub>257</sub> (1:4) tetramers, each conjugated to PE. For surface marker staining, a 20  $\mu$ l of a 3x mastermix containing the surface antibodies was added to each well without prior washing, followed by incubation for another 25 minutes on ice in the dark (60  $\mu$ l total volume). Cells were then washed twice with 200  $\mu$ l FACS buffer, transferred to a FACS tube in a 400  $\mu$ l volume of FACS buffer, and stored at 4°C until FACS analysis.

#### **4.2.17 Sorting and adoptive transfer of OT-I cells**

OT-I cells were purified from the spleens of naïve OT-I mice either for by flow cytometric sorting (BD Aria II) or by MACS cell separation using anti-FITC MicroBeads.

For flow cytometric sorting, splenic cell suspensions were stained in FACS buffer containing anti-CD8a-APC (1:200), anti-CD45.1-eFluor450 (1:100) and anti-CD44-FITC

(1:300) and sorted for the PI- CD44<sup>lo</sup> CD8<sup>+</sup> CD45.1<sup>+</sup> cell population, commonly resulting in a purity of approximately 98%.

For MACS cell separation, OT-I cells were sorted by negative depletion over an LS column. In short, splenic cell suspensions were stained in MACS buffer with FITC-labeled antibodies against MHC II (1:100), B220 (1:100), NK1.1 (1:100), CD4 (1:100) followed by magnetic labelling with anti-FITC Microbeads (according to manufacturer's instructions). Magnetically labeled cells were loaded on a LS column and the flow through (containing unlabeled OT-I cells) was collected. Purity of the magnetic cell separation was determined by FACS analysis after staining with anti-TCR V alpha 2-FITC (1:200), anti-CD45.2-PE (1:200), anti-CD45.1-eFluor450 (1:200) and anti-CD8a-APC (1:200) antibodies and was commonly between 90-95%, with a less than 5% fraction of cells with CD44<sup>hi</sup> phenotype.

For adoptive transfer of OT-I cells, sorted cells were thoroughly washed in sterile PBS, adjusted to a cell density of 250,000 cells per ml and 50,000 cells were into the tail vein of each recipient mouse.

## 5 Results

### 5.1 MVA skin inoculation by tattooing

Recent data have shown that after clearance of localized infection, certain non-lymphoid tissues (including the skin, the mucosae of the gut, lung or the female reproductive tract) retain a population of pathogen-specific memory CD8<sup>+</sup> T cells that remain permanently resident within the tissue and form a critical first line of defense against local reinfection (Cuburu et al., 2012; Gebhardt et al., 2009; Hofmann & Pircher, 2011; Jiang et al., 2012; Shin & Iwasaki, 2012; Wakim et al., 2013; Wakim et al., 2010).

One of the primary aims of this thesis was to assess whether such tissue-resident memory (TRM) CD8<sup>+</sup> T cells could also be established after a local, non-replicating skin infection with the viral vector MVA. To induce an acute local MVA skin infection, MVA was inoculated into the skin via tattooing.

The rationale for using tattooing for the skin delivery of MVA was that i) it resembles the traditional skin scarification route used for smallpox vaccination, in that it introduces the virus into the upper skin layer by multiple needle punctures and ii) that it additionally allows for an easy and controlled application of MVA over a larger skin surface area (Fig. 1), which should increase the local infection rate with this non-replicating vector and thus enhance its immunogenicity.

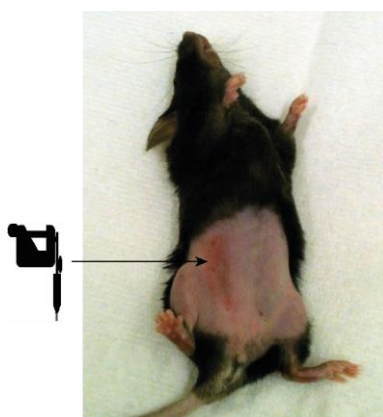


**Figure 1: Abdominal skin shortly after MVA tattooing.**

In order to visualize the localization of infection upon tattoo delivery of MVA, mice were tattooed for 20 s on abdominal skin (spanning an area of approximately 2 cm<sup>2</sup>) with 1x10<sup>8</sup> IU recombinant MVA that expresses  $\beta$ -galactosidase under control of the early PK1L

promoter (MVA-lacZ) (Fig. 2). Frozen cross-sections of MVA-lacZ-tattooed skin and untreated contralateral control skin were prepared 8 hours later and stained with X-Gal (5-bromo-4-chloro-3-indolyl- $\beta$ -D-galactopyranoside) substrate reagent. Upon X-Gal staining, MVA-lacZ-infected cells will turn blue due to the  $\beta$ -galactosidase-mediated hydrolysis of X-Gal, which yields a water-insoluble blue precipitate. The assay revealed that MVA-lacZ-infected cells were dispersed throughout the entire inoculated skin area and were primarily located within the epidermis or in close proximity to dermal-epidermal junction (Fig. 2).

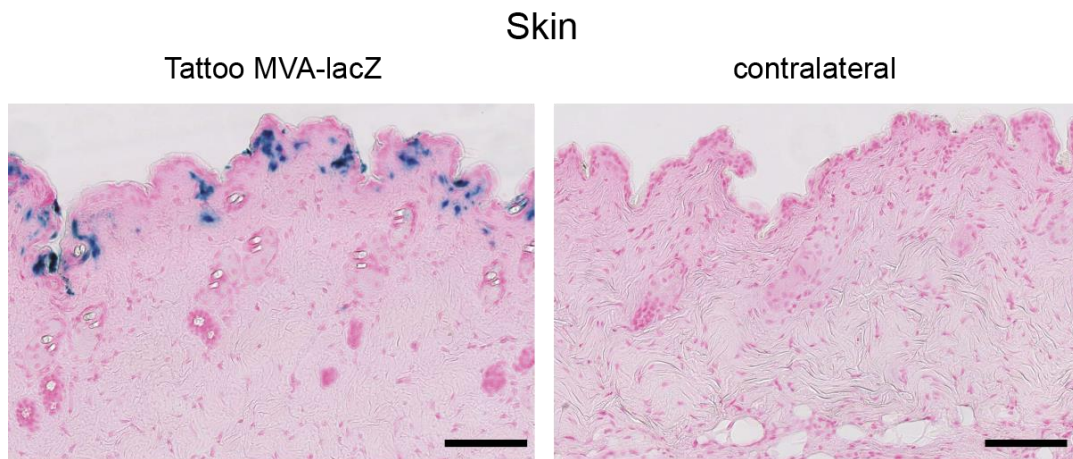


**Figure 2: MVA tattooing largely restricts viral antigen expression to the epidermis.**

Representative X-Gal staining of MVA-lacZ-tattooed ( $1 \times 10^8$  IU) and uninfected contralateral abdominal skin 8 hours post infection. Skin cryo sections were counterstained with nuclear fast red. 20x magnification. Scale bars: 100  $\mu$ m. Data are representative of at least 3 independent experiments.

In contrast, MVA-lacZ-infected cells were not observed in abdominal skin contralateral to the tattoo inoculation site (Fig. 2), indicating that MVA-derived recombinant gene expression following local skin tattooing remains confined to the primary site of virus delivery.

The results shown in Fig. 2 are consistent with existing data from our lab, which showed that MVA-encoded recombinant antigen expression, as determined by *in vivo* imaging of luciferase activity upon tattooing with a luciferase-expressing MVA (MVA-Luc; PK1L promoter), remains largely concentrated to the initial tattoo inoculation site (Fig. 3a).

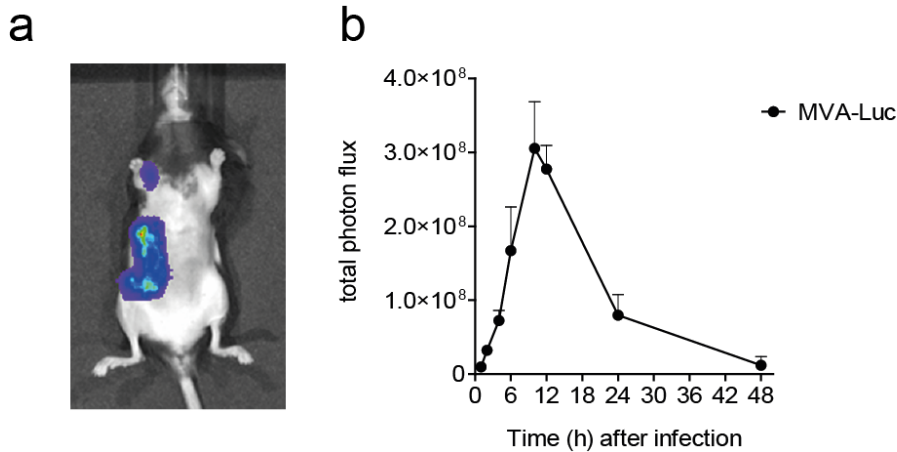


**Figure 3: *In vivo* imaging of luciferase activity following cutaneous infection with MVA-Luc.**

(a) Representative image taken 6 hours after tattooing with MVA-Luc ( $1 \times 10^8$  IU). (b) Time course of luciferase activity in MVA-Luc-tattooed abdominal skin ( $n=2$ ). Error bars represent SEM.

*In vivo* imaging of MVA-Luc-tattooed mice further indicated that luciferase activity in the skin was highest at around 10-12 hours post infection and thereafter rapidly decreased (Fig. 3b), suggesting that MVA-driven recombinant protein synthesis in the skin is limited to a relatively short time frame after tattoo application, which is in line with the inability of MVA to undergo productive replication in mammalian cells (Sutter & Moss, 1992).

In summary, these data show that MVA tattooing induces a highly localized and transient infection of the skin, during which viral antigen is mainly expressed within cells of epidermal origin.

## 5.2 Viral tattooing induces CD8<sup>+</sup> T cell responses of similar quality and magnitude as the conventional intramuscular route

Next, it was asked whether a skin tattoo with MVA is capable of priming a systemic antiviral CD8<sup>+</sup> T cell response. To this end, mice were infected by tattooing the right abdominal skin with  $2 \times 10^6$  IU MVA expressing the model antigen ovalbumin (OVA) under the control of the vaccinia viral early/late promoter PH5 (MVA-OVA). For comparison, a second group of mice received the same dose of MVA-OVA by intramuscular (i.m.) route, which currently represents one of the standard routes for the delivery of MVA vectors in clinical trials (Romani et al., 2012a). Seven days post infection, splenocytes of immunized mice were harvested and analyzed for the presence of MVA- and OVA-specific CD8<sup>+</sup> T cells using intracellular cytokine staining (ICS) after short-term *ex vivo* re-stimulation with K<sup>b</sup>-restricted peptides derived from the vector

backbone (B8R<sub>20</sub>, A3L<sub>270</sub>), the recombinant antigen OVA (OVA<sub>257</sub>) or an irrelevant control peptide derived from  $\beta$ -galactosidase ( $\beta$ Gal<sub>96</sub>). The ICS analysis showed that both routes of MVA inoculation elicited robust vector- and recombinant OVA-specific CD8<sup>+</sup> T cell responses, with roughly similar frequencies and total numbers of antigen-specific CD8<sup>+</sup> T cells producing the effector cytokine IFN- $\gamma$  (Fig. 4a, b).

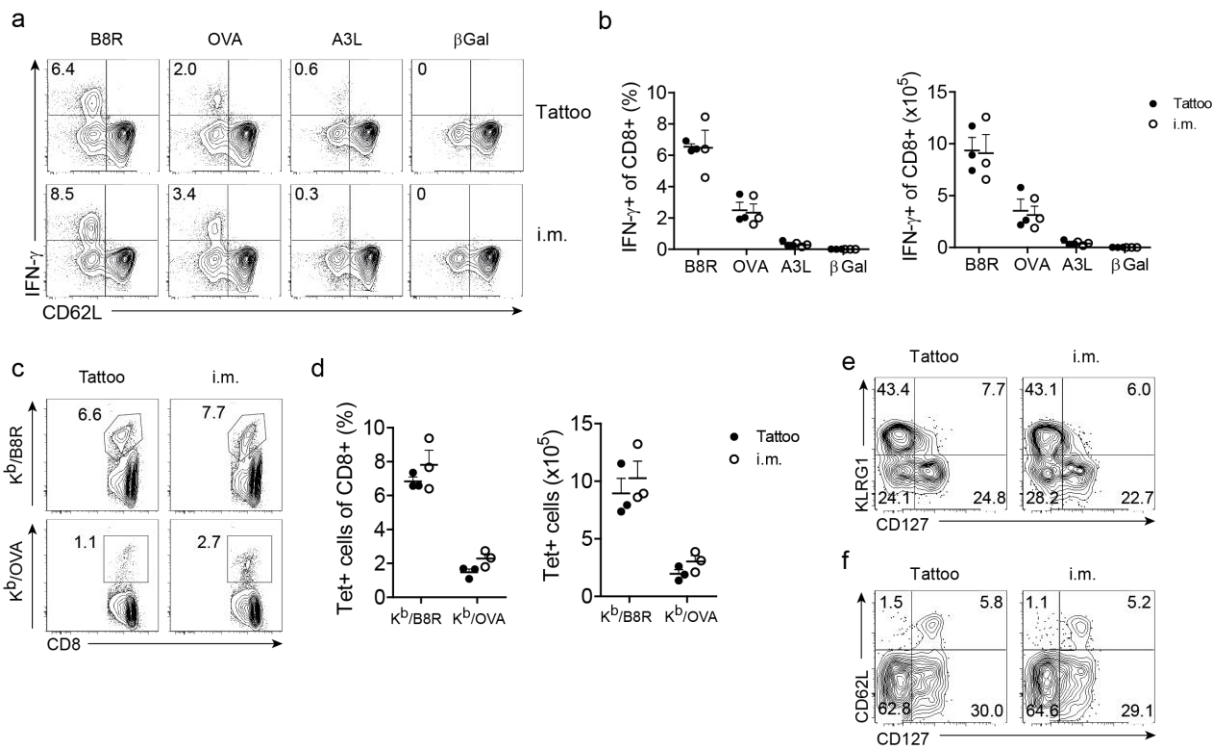


**Figure 4: CD8<sup>+</sup> T cell response in the spleen 7 days after MVA-OVA immunization by tattooing or intramuscular (i.m.) injection.**

(a) Representative plots showing IFN- $\gamma$  producing (IFN- $\gamma$ <sup>+</sup>) splenic CD8<sup>+</sup> T cells after short-term *ex vivo* re-stimulation with the indicated peptides, as determined by intracellular cytokine staining (ICS). (b) Frequency (left panel) and absolute numbers (right panel) of IFN- $\gamma$ <sup>+</sup> CD8<sup>+</sup> T cells in the spleen. (c) Representative plots showing the percentage of B8R- and OVA-specific CD8<sup>+</sup> T cells in the spleen, as determined by K<sup>b</sup>/B8R and K<sup>b</sup>/OVA tetramer staining. (d) Percentage (left panel) and total number (right panel) of splenic B8R- and OVA-specific CD8<sup>+</sup> T cells. (e) Expression of CD127 and KLRG1 or (f) CD127 and CD62L on B8R-specific CD8<sup>+</sup> T cells. Numbers in plots indicate the percentages among all events shown. Dots in graphs represent individual mice. Horizontal bars indicate the mean and error bars represent SEM (n=3).

In line with published studies (Kastenmuller et al., 2007; Kastenmuller et al., 2009; Tschärke et al., 2005), the CD8<sup>+</sup> T cell response elicited by either route was dominated by CD8<sup>+</sup> T cells recognizing the early MVA-derived epitope B8R<sub>20</sub> (Fig. 4a, b). Similar results were obtained after surface staining of splenocytes with peptide/MHC class I (K<sup>b</sup>) tetramers (K<sup>b</sup>/B8R, K<sup>b</sup>/OVA) without prior *ex vivo* peptide re-stimulation (Fig. 4c, d). Tetramer staining further allowed for an analysis of the differentiation profile of antigen-specific effector CD8<sup>+</sup> T cells, which may provide early information about the memory potential within the responding CD8<sup>+</sup> T cell population. For instance, those effector CD8<sup>+</sup>

T cells that express CD127 (IL-7 $\alpha$ ) but lack expression of the killer cell lectin-like receptor G1 (KLRG1) represent a subpopulation of effector cells which more likely survive contraction and become long-lived memory CD8<sup>+</sup> T cells and have therefore been defined as memory precursor effector cells (MPECs). In contrast, effector CD8<sup>+</sup> T cells that lack CD127 but express KLRG1 have been designated as short-lived effector cells (SLECs) and are destined to undergo apoptosis after antigen clearance (Joshi et al., 2007; Kaech et al., 2003). Notably, recent data have suggested that the precursors of TRM cells are found among early effector CD8<sup>+</sup> T cells which lack KLRG1 (Mackay et al., 2013). A similar distinction of effector CD8<sup>+</sup> T cell subpopulations can be made on the basis of expression of CD62L (L-selectin) and CD127, which allows for a categorization into CD62L<sup>hi</sup> CD127<sup>hi</sup> central memory (TCM) T cell precursors, CD62L<sup>lo</sup> CD127<sup>hi</sup> effector memory (TEM) T cell precursors or CD62L<sup>lo</sup> CD127<sup>lo</sup> terminally differentiated effector T cells (Huster et al., 2004; Obar & Lefrancois, 2010).

As illustrated in Figs. 4e and 4f, similar relative fractions of each of the described effector subpopulations were found within the K<sup>b</sup>/B8R tetramer<sup>+</sup> pool of effector CD8<sup>+</sup> T cells after MVA tattooing and i.m. MVA injection (Fig. 4e, f).

Combined, these data demonstrate that MVA immunization by tattooing is able to generate a robust primary recombinant antigen- and vector-specific CD8<sup>+</sup> T cell response that is comparable in both magnitude and quality to the one elicited after immunization by the i.m. route of MVA infection.



### 5.3 MVA tattooing confers protective immunity against infection with replication-competent VV

To determine whether a local MVA tattoo would confer protective immunity in the memory phase, MVA-tattooed mice were challenged intranasally with a lethal dose ( $1 \times 10^6$  PFU) of the replication-competent vaccinia virus strain Western Reserve (VV-WR) on day 50 post primary immunization.

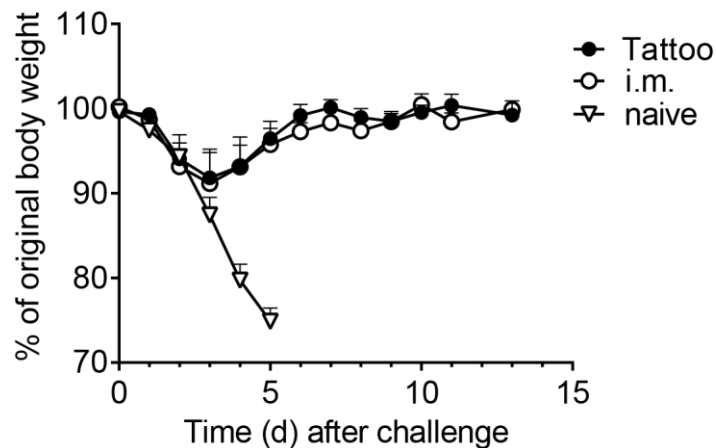


**Figure 5: MVA tattooing is comparable to the i.m. MVA immunization route in providing protective immunity against lethal respiratory VV infection.**

Mice were immunized with wild-type MVA ( $1 \times 10^8$  IU) by either tattooing or i.m. injection and challenged intranasally with a lethal dose of vaccinia virus Western Reserve (VV-WR;  $1 \times 10^6$  PFU) 50 days later. Shown is the percentage of original body weight of immunized and non-immunized (naïve) animals following VV-WR challenge. Data are representative of 3 independent experiments with 4 mice per group ( $n=4$ ). Dots show the mean of each group and error bars represent SEM.

The respiratory VV-WR challenge infection induced progressive weight loss in non-immunized (naïve) animals that was accompanied by typical signs of disease (ruffled fur, lack of activity and movement) and these mice rapidly succumbed to the infection (Fig. 5). In contrast, mice that had been immunized with MVA by tattooing or i.m. injection showed markedly reduced clinical signs of disease and lost only around 10% of their original body weight (by day 3 post challenge), which they fully regained one week post challenge (Fig. 5). The data demonstrate that a local skin application of MVA provides long-lasting protective immunity against secondary respiratory VV infection, which is as robust as that induced upon MVA immunization by i.m. injection.

## 5.4 MVA tattooing promotes effector CD8<sup>+</sup> T cell recruitment to the skin

Next, it was analyzed whether the localized MVA skin infection would promote a recruitment of circulating antigen-specific effector CD8<sup>+</sup> T cells to the tissue. In order to track virus-specific CD8<sup>+</sup> T cells *in vivo*, 50,000 naïve CD45.1<sup>+</sup> CD8<sup>+</sup> OT-I cells (expressing a transgenic T cell receptor (TCR) specific for the OVA-derived H-2K<sup>b</sup>-restricted epitope OVA<sub>257</sub>) were adoptively transferred into C57BL/6 recipient mice (CD45.2), which one day later received an MVA-OVA tattoo on the right abdominal skin. One week after tattooing, spleens of immunized animals as well as right (MVA-OVA-infected) and left (untreated) abdominal skin were isolated and subsequently analyzed by flow cytometry (Fig. 6a). Prior to excision of skin, mice were perfused with PBS through the heart ventricle to minimize contamination of the skin cell preparations with OT-I cells from the blood circulation. MVA-OVA tattooing induced a robust expansion of the adoptively transferred OT-I cells, which on average constituted about 5% of the total CD8<sup>+</sup> T cell population in the spleen (Fig. 6b, c). FACS analysis of skin tissue showed that OT-I cells also readily infiltrated MVA-OVA-infected skin, as demonstrated by a pronounced local increase in OT-I cell numbers and frequency when compared to uninfected contralateral skin (Fig. 6c, d).

To determine the localization of effector OT-I cells in virus-infected skin, frozen sections of abdominal skin tissue of MVA-OVA-tattooed mice were analyzed on day 7 post tattooing by immunohistochemical (IHC) staining of the OT-I congenic marker CD45.1.

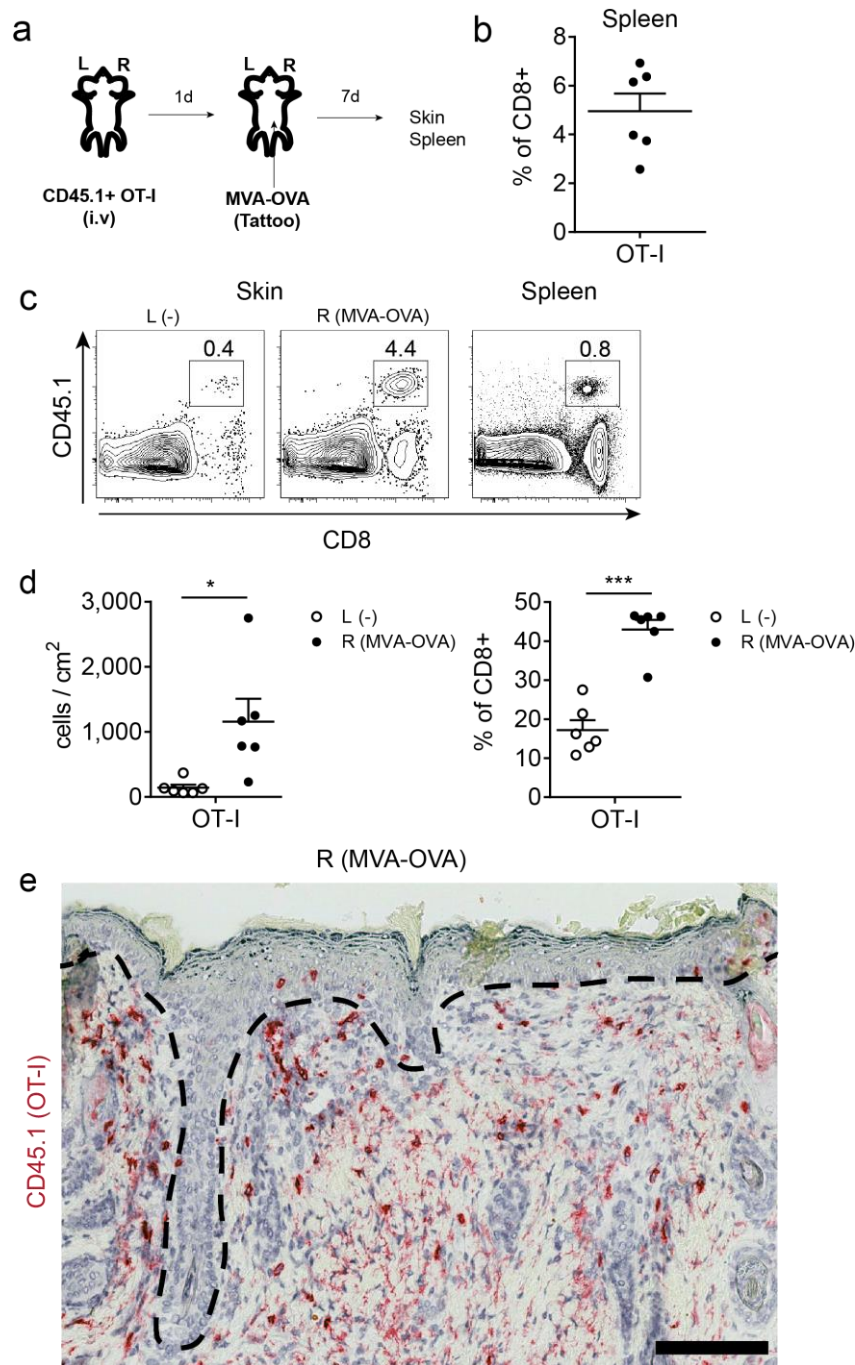


**Figure 6: Virus-specific effector CD8<sup>+</sup> T cells accumulate in MVA-tattooed skin.**

(a) Mice were adoptively transferred (i.v.) with 50,000 naïve CD45.1<sup>+</sup> OT-I cells and one day later tattooed with  $2 \times 10^6$  IU MVA-OVA on right (R) abdominal skin. On day 7 post infection, OT-I cells were identified in MVA-OVA-infected right (R) and uninfected left (L) abdominal skin and the spleen by flow cytometry. (b) Frequency of OT-I cells in the total CD8<sup>+</sup> T cell population in the spleen. (c) Representative plots showing the percentage of OT-I cells in the CD45<sup>+</sup> leukocyte population in uninfected left (L) and MVA-OVA-infected right (R) abdominal skin and the spleen. (d) Absolute number (per cm<sup>2</sup> skin; left panel) and frequency of OT-I cells (in the skin CD8<sup>+</sup> T cell population; right panel) in MVA-OVA-infected right (R) and uninfected left (L) abdominal skin. (e) Localization of OT-I cells in MVA-OVA-infected skin 7 days after tattooing, as determined by IHC staining of the congenic marker CD45.1 (red). 20x magnification; Scale bar 100  $\mu$ m. Dotted line indicates the border between epidermis and dermis. Dots in graphs represent individual mice. Horizontal bars indicate the mean and error bars represent SEM. Data are pooled from 2 independent experiments (n=6). Statistical analysis (paired Student's *t*-test), \*  $P < 0.05$ , \*\*\*  $P < 0.001$

The staining revealed that at this early time point post infection, effector OT-I cells mainly populated the dermis of MVA-OVA-infected skin, but seemed to accumulate near the dermal-epidermal junction (Fig. 6e). Few effector OT-I cells were also observed within the epidermal layer (Fig. 6e). Note that the epidermis appeared quite enlarged at this stage of the immune response (Fig. 6e), which could be due to a local hyperproliferation of keratinocytes in response to the mechanical skin injury or a local expression of the MVA-encoded epidermal growth factor homologue VGF (vaccinia virus growth factor) (Tscharke & Smith, 1999).

In summary, these data show that the acute viral skin infection generated upon MVA tattooing provides a potent signal for the acute recruitment of effector CD8<sup>+</sup> T cells from the circulation, and thus promotes a strong local accumulation of virus-specific CD8<sup>+</sup> T cells in the initial virus application site.

## 5.5 Virus-specific CD8<sup>+</sup> T cells persist in MVA-tattooed skin

To investigate whether OT-I cells that had been attracted to MVA-OVA-infected skin during the acute phase of the response were able to form a skin-resident population of memory T cells, mice that had received transfer of 50,000 naïve OT-I cells were again tattooed with MVA-OVA on right abdominal skin and analyzed during the memory phase of the response (40 days after infection) (Fig. 7a). At this time point, memory OT-I cells were still detectable in the spleens of immunized mice (Fig. 7b, c), albeit at a considerably lower frequency than during the acute phase on day 7. Analysis of skin tissue revealed that previously MVA-OVA-tattooed abdominal skin was significantly enriched with memory OT-I cells (with an average of 140 cells per cm<sup>2</sup> skin) when compared to skin from the contralateral abdominal skin region, from which only very few memory OT-I cells could be isolated (around 25 cells per cm<sup>2</sup>) (Fig. 7c, d). Low amounts of memory OT-I cells were also detected in more distant skin locations, such as the ear (around 6 cells per ear) (Fig. 7c, e). The strong enrichment of memory OT-I cells in previously MVA-OVA-tattooed skin was further indicated by a substantially higher local frequency of OT-I cells compared to contralateral skin and distant ear skin (around 40% of the total cutaneous CD8<sup>+</sup> T cell population versus around 20% and 10%, respectively) (Fig. 7d, e).

Together, these data demonstrate that the acute skin infection with MVA is able to support the development of skin-resident memory CD8<sup>+</sup> T cells, but also indicate that the

lodgment of these memory T cells to the skin is highly restricted to previously virus-infected skin region.

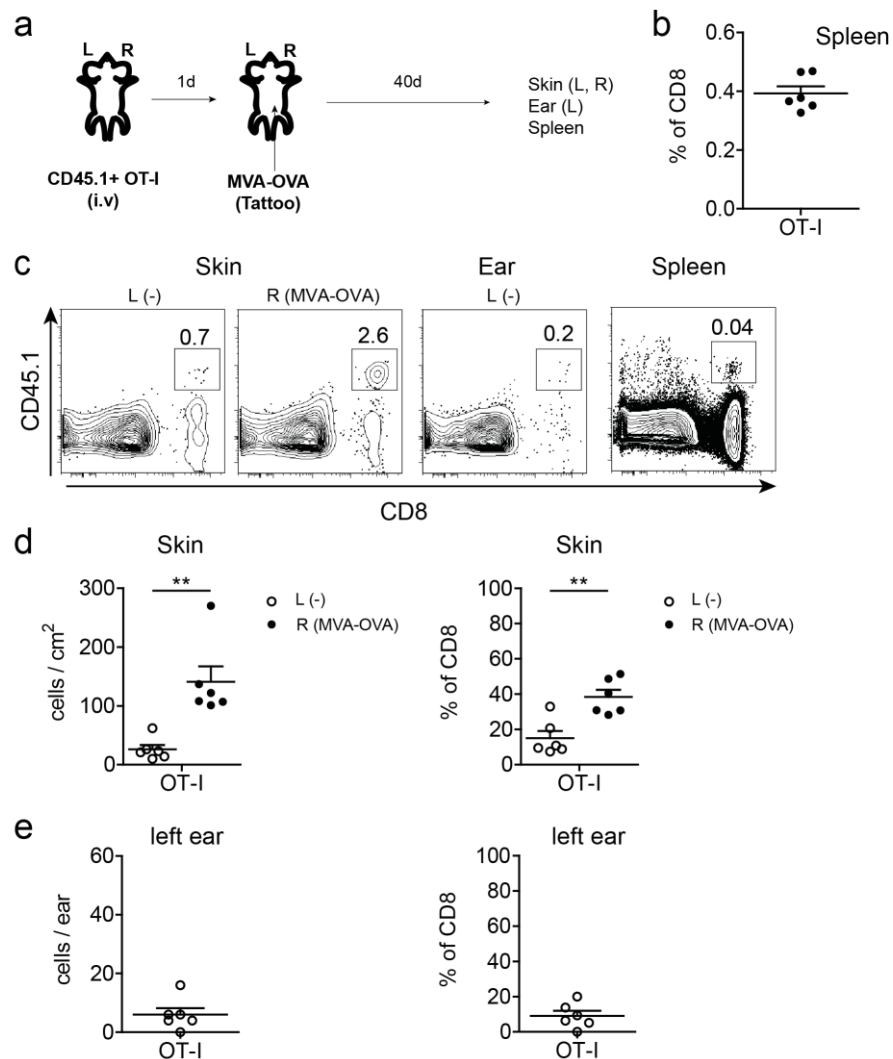


**Figure 7: Virus-specific CD8<sup>+</sup> T cells persist in previously MVA-tattooed skin.**

(a) Mice were adoptively transferred (i.v.) with 50,000 naïve CD45.1<sup>+</sup> OT-I cells and one day later tattooed with  $2 \times 10^6$  IU MVA-OVA on right (R) abdominal skin. On day 40 post infection, OT-I cells were identified in MVA-OVA-infected right (R) and uninfected left (L) abdominal skin, the left (L) ear and the spleen by flow cytometry. (b) Frequency of OT-I cells in the total CD8<sup>+</sup> T cell population in the spleen. (c) Representative plots showing the percentage of OT-I cells in the CD45<sup>+</sup> leukocyte population in MVA-OVA-infected right (R) and uninfected left (L) abdominal skin, the left (L) ear and the spleen. (d) Absolute number (per cm<sup>2</sup> skin; left panel) and frequency of OT-I cells (in the skin CD8<sup>+</sup> T cell population; right panel) in MVA-OVA-infected right (R) and uninfected left (L) abdominal skin. (e) Absolute number (per ear; left panel) and frequency of OT-I cells (in the skin CD8<sup>+</sup> T cell population; right panel) in the skin of the left ear. Dots in graphs represent individual mice. Horizontal bars indicate the mean and error bars represent SEM. Data are derived from 1 experiment with 6 mice (n=6). Statistical analysis (paired Student's *t*-test), \*\*  $P < 0.01$

In order to confirm the above findings and to address whether virus-specific memory CD8<sup>+</sup> T cells which accumulated at the site of prior MVA tattooing would be maintained long-term in the skin, the above experiment was repeated and mice were analyzed during the late memory phase (more than 100 days after tattooing). Additionally, in order to test the capacity of a non-cutaneous MVA delivery route to generate TRM cells in the skin,

OT-I-infused mice which had been immunized with MVA-OVA by i.m. injection into the right hind leg were analyzed in parallel (Fig. 8a).

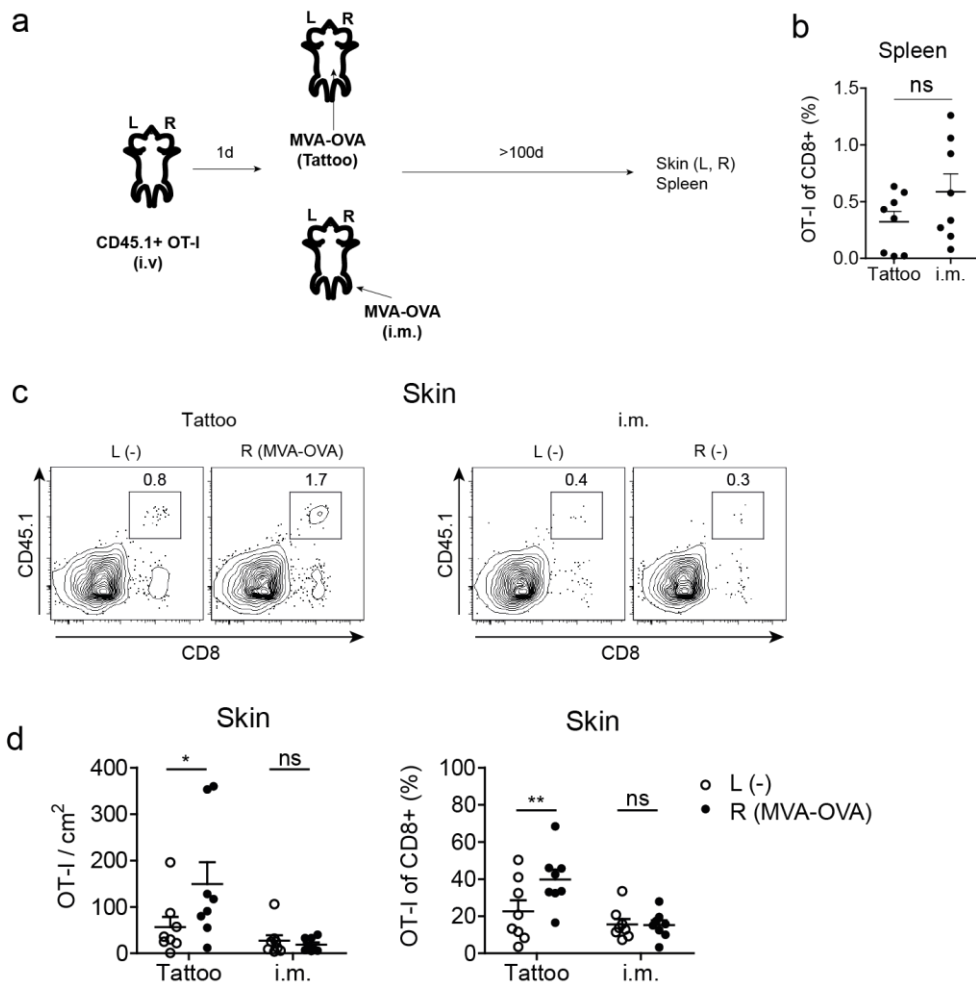


**Figure 8: Virus-specific CD8<sup>+</sup> T cells persist long-term in previously MVA-tattooed skin.**

(a) Mice were adoptively transferred (i.v.) with 50,000 naïve CD45.1<sup>+</sup> OT-I cells and one day later immunized with  $2 \times 10^6$  IU MVA-OVA by tattooing the right (R) abdominal skin or by i.m. injection into the right (R) anterior tibial muscle. In the late memory phase (between day 130 – 200 post infection), OT-I cells were identified in right (R) and left (L) abdominal skin as well as the spleen of immunized mice by flow cytometry. (b) Comparison of the frequency of OT-I cells in the total CD8<sup>+</sup> T cell population in the spleen between MVA-OVA-tattooed and i.m. MVA-OVA-injected mice. (c) Representative plots showing the percentage of OT-I cells in the CD45<sup>+</sup> leukocyte population in right (R) and left (L) abdominal skin of MVA-OVA-tattooed and i.m. MVA-OVA-injected mice. (d) Absolute number (per cm<sup>2</sup> skin; left panel) and frequency of OT-I cells (in the skin CD8<sup>+</sup> T cell population; right panel) in right (R) and left (L) abdominal skin. Dots in graphs represent individual mice. Horizontal bars indicate the mean and error bars represent SEM. Data are pooled from 5 independent experiments with 1-2 mice per group and time point. (n=8). Statistical analysis (in b, unpaired Student's *t*-test; in d; paired Student's *t*-test), ns, not significant. \*  $P < 0.05$ , \*\*  $P < 0.01$

Analysis of the systemic memory T cell compartment in the spleen showed that the two immunized groups had roughly comparable frequencies of OT-I cells during this late phase of memory (Fig. 8b). Notably, the frequency of OT-I cells in the spleens of MVA-OVA-tattooed mice was similar to that detected 40 days after MVA-OVA tattooing (Fig. 8b, Fig.

7b), indicating that the established pool of systemic memory OT-I cells was maintained at a stable level between the early (d40) and late (>d100) memory stage.

Consistent with the results obtained from the previous experiment, analysis of the skin tissue of MVA-OVA-tattooed mice revealed a significant enrichment of memory OT-I cells (in both frequency and absolute number) in previously MVA-OVA-inoculated skin as compared to untreated contralateral skin (Fig. 8c, d). Interestingly, the total amount of memory OT-I cells residing in the prior MVA-OVA inoculation site was roughly comparable between the late and early memory phase (Fig. 8d, Fig. 7d), suggesting that the local pool of skin TRM cells is indeed long-lived and maintained within the tissue at a constant level even well after clearance of the non-replicating virus infection. Notably, memory OT-I cells remained detectable in MVA-OVA-infected skin even as late as 1 year after tattooing (data not shown), suggesting that these skin TRM cells may even persist locally throughout the whole lifespan of an immunized mouse.

In contrast to MVA-OVA-tattooed mice, mice that had received an i.m. MVA-OVA immunization harbored only very low numbers (as well as frequencies) of memory OT-I cells in either of the two analyzed abdominal skin regions (Fig. 8c, d). The total number of skin-resident OT-I cells in i.m. immunized mice was found to be even lower than that detected in contralateral skin of MVA-OVA-tattooed animals (Fig. 8c, d), although the slightly higher numbers found in this site may be due to a minor contamination with OT-I TRM cells from the tattoo inoculation site. The data obtained from i.m. immunized mice however, suggest that this non-cutaneous route of MVA delivery may not be suitable for an efficient generation of TRM cells in the skin.

To further validate these findings, it was next investigated whether skin TRM cells could also be induced by an MVA-OVA tattoo in a different skin location. For this, mice were again adoptively transferred with OT-I cells and one day later tattooed with  $2 \times 10^6$  IU MVA-OVA on the dorsal skin of the right ear. In analogy to the experiment shown in Fig. 8, mice immunized with MVA-OVA by the i.m. route were analyzed in parallel (Fig. 9a). Due to the smaller surface area of the ear, virus was applied in a 5  $\mu$ l-volume, compared to the 10  $\mu$ l-volume used for tattooing on abdominal skin.

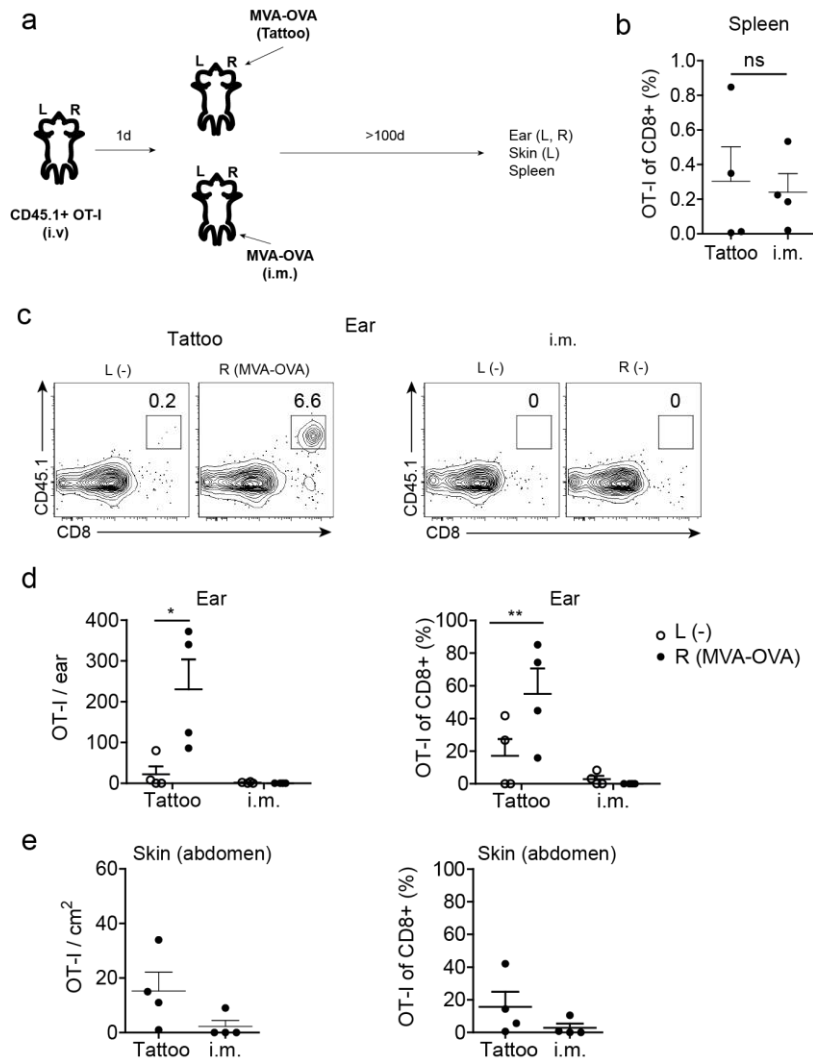


**Figure 9: Virus-specific CD8+ T cells persist long-term in previously MVA-tattooed ears.**

(a) Mice were adoptively transferred (i.v.) with 50,000 naïve CD45.1+ OT-I cells and one day later immunized with  $2 \times 10^6$  IU MVA-OVA by tattooing the right (R) dorsal ear pinna or by i.m. injection into the right (R) anterior tibial muscle. In the late memory phase (more than 100 day post infection), OT-I cells were identified in right (R) and left (L) ears, left (L) abdominal skin as well as the spleen of immunized mice by flow cytometry. (b) Comparison of the frequency of OT-I cells in the total CD8+ T cell population in the spleen between MVA-OVA-tattooed and i.m. MVA-OVA-injected mice. (c) Representative plots showing the percentage of OT-I cells in the CD45+ leukocyte population in right (R) and left (L) ears of MVA-OVA-tattooed and i.m. MVA-OVA-immunized mice. (d) Absolute number (per ear; left panel) and frequency of OT-I cells (in the skin CD8+ T cell population; right panel) in right (R) and left (L) ears. (e) Absolute number (per  $\text{cm}^2$  skin; left panel) and frequency of OT-I cells (in the skin CD8+ T cell population; right panel) in left (L) abdominal skin. Dots in graphs represent individual mice. Horizontal bars indicate the mean and error bars represent SEM. Data are derived from 1 experiment with 4 mice per group ( $n=4$ ). Statistical analysis (in **b**, unpaired Student's *t*-test; in **d**; paired Student's *t*-test), ns, not significant. \*  $P < 0.05$ , \*\*  $P < 0.01$

In line with the previous data, analysis of the splenic memory T cell compartment more than 100 days post infection revealed no difference in the frequencies of OT-I cells between MVA-OVA-tattooed and i.m. MVA-OVA-injected animals (Fig. 9b). During this late memory phase, memory OT-I cells were again found to be highly enriched in MVA-OVA-tattooed ears when compared to untreated contralateral ears (Fig. 9c, d) or distant abdominal skin (Fig. 9e). These data are consistent with the results obtained after MVA-OVA tattooing on abdominal skin and confirm that MVA tattooing also leads to the



establishment of TRM cells in the ear. The data further confirm the previous finding that upon MVA tattooing TRM cells are most efficiently generated at the site of prior MVA skin infection. As expected, in i.m. MVA-OVA-immunized mice hardly any memory OT-I cells could be recovered from ear skin (Fig. 9c, d) or abdominal skin (Fig. 9e), recapitulating the finding that i.m. virus delivery does not promote an appreciable formation of TRM cells in the skin.

## **5.6 Virus-specific memory CD8<sup>+</sup> T cells generated in MVA-tattooed skin predominantly reside within the epidermis and express markers of tissue residence**

Multiple studies have shown that skin TRM cells typically take up residence within the skin epithelium (Ariotti et al., 2012; Gebhardt et al., 2009; Gebhardt et al., 2011; Jiang et al., 2012; Zaid et al., 2014). It has been suggested that their persistence within this anatomical niche is - at least in part - mediated by the integrin  $\alpha$ E subunit CD103, which is expressed at high levels on skin TRM cells (but also on TRM cells in other tissues). CD103 is known to interact with E-cadherin (Cepek et al., 1993; Cepek et al., 1994), a cell adhesion molecule expressed by most epithelial cells (including keratinocytes) and it is believed that skin TRM cells might use this molecule to anchor to the epidermal layer (Gebhardt & Mackay, 2012). In murine epidermis, CD103 is also highly expressed on dendritic epidermal T cells (DETCs), a subpopulation of epidermis-resident  $\gamma\delta$  T cells and it has been shown that this subset is dramatically diminished in CD103<sup>-/-</sup> mice (Schon et al., 2002), highlighting the importance of this molecule for the maintenance of lymphocytes within the epidermal niche.

In order to determine the localization of virus-specific TRM cells in previously MVA-infected skin, MVA-OVA-tattooed abdominal skin tissue of OT-I recipient mice was analyzed during the late memory phase (200 days after tattooing) by IHC staining of the OT-I congenic marker CD45.1.

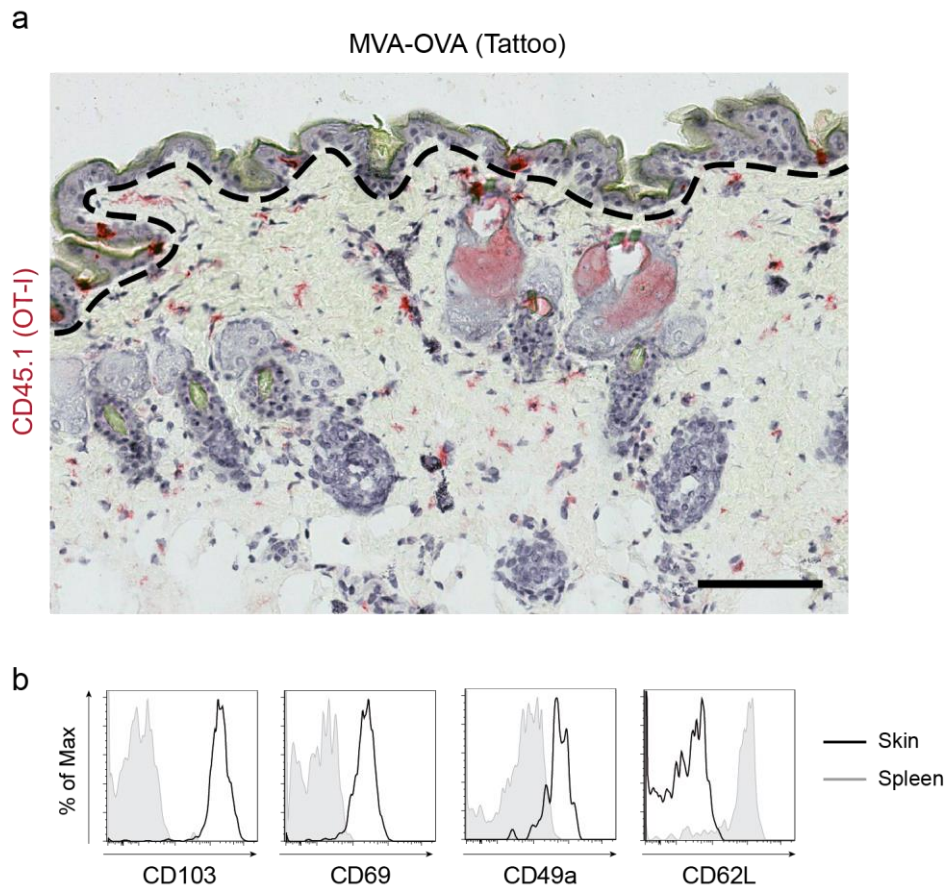


**Figure 10: Virus-specific memory CD8<sup>+</sup> T cells preferentially lodge to the epidermis of MVA-tattooed skin and exhibit a TRM phenotype.**

(a) Localization of OT-I cells in previously MVA-OVA-tattooed abdominal skin 200 days after infection, as determined by IHC staining of the congenic marker CD45.1 (red). 20x magnification; Scale bar, 100  $\mu$ m. Dotted line indicates the border between epidermis and dermis. (b) Expression of CD103, CD69, CD49a and CD62L on OT-I cells isolated from MVA-OVA-tattooed abdominal skin (black histograms) and the spleen (grey shaded histograms) 200 days after tattooing. Data are representative of more than 3 independent experiments.

The analysis revealed that the vast majority of CD45.1<sup>+</sup> OT-I cells retained in previously MVA-OVA-infected skin indeed resided within the epidermis, but were only scarcely found in the underlying dermal compartment (Fig. 10a). The specificity of the IHC staining of OT-I was further confirmed by double staining using antibodies to both CD8 and CD45.1, which clearly suggested a co-localization of these two markers on cells within the epidermis (data not shown). Consistent with the preferential lodgment of OT-I cells to the epithelium of previously MVA-OVA-infected skin, flow cytometric analysis showed that majority of skin-derived OT-I cells expressed high levels of CD103, in contrast to their counterparts in lymphoid organs (Fig. 10b). Unlike memory OT-I cells from lymphoid tissue, which at this time point consisted mostly of CD62L<sup>+</sup> central memory T cells (TCM) cells, memory OT-I cells isolated from MVA-OVA-tattooed skin were uniformly CD62L<sup>-</sup> and displayed higher levels of the TRM-associated surface receptors CD69 and CD49a (integrin subunit  $\alpha$ 1; VLA-1) (Fig. 10b).

Note that the few OT-I cells found in skin contralateral to the site of the prior MVA-OVA tattoo inoculation or in skin of i.m. MVA-OVA-immunized mice were phenotypically indistinguishable from those found in MVA-OVA-tattooed skin (data not shown). Taken together, these data indicate that memory OT-I cells, which persist at the site of prior MVA skin infection, are phenotypically distinct from their circulating memory CD8<sup>+</sup> T cell counterparts, exhibit a similar phenotypic profile as skin TRM cells described in other models (including skin infections with replicating viruses, such as HSV-1 and VV) (Gebhardt et al., 2009; Jiang et al., 2012), and preferentially lodge to the skin epithelium. Because of these characteristics, it can be concluded that antiviral memory CD8<sup>+</sup> T cells established in the skin upon acute MVA skin infection represent bona fide skin TRM cells.

### **5.7 Formation of endogenous virus-specific TRM cells**

A recent study has pointed out that adoptive transfer of unphysiologically high numbers of monoclonal high-avidity TCR expressing T cells in infection or immunization studies may not accurately model the endogenous response of lower affinity polyclonal T cells in terms of kinetics, expansion, differentiation and efficiency of memory generation (Badovinac et al., 2007). Therefore, it was decided to study the local skin-resident memory CD8<sup>+</sup> T cell formation of endogenous virus-specific CD8<sup>+</sup> T cells without prior transfer of OT-I cells. To this end, mice were tattooed on dorsal skin of the right ear pinna with MVA-OVA ( $2 \times 10^6$  IU) and more than 70 days later, endogenous B8R-specific CD8<sup>+</sup> T cells, which in the absence of OT-I cells represent the immunodominant population of responding CD8<sup>+</sup> T cells, were analyzed in ear skin and spleen via staining with K<sup>b</sup>/B8R tetramers (Fig. 11a).

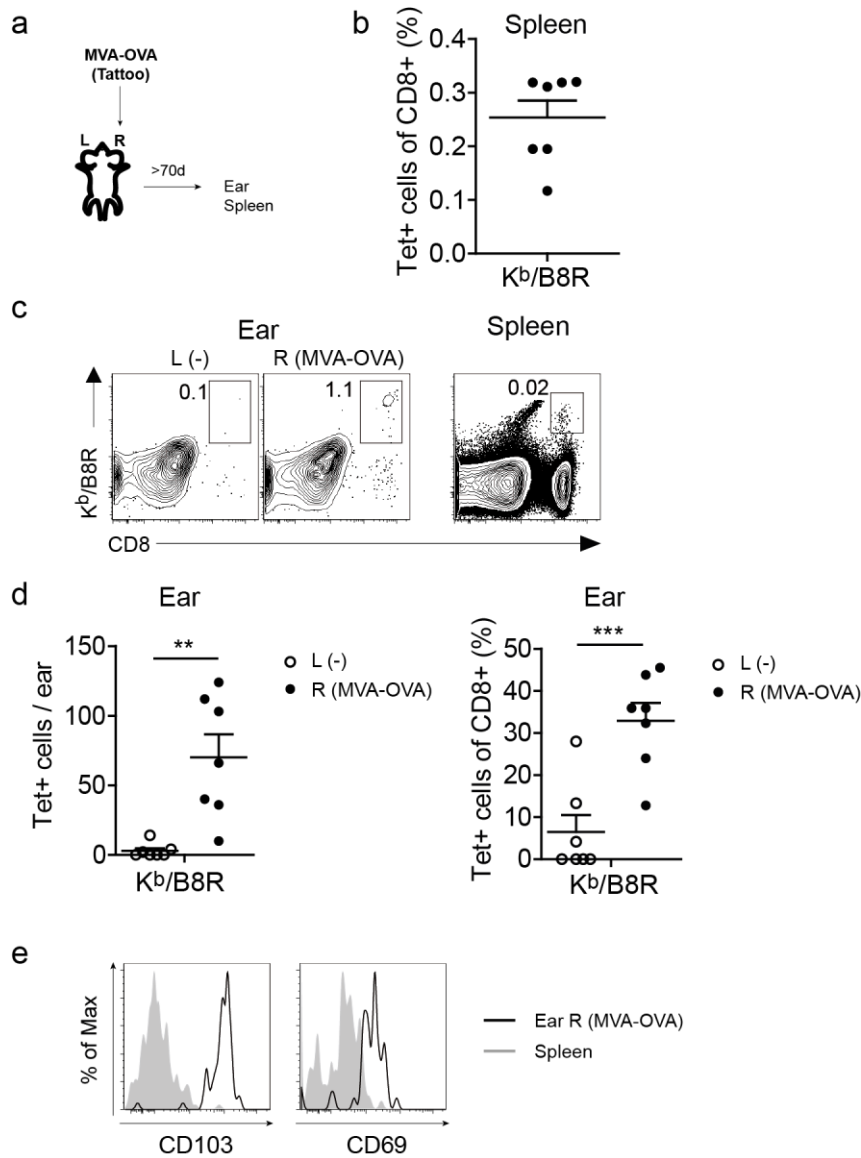


**Figure 11: MVA tattooing also induces formation of endogenous virus-specific TRM cells.**

(a) Mice were tattooed on the right (R) dorsal ear pinna with  $2 \times 10^6$  IU MVA-OVA and endogenous B8R-specific CD8<sup>+</sup> T cells were identified in right (R) and left (L) ears as well as the spleen between day 70 and day 120 post infection by K<sup>b</sup>/B8R tetramer staining. (b) Frequency of B8R-specific CD8<sup>+</sup> T cells in the total CD8<sup>+</sup> T cell population in the spleen. (c) Representative plots showing the percentage of B8R-specific CD8<sup>+</sup> T cells in the CD45<sup>+</sup> leukocyte population in right (R) and left (L) ears and the spleen. (d) Absolute number (per ear; left panel) and frequency of B8R-specific CD8<sup>+</sup> T cells (in the skin CD8<sup>+</sup> T cell population; right panel) in right (R) and left (L) ears. (e) Expression of CD103 and CD69 on B8R-specific CD8<sup>+</sup> T cells isolated from MVA-OVA-tattooed right (R) ears (black histograms) and the spleen (grey shaded histograms). Dots in graphs represent individual mice. Horizontal bars indicate the mean and error bars represent SEM. Data are pooled from 3 independent experiments with 2-3 mice per time point ( $n=7$ ). Statistical analysis (paired Student's *t*-test), \*\*  $P < 0.01$ , \*\*\*  $P < 0.001$

At this memory time point, spleens of MVA-OVA-tattooed mice still harbored a readily detectable population of B8R-specific memory CD8<sup>+</sup> T cells (Fig. 11b, c). Importantly, B8R-specific memory CD8<sup>+</sup> T cells were also found to be significantly enriched both in absolute and relative number in previously MVA-OVA-tattooed ears when compared to untreated ears (Fig. 11c, d). Phenotypic analysis of skin-derived B8R-specific memory CD8<sup>+</sup> T cells further revealed that these cells exhibited increased expression of the TRM

signature markers CD103 and CD69 (CD49a, not determined) in comparison to their counterparts in lymphoid tissue (Fig. 12e). Thus, these data demonstrate that a local pool of antiviral skin TRM cells can also be induced from the endogenous polyclonal repertoire of antigen-specific CD8<sup>+</sup> T cells, whose initial precursor frequency in a naive T cell pool is extremely low (Blattman et al., 2002; Haluszczak et al., 2009).

## **5.8 Skin TRM provide enhanced protection against a local VV reinfection**

Recent evidence suggests that TRM cells play a dominant role in the control of infections that originate within non-lymphoid tissues, presumably owing to their strategic positioning in immediate proximity to the site of pathogen entry (Ariotti et al., 2012; Gebhardt et al., 2009; Gebhardt et al., 2011; Hofmann & Pircher, 2011; Jiang et al., 2012; Mackay et al., 2012; Shin & Iwasaki, 2012). In contrast, circulating populations of memory CD8<sup>+</sup> T cells (including TCM and TEM cells) were found to be surprisingly ineffective in dealing with localized infections (Jiang et al., 2012; Mackay et al., 2012). This is likely due to the fact that these cells do not routinely traffic through non-lymphoid tissues in the steady state and therefore require a period of reactivation in SLOs before they can migrate to the site of infection to participate in host defense (Gebhardt et al., 2011; Klonowski et al., 2004). To evaluate whether skin TRM cells generated at the site of prior MVA tattooing were able to protect against a secondary virus infection of the skin, a cutaneous VV challenge was performed in the memory phase (> 50 days) after primary immunization. For this, groups of mice were tattooed with MVA-OVA ( $2 \times 10^6$  IU) either on the left abdominal skin (group 1) or on the right ear pinna (group 2), to generate enriched populations of virus-specific TRM cells in these two different skin locations (Fig. 12a). Note that the two cutaneous immunization protocols (abdomen versus ear) elicited roughly equal frequencies of systemic virus-specific memory CD8<sup>+</sup> T cells (as measured in the spleen for OT-I cells, Fig. 8b and Fig. 9b). Thus, groups 1 and 2 should only differ in the regional distribution of skin TRM. Mice that received the same dose of MVA-OVA by i.m. injection were included as a third group (group 3) (Fig. 12a), which largely lacks virus-specific TRM cells in the skin, but contains comparable levels of systemic memory CD8<sup>+</sup> T cells to MVA-tattooed mice (Figs 8b, 9b). Naïve animals served as negative controls (group 4) (Fig. 12a). The different groups also exhibited similar levels of vaccinia virus-specific IgG/M, as

measured by ELISA in the serum 40 days after MVA-OVA immunization (data not shown).

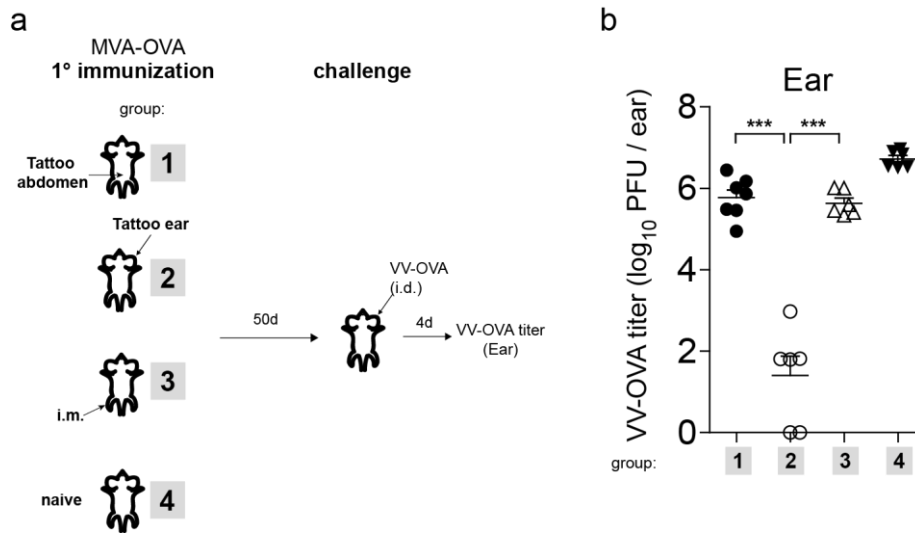


**Figure 12: Virus-specific CD8<sup>+</sup> TRM cells confer enhanced local protection against skin infection with replication-competent VV-OVA.**

(a) Groups of mice were immunized with  $2 \times 10^6$  IU MVA-OVA by tattooing on the left abdominal skin (group 1), by tattooing on the right dorsal ear pinna (group 2) or by i.m. injection into the anterior tibial muscle of the left hind leg (group 4). Non-immunized (naïve) mice served as controls (group 4). In the memory phase after primary MVA-OVA immunization (day 50), all groups were challenged with  $2 \times 10^6$  PFU VV-OVA by intradermal (i.d.) injection into the right ear. VV-OVA titers in VV-OVA-injected ears were determined 4 days later by standard plaque assay. (b) VV-OVA titer in challenged right ears, expressed as  $\log_{10}$  PFU VV-OVA per ear. Dots in graphs represent individual mice. Horizontal bars indicate the mean and error bars represent SEM. Data are pooled from 2 independent experiments with 3-4 mice per group ( $n=6-7$ ). Statistical analysis (one-way ANOVA followed by Tukey's post-test comparison), \*\*\*  $P < 0.001$

All mice were challenged 50 days after primary immunization with  $2 \times 10^6$  PFU VV-OVA by intradermal injection into the right ear and VV-OVA titers were measured 4 days later in homogenized ear tissue by standard plaque assay on RK-13 cells.

As expected, high VV-OVA titers were detected in ears of non-immunized animals (Fig. 12b). Interestingly, mice challenged on previously MVA-OVA-tattooed ears (group 2) almost completely eliminated VV from the challenged ear (around 10,000-fold reduction compared to naïve mice), while those that had received the primary MVA-OVA tattoo on the abdomen (group 1) only partially cleared VV-OVA from the ear (around 10-fold reduction). Similar to group 1, mice immunized by the i.m. route (group 3) also demonstrated incomplete clearance of VV-OVA from the challenged ear (Fig. 12b), further supporting recent data showing that circulating TCM or TEM populations have only a limited capacity to protect from infections encountered within peripheral tissues (Jiang et al., 2012; Mackay et al., 2012). Together, these data demonstrate that virus-specific TRM cells, which are seeded into the skin upon MVA-OVA tattooing, are capable of providing

rapid protective immunity against renewed local infection, but also reveal that the establishment of a protective TRM pool after MVA tattooing is largely restricted to the site of the initial virus inoculation.

## **5.9 Role of Foxp3<sup>+</sup> CD4<sup>+</sup> regulatory T cells in TRM formation in the skin**

Having established that MVA skin infection is capable of triggering the local formation of virus-specific skin TRM cells, it was decided to use this model to explore possible factors that contribute to TRM generation. It has recently been described that Foxp3<sup>+</sup> CD4<sup>+</sup> regulatory T cells (Tregs) are highly abundant in both human and murine skin (Dudda et al., 2008). Tregs are known to play a pivotal role in maintaining tissue homeostasis and self-tolerance (Belkaid, 2007; Belkaid & Tarbell, 2009; Kim et al., 2007; Lahl et al., 2007). Impaired Treg migration to the skin has been associated with the development of a severe cutaneous inflammatory disease (Dudda et al., 2008). Moreover, upon cutaneous immunization with OVA protein emulsified in IFA (incomplete Freund's adjuvant), Tregs have been found to accumulate at the site of skin inflammation and dampen effector cytokine production of infiltrating CD4<sup>+</sup> helper T cells *in situ* (McLachlan et al., 2009). Previous work from our laboratory demonstrated that Tregs also modulate the response to (systemic) MVA infection by suppressing the priming and expansion of virus-specific CD8<sup>+</sup> effector T cells (Kastenmuller et al., 2011). Interestingly, although the absence of Tregs during the priming phase resulted in enhanced induction of MVA-specific effector CD8<sup>+</sup> T cells, no influence on subsequent systemic CD8<sup>+</sup> T cell memory generation was noticeable in Treg-depleted mice when compared to (non-depleted) wild-type animals (Kastenmuller et al., 2011). In light of the described findings, it was of interest to find out whether the absence of this regulatory subset during the course of an MVA skin infection might have an impact on the local CD8<sup>+</sup> T cell memory formation in the skin. To address this question, the bacterial artificial chromosome (BAC)-transgenic DERE (DEpletion of REGulatory T cells) mouse model was used (Lahl et al., 2007). DERE mice express the simian diphtheria toxin receptor (DTR) fused to an enhanced GFP (green fluorescent protein) under the control of the Foxp3 gene locus. Administration of diphtheria toxin (DTX) results in selective but transient (lasting approximately 6 to 8 days) depletion of regulatory T cells (Kastenmuller et al., 2011). DERE mice and non-transgenic littermates were infected with  $2 \times 10^6$  IU MVA-OVA by abdominal skin tattoo and skin recruitment

and local memory formation of B8R-specific CD8<sup>+</sup> T cells were examined. Both groups of mice received three intraperitoneal injections of 1 μg DTX on day 0, 1 and 2 after tattooing (Fig. 13a).

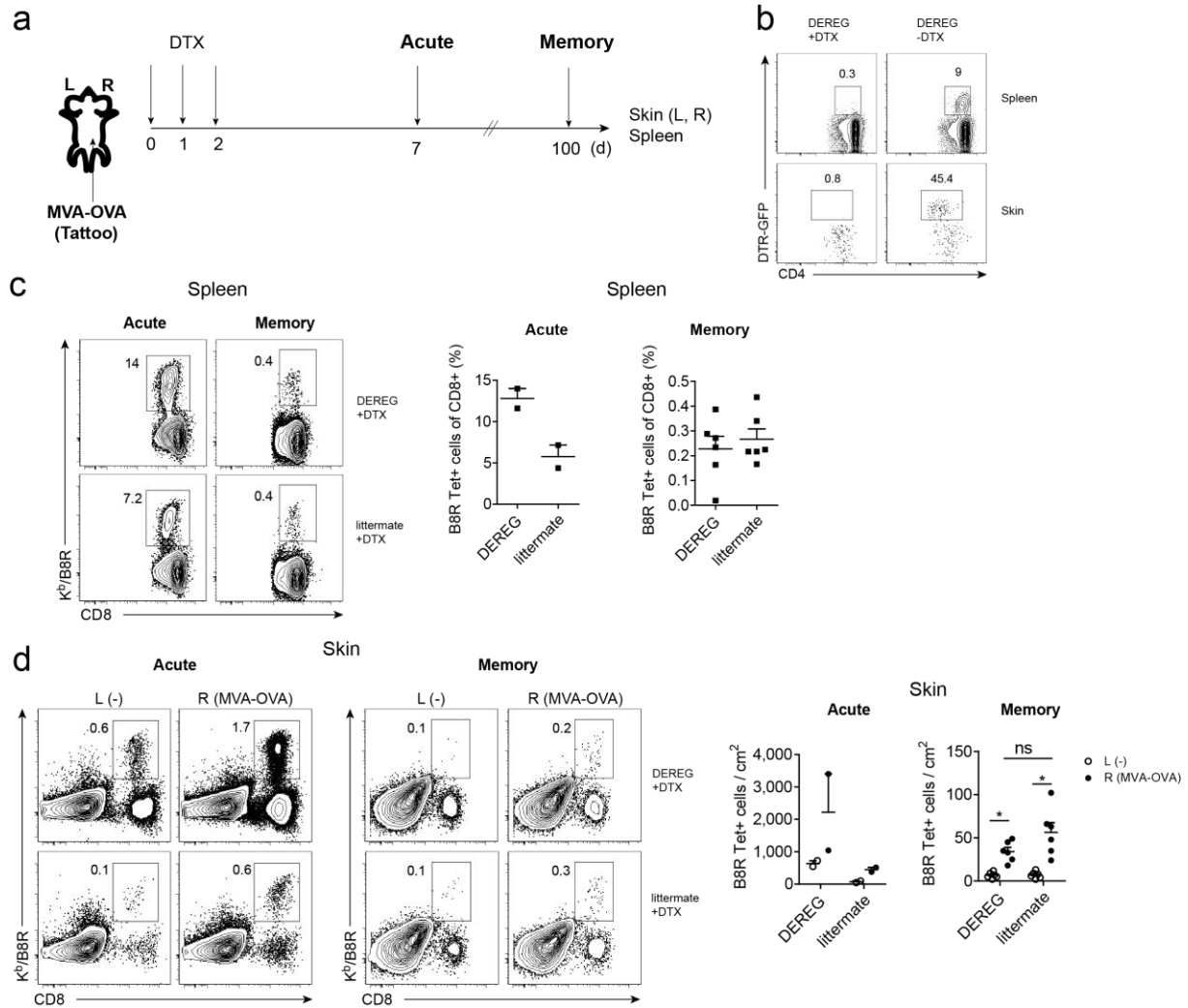


**Figure 13: Absence of Foxp3<sup>+</sup> CD4<sup>+</sup> regulatory T cells during acute MVA skin infection does not impact the formation of skin TRM cells.**

(a) DEREg mice or wild-type littermate controls were tattooed on right abdominal skin with  $2 \times 10^6$  IU MVA-OVA and received 3 intraperitoneal (i.p.) injections (d0, d1, d2) of 1 μg diphtheria toxin (DTX) in order to deplete Foxp3<sup>+</sup> Tregs. During the acute phase (Acute, day 7) and the memory phase (Memory, day 100) after infection, B8R-specific CD8<sup>+</sup> T cells were identified in right (R) and left (L) abdominal skin and the spleen by K<sup>b</sup>/B8R tetramer staining. (b) Efficiency of depletion of Foxp3<sup>+</sup> Tregs (identified by expression of the DTR-GFP fusion protein) in abdominal skin and spleen of DTX-treated or untreated DEREg mice, as measured one day after two daily DTX injections. (c) Representative plots (left panel) and graphs (right panels) showing the frequency B8R-specific CD8<sup>+</sup> T cells in the spleen of DTX-treated DEREg mice and littermate controls during the acute phase and the memory phase. (d) Representative plots showing the frequency of B8R-specific CD8<sup>+</sup> T cells in the CD45<sup>+</sup> leukocyte population in right (R) and left (L) abdominal skin of DTX-treated DEREg mice and littermate controls (left panel). Absolute number (per cm<sup>2</sup> skin) of B8R-specific CD8<sup>+</sup> T cells in the indicated skin regions of DTX-treated DEREg mice and littermate controls (right panel). Dots in graphs represent individual mice. Horizontal bars indicate the mean and error bars represent SEM. Data are derived from 1 experiment (Acute, n=2) or are pooled from 2 independent experiments (Memory, n=6). Statistical analysis (unpaired Student's *t*-test for comparison between groups; paired Student's *t*-test for comparisons between left and right skin regions), ns, not significant. \* *P* < 0.05



As illustrated in Fig. 13b, DTX application efficiently depleted Tregs from both the spleen as well as the skin of DERE mice, as indicated by the absence of DTR-GFP<sup>+</sup> CD4<sup>+</sup> T cells in either compartment on day 2 (Fig. 13b).

In line with previous data from our lab (Kastenmuller et al., 2011), analysis of the spleen 7 days after tattooing showed a strongly enhanced systemic effector CD8<sup>+</sup> T cell response in DTX-treated DERE mice, as indicated by an about 2-fold increased frequency of B8R-specific CD8<sup>+</sup> T cells in comparison to littermate controls (Fig 13c). After establishment of memory, however, both groups exhibited similar frequencies of B8R-specific CD8<sup>+</sup> T cells in the spleen (Fig. 13c), suggesting that the absence of Tregs during the priming phase after cutaneous MVA immunization does not seem to alter the generation of systemic CD8<sup>+</sup> T cell memory, similar to what has been described after systemic MVA vaccination (Kastenmuller et al., 2011).

Analysis of skin tissue on day 7 after tattooing showed that the depletion of Tregs also led to a markedly enhanced infiltration of virus-specific effector CD8<sup>+</sup> T cells into MVA-OVA-infected skin, as indicated by a considerably increased frequency and absolute number of B8R-specific CD8<sup>+</sup> T cells in MVA-OVA-tattooed abdominal skin of DTX-treated DERE mice (Fig. 13d). It is interesting to note that at this time point, non-involved contralateral skin of Treg-depleted animals even contained higher numbers of B8R-specific CD8<sup>+</sup> T cells when compared to the MVA-OVA-tattooed skin region of littermate controls (Fig. 13d). Importantly, despite an increased accumulation of virus-specific effector CD8<sup>+</sup> T cells on day 7 after tattooing, of DTX-treated DERE mice harbored a similar number of B8R-specific CD8<sup>+</sup> T cells in MVA-OVA-tattooed skin as littermate controls after establishment of memory (Fig. 13d). Furthermore, comparable numbers of B8R-specific memory CD8<sup>+</sup> T cells were detected in non-involved contralateral skin between the two analyzed groups (Fig. 13d).

Together, these data demonstrate that upon MVA tattooing Tregs dampen the acute antiviral effector CD8<sup>+</sup> T cell response both systemically as well as in MVA-infected tissue, but do not seem to play an important functional role in regulating the formation of systemic or local skin-resident CD8<sup>+</sup> T cell memory. The results further indicate that the size of the established antiviral CD8<sup>+</sup> TRM cell pool in MVA-infected skin does not necessarily correlate with size of the local effector CD8<sup>+</sup> T cell pool in the tissue during the acute phase of the response.

## 5.10 Skin injury alone promotes local effector CD8<sup>+</sup> T cell accumulation

Recent data have suggested that local inflammation alone can support the development of TRM cells in the skin even in the absence of antigen in the tissue (Mackay et al., 2012). Since the above experiments have shown virus-specific TRM cells predominantly took up residence in MVA-tattooed skin, it was asked whether this site-specific TRM cell accumulation might have been instructed by local inflammatory signals that were released in response to the epidermal injury or the subsequent cutaneous viral infection. First, it was addressed whether local inflammation triggered by epidermal injury alone would be sufficient to promote a local recruitment of virus-specific CD8<sup>+</sup> T cells to the skin.

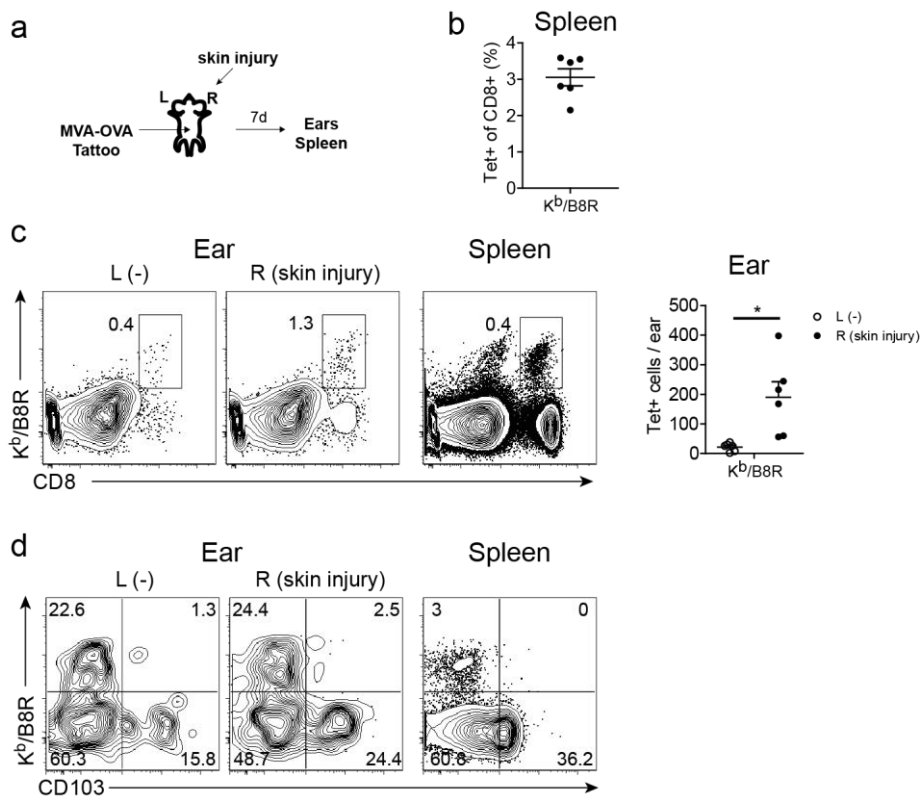


**Figure 14: Epidermal injury promotes recruitment of virus-specific effector CD8<sup>+</sup> T cells from the circulation.**

(a) Mice were tattooed on left abdominal skin with  $2 \times 10^6$  IU MVA-OVA and were shortly thereafter injured on the right ear by superficial scratches with the tattoo needle. On day 7 after immunization, B8R-specific CD8<sup>+</sup> T cells were analyzed in superficially injured right (R) ears and untreated left (L) ears as well as the spleen by K<sup>b</sup>/B8R tetramer staining. (b) Frequency of B8R-specific CD8<sup>+</sup> T cells (in the total CD8<sup>+</sup> T cell population) in the spleen. (c) Representative plots showing the percentage of B8R-specific CD8<sup>+</sup> T cells in the CD45<sup>+</sup> leukocyte population in left and right ears and the spleen (left panel). Absolute number of B8R-specific CD8<sup>+</sup> T cells in ear skin (right panel). (d) Analysis of CD103 expression on B8R-specific CD8<sup>+</sup> T cells isolated from left and right ears and the spleen. Dots in graphs represent individual mice. Horizontal bars indicate the mean and error bars represent SEM. Data are pooled from 2 independent experiments ( $n=6$ ). Statistical analysis (paired Student's *t*-test), \*  $P < 0.05$

To this end, mice were tattooed on abdominal skin with  $2 \times 10^6$  IU MVA-OVA and shortly thereafter skin injury was induced on one ear by multiple superficial scratches with a tattoo

needle. At the peak of the immune response (day 7), cell suspensions were obtained from injured right ears, untreated contralateral ears and the spleen and were analyzed by K<sup>b</sup>/B8R tetramer staining (Fig. 14a).

The analysis showed that the abdominal MVA-OVA tattoo induced a robust systemic B8R-specific CD8<sup>+</sup> T cell response, as determined in the spleen (Fig. 14b, c). Analysis of ear tissue revealed that B8R-specific effector CD8<sup>+</sup> T cells were present in significantly greater numbers in previously injured ear skin when compared to untreated ears, indicating that the acute skin injury was able to trigger a local recruitment of virus-specific effector CD8<sup>+</sup> T cells from the circulation (Fig. 14c). Notably, B8R-specific effector CD8<sup>+</sup> T cells that had been recruited to both inflamed and untreated skin were predominantly CD103<sup>-</sup>, similar to their counterparts in the spleen (Fig. 14d).

To further confirm this finding, the experiment was repeated in mice that were immunized with MVA-OVA by intradermal injection into abdominal skin (Fig. 15a). This route of MVA immunization was chosen as it should largely prevent a possible carry-over of infectious virus from the abdominal inoculation site to the injured ear (transferred by the mice themselves), since injected virus suspension remains confined within a bleb below the skin surface.

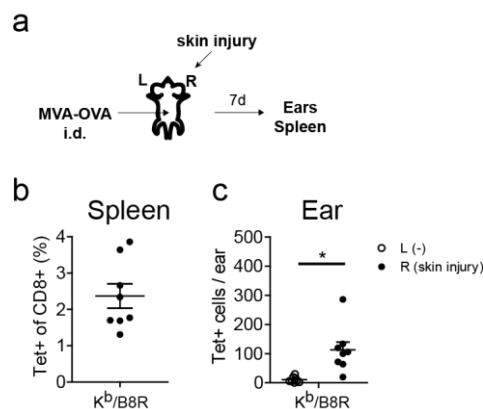


**Figure 15: Recruitment of i.d. primed MVA-specific CD8<sup>+</sup> T cells to the site of skin injury.**

(a) Mice were injected i.d. with  $2 \times 10^6$  IU MVA-OVA into the left abdominal skin and were shortly thereafter injured on the right ear by superficial scratches with the tattoo needle. On day 7 after immunization, B8R-specific CD8<sup>+</sup> T cells were analyzed in superficially injured right (R) ears and untreated left (L) ears as well as the spleen by K<sup>b</sup>/B8R tetramer staining. (b) Frequency of B8R-specific CD8<sup>+</sup> T cells (in the total CD8<sup>+</sup> T cell population) in the spleen. (c) Absolute number of B8R-specific CD8<sup>+</sup> T cells in left and right ears. Dots in graphs represent individual mice. Horizontal bars indicate the mean and error bars represent SEM. Data are pooled from 2 independent experiments (n=6). Statistical analysis (paired Student's *t*-test), \*  $P < 0.05$

Intradermal injection of MVA-OVA elicited roughly similar frequencies of B8R-specific CD8<sup>+</sup> T cells in the spleen as did MVA-OVA immunization by tattooing (Fig. 15b, Fig. 14b). Consistent with above data, i.d. primed B8R-specific CD8<sup>+</sup> T cells also markedly

accumulated in previously injured ears, whereas the contralateral untreated ears again harbored only low amounts of B8R-specific effector CD8<sup>+</sup> T cells (Fig. 15c).

This result thus confirmed that the increased recruitment and accumulation of virus-specific effector CD8<sup>+</sup> T cells in superficially damaged ears was likely mediated only by the local inflammatory response to tissue injury.

Since it is known that T cells which are primed in skin-draining lymph nodes preferentially acquire expression of homing receptors that facilitate their entry into inflamed skin (Campbell & Butcher, 2002; Mora et al., 2005), it was of interest to examine if virus-specific CD8<sup>+</sup> T cells primed by a non-cutaneous MVA immunization route would also be able to migrate to superficially injured skin. To address this, mice were immunized intranasally with  $2 \times 10^6$  IU MVA-OVA and right ears were again injured by scratching with the tattoo needle (Fig. 16a).

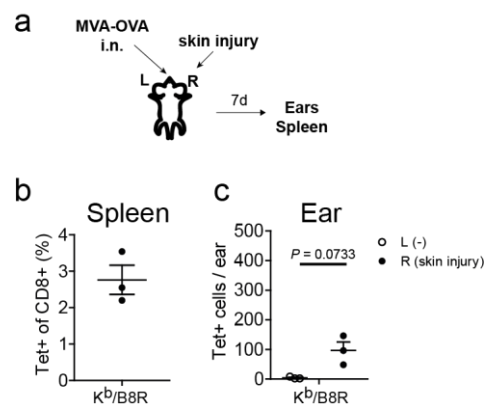


**Figure 16: Recruitment of mucosally primed MVA-specific CD8<sup>+</sup> T cells to the site of skin injury.**

(a) Mice were immunized intranasally (i.n.) with  $2 \times 10^6$  IU MVA-OVA and were shortly thereafter injured on the right ear by superficial scratches with the tattoo needle. On day 7 after immunization, B8R-specific CD8<sup>+</sup> T cells were analyzed in superficially injured right (R) ears and untreated left (L) ears as well as the spleen by K<sup>b</sup>/B8R tetramer staining. (b) Frequency of B8R-specific CD8<sup>+</sup> T cells (in the total CD8<sup>+</sup> T cell population) in the spleen. (c) Absolute number of B8R-specific CD8<sup>+</sup> T cells in left and right ears. Dots in graphs represent individual mice. Horizontal bars indicate the mean and error bars represent SEM. Data are derived from 1 experiment (n=3). Statistical analysis (paired Student's *t*-test)

K<sup>b</sup>/B8R tetramer staining in the spleen 7 day post immunization showed that this mucosal route of MVA-OVA immunization primed a robust systemic B8R-specific CD8<sup>+</sup> T cell response that was similar in magnitude to that elicited by the cutaneous routes of MVA-OVA administration (Fig. 16b, Fig. 15b, Fig. 14b). Analysis of skin tissue again revealed a considerable local accumulation of B8R-specific CD8<sup>+</sup> T cells in recently injured ears as compared to untreated ears (Fig. 16c), indicating that virus-specific effector CD8<sup>+</sup> T cells with the capacity to traffic into inflamed skin are also generated upon mucosal MVA immunization.

A recent study reported that mobilization of virus-specific effector CD8<sup>+</sup> T cells into HSV-2-infected vaginal mucosal tissue critically requires the help of CD4<sup>+</sup> T cells. The report showed that virus-specific CD4<sup>+</sup> helper T cells, which infiltrate the infected mucosa early after infection, secrete the cytokine IFN- $\gamma$  and thereby induce a local expression of the chemokines CXCL9 and CXCL10 within the tissue that permits the subsequent entry of HSV-specific CD8<sup>+</sup> T cells (Nakanishi et al., 2009). It is interesting to note that after MVA tattooing, virus-specific effector CD8<sup>+</sup> T cells present in the systemic circulation expressed higher levels of the chemokine receptor CXCR3 (the receptor for CXCL9 and CXCL10) compared to those that had entered virus-infected skin (data not shown). As reduced expression of CXCR3 on skin-infiltrating effector CD8<sup>+</sup> T cells could be indicative of a recent engagement of the CXCR3 with its ligands CXCL9 and/or CXCL10, it is possible that these IFN- $\gamma$ -inducible chemokines might also be involved in the recruitment of effector CD8<sup>+</sup> T cells to inflamed MVA-tattooed skin.

To test whether virus-specific CD8<sup>+</sup> T cell entry into injured skin might be controlled by such a local IFN- $\gamma$  dependent mechanism, it was decided to study the CD8<sup>+</sup> T cell infiltration into injured ear skin in mice deficient in the expression of IFN- $\gamma$ R (IFN- $\gamma$ R<sup>-/-</sup> mice) (Fig. 17a).

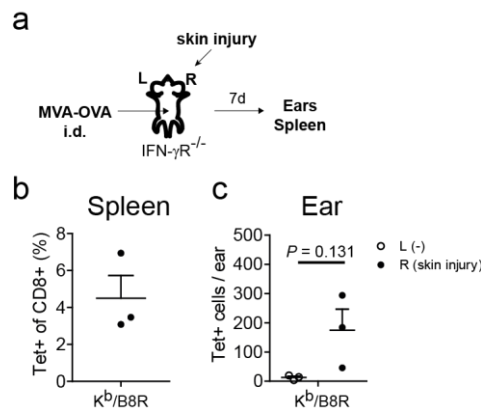


**Figure 17: Recruitment of MVA-specific CD8<sup>+</sup> T cells to the site of skin injury does not require local IFN- $\gamma$  signaling.**

(a) IFN- $\gamma$ R<sup>-/-</sup> mice were injected i.d. with  $2 \times 10^6$  IU MVA-OVA into the left abdominal skin and were shortly thereafter injured on the right ear by superficial scratches with the tattoo needle. On day 7 after immunization, B8R-specific CD8<sup>+</sup> T cells were analyzed in superficially injured right (R) ears and untreated left (L) ears as well as the spleen by K<sup>b</sup>/B8R tetramer staining. (b) Frequency of B8R-specific CD8<sup>+</sup> T cells (in the total CD8<sup>+</sup> T cell population) in the spleen. (c) Absolute number of B8R-specific CD8<sup>+</sup> T cells in left and right ears. Dots in graphs represent individual mice. Horizontal bars indicate the mean and error bars represent SEM. Data are derived from 1 experiment (n=3). Statistical analysis (paired Student's *t*-test).

IFN- $\gamma$ R<sup>-/-</sup> mice mounted a normal systemic B8R-specific CD8<sup>+</sup> T cell response after i.d. immunization with MVA-OVA, as indicated by a comparable frequency of K<sup>b</sup>/B8R tetramer binding CD8<sup>+</sup> T cells in the spleen on day 7 post infection when compared to wild-type mice (Figs. 17b, 15b). Importantly, the analysis further demonstrated that the

absolute number of B8R-specific CD8<sup>+</sup> T cells recruited to injured ears of IFN- $\gamma$ R<sup>-/-</sup> mice was similar to that detected in wild-type animals (Figs. 17c, Fig. 15c).

In conclusion, these data suggest that infiltration of circulating virus-specific CD8<sup>+</sup> T cells into sites of acute cutaneous injury is likely not as dependent on local IFN- $\gamma$  signals as migration of the cells to inflamed, virus-infected mucosal tissue (Nakanishi et al., 2009).

### 5.11 Local skin injury alone poorly supports the establishment of CD8<sup>+</sup> TRM cells

The above data have shown that an acute local skin inflammation alone, as elicited by a superficial mechanical disruption of the epidermal barrier, was sufficient to promote the recruitment of virus-specific CD8<sup>+</sup> T cells from the circulation. It was next investigated whether virus-specific CD8<sup>+</sup> T cells that had accumulated in the site of cutaneous injury during the acute phase were able to form a local population of skin TRM cells. Mice which had been tattooed on left abdominal skin with MVA-OVA and received a local skin injury on the right ear were therefore analyzed after establishment of immunological memory (>50 days post immunization) (Fig. 18a).

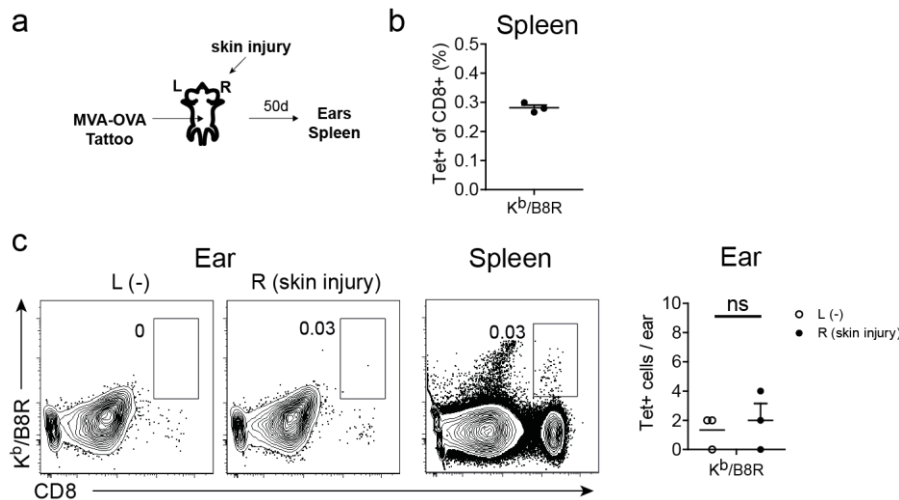


**Figure 18: Acute skin injury is not sufficient to induce permanent lodgment of MVA-specific CD8<sup>+</sup> T cells to the skin.**

(a) Mice were tattooed with  $2 \times 10^6$  IU MVA-OVA on the left abdominal skin and were shortly thereafter injured on the right ear by superficial scratches with the tattoo needle. In the memory phase (>50 days) after immunization, B8R-specific CD8<sup>+</sup> T cells were analyzed in superficially injured right (R) ears and untreated left (L) ears as well as the spleen by K<sup>b</sup>/B8R tetramer staining. (b) Frequency of B8R-specific CD8<sup>+</sup> T cells (in the total CD8<sup>+</sup> T cell population) in the spleen. (c) Representative plots showing the percentage of B8R-specific CD8<sup>+</sup> T cells in the CD45<sup>+</sup> leukocyte population in left and right ears and the spleen (left panel). Absolute number of B8R-specific CD8<sup>+</sup> T cells in left and right ears (right panel). Dots in graphs represent individual mice. Horizontal bars indicate the mean and error bars represent SEM. Data are derived from 1 experiment (n=3). Statistical analysis (paired Student's *t*-test). ns, not significant.

At this time point, mice still harbored detectable levels of B8R-specific memory CD8<sup>+</sup> T cells in the spleen, as determined by K<sup>b</sup>/B8R tetramer staining (Fig. 18b, c). However, barely any B8R-specific memory CD8<sup>+</sup> T cells could be detected in previously injured ear skin (Fig. 18c). A similar result was obtained in a parallel experiment using mice that had been immunized with MVA-OVA by i.d. injection (data not shown).

Together, these results suggested that the cutaneous inflammatory response evoked by the mechanical skin injury alone, although sufficient to trigger a local influx and accumulation of activated effector CD8<sup>+</sup> T cells, was largely unable to support the formation of local TRM cells.

### **5.12 Homing of effector CD8<sup>+</sup> T cells to inflamed skin does not depend on the presence of their cognate antigen *in situ***

The above experiments indicated that epidermal injury-associated inflammatory signals alone unlikely contributed to the observed TRM cell accumulation in previously MVA-tattooed skin and suggested that some other factor, most likely related to the local viral infection, might have been responsible for the enhanced formation of TRM cell at the prior tattoo inoculation site.

To explore the basis of the location-restricted TRM lodgment in more detail, an experimental model was established based on adoptive transfer of OT-I cells, which should allow to dissect the relative role of the skin inflammation (resulting from skin injury alone or skin injury combined with local viral infection) and local antigen recognition in the formation of virus-specific TRM cells in the skin.

Naïve OT-I cells were transferred into mice and subsequently primed by i.v. MVA-OVA immunization, in order to generate a circulating pool of effector CD8<sup>+</sup> T cells specific for the model antigen OVA. On the same day, MVA-OVA-primed OT-I recipient mice were divided into three groups, which were treated as follows: (i) Mice of group 1 were tattooed on the right ear with PBS to induce a local skin injury, while the other ear was left untreated. (ii) Mice of group 2 were tattooed on left and right ears with PBS and wild-type MVA (MVA), respectively, to induce either a local skin injury or to create a local virus infection in the absence of OVA expression *in situ*. (iii) Mice of group 3 were tattooed on left and right ears with wild-type MVA and MVA-OVA, respectively, to model a local virus infection in the absence or presence of OVA expression in the skin (Fig. 19a).

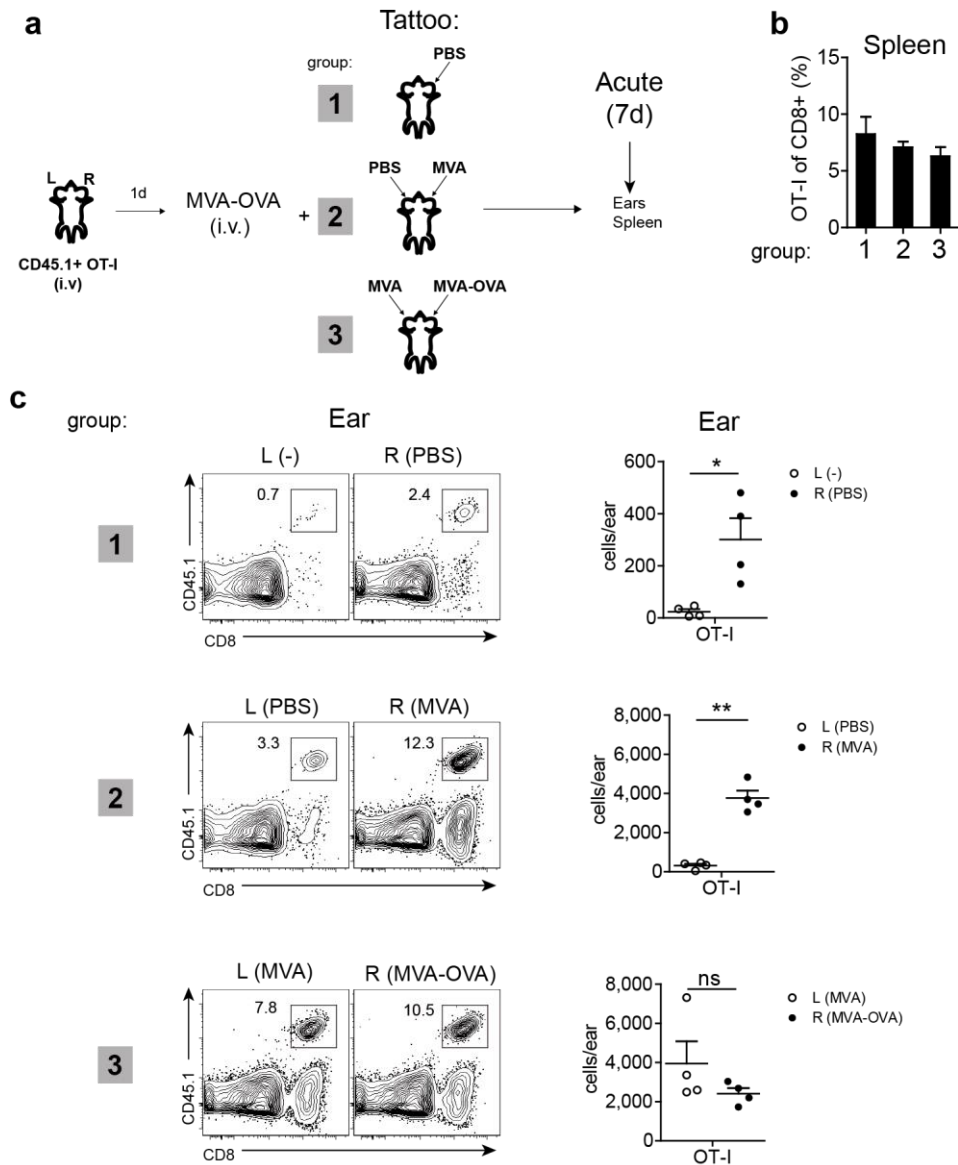


**Figure 19: Effector CD8+ T cell infiltration into MVA-tattooed skin is governed by local inflammation and occurs independently of local antigen expression.**

(a) Mice were adoptively transferred (i.v.) with 50,000 naïve CD45.1+ OT-I cells and immunized i.v. with  $2 \times 10^6$  IU MVA-OVA. Shortly after immunization, one group of mice was tattooed on the right (R) ear with PBS (group 1). A second group (group 2) was tattooed on the left (L) and right (R) ear with PBS and  $2 \times 10^6$  IU MVA, respectively. A third group (group 3) was tattooed on the left and right ear with  $2 \times 10^6$  IU MVA and  $2 \times 10^6$  IU MVA-OVA, respectively. During the acute phase after immunization (day 7), ears and spleens of the different groups were analyzed for the presence of OT-I cells. (b) Frequency of OT-I cells within the CD8+ T cell population in the spleen of groups 1-3. (c) Representative plots depicting the frequency of OT-I cells in the CD45+ leukocyte population in left (L) and right (R) ears of group 1-3 (left panel). Absolute number of OT-I cells isolated from left (L) and right (R) ears (right panel). Dots in graphs represent individual mice. Horizontal bars indicate the mean and error bars represent SEM. Data are derived from 1 experiment (representative of 2 independent experiments) (n=4). Statistical analysis (paired Student's *t*-test). ns, not significant. \*  $P < 0.05$ ; \*\* \*  $P < 0.001$

The three groups were first analyzed on day 7 post infection to study the extent of OT-I cell recruitment to the differentially tattooed skin locations. Analysis in the spleen showed similar frequencies of OT-I cells between the three groups, indicating that the additional local MVA infections (in particular the local MVA-OVA infection in group 3) did not considerably influence the systemic expansion of the adoptively transferred donor cells



(Fig. 19b). Analysis of group 1 showed that primed OT-I cells significantly accumulated (about 10-fold) in PBS-tattooed ears when compared to untreated contralateral ears, in which only few OT-I cells were detectable (Fig. 19c, group 1), supporting the previous finding that recruitment of circulating effector CD8<sup>+</sup> T cells to the skin is increased in the presence of a local tissue injury.

Consistently, previously PBS-tattooed ears from mice of group 2 also harbored a considerable population of effector OT-I cells that was similar in size to that detected in PBS-tattooed ears of group 1 (Fig. 19c, group 2). In group 2, however, a much stronger local accumulation of OT-I cells was detected in contralateral MVA-tattooed ears, which contained approximately 10 times more OT-I cells than ears tattooed with PBS alone (Fig. 19c, group 2), demonstrating that local inflammation induced by the cutaneous viral infection represented a more potent signal for the recruitment of CD8<sup>+</sup> T cells to the tissue than mechanical injury alone.

Interestingly, additional expression of OVA in virus-infected skin appeared to have no further impact on the local recruitment of OT-I effector cells, as indicated by similar numbers of these cells between MVA-OVA-tattooed and MVA-tattooed ears of group 3 (Fig. 19c, group 3). It is also interesting to note that a similar total number of OT-I cells was detected in MVA-infected ears when comparing group 2 and group 3 (Fig. 19c, groups 2-3), which suggests that the additional priming of OT-I cells in lymph nodes draining MVA-OVA-infected ears of group 3, did not seem to have a noticeable impact on the overall skin-homing potential of the circulating OT-I effector pool. Of note, OT-I effector cells which were present in the differentially treated ears at the time of analysis did not express CD103, similar to their systemic OT-I cell counterparts in the spleen (data not shown).

Taken together, the above results suggest that the initial migration of circulating effector CD8<sup>+</sup> T cells to the site of viral tattooing occurs mainly in response to the local infection and to a minor extent also to skin injury, whereas cognate antigen expression within inflamed virus-infected skin appears to be dispensable for this process.

### **5.13 Local antigen recognition drives TRM development in MVA-infected skin**

In order to find out to what extent skin-infiltrating effector OT-I cells were able to establish tissue residence in the differentially tattooed skin locations, the three experimental groups were next analyzed during the memory phase (day 40 post infection). In addition to detection of OT-I cells, tetramer staining of B8R-specific CD8<sup>+</sup> T cells was included into the analysis to control for possible variations in the efficacy of local TRM induction in ears tattooed with the different MVA vectors (as used in group 3) (Fig. 20a).

As shown in Fig. 20b, memory populations of OT-I cells and endogenous B8R-specific CD8<sup>+</sup> T cells were readily detected in the spleen and were present at similar frequencies in all groups examined (Fig. 20b).

Quantification of OT-I cells in ears of group 1 showed that previously PBS-tattooed ears contained only a small population of memory OT-I cells, which was nearly equal in size to that detected in contralateral untreated ears (Fig. 20c, group 1). Similar results were obtained from analysis of endogenous B8R-specific memory CD8<sup>+</sup> T cells, whose numbers in both untreated and PBS-tattooed ears were close to the limit of detection (Fig. 20c, group 1). The results from group 1 therefore suggest that effector CD8<sup>+</sup> T cells which had infiltrated the site of acute skin injury were largely unable to form a local pool of skin-resident memory CD8<sup>+</sup> T cells in this site, consistent with the data obtained from the experiment shown in Fig. 18.

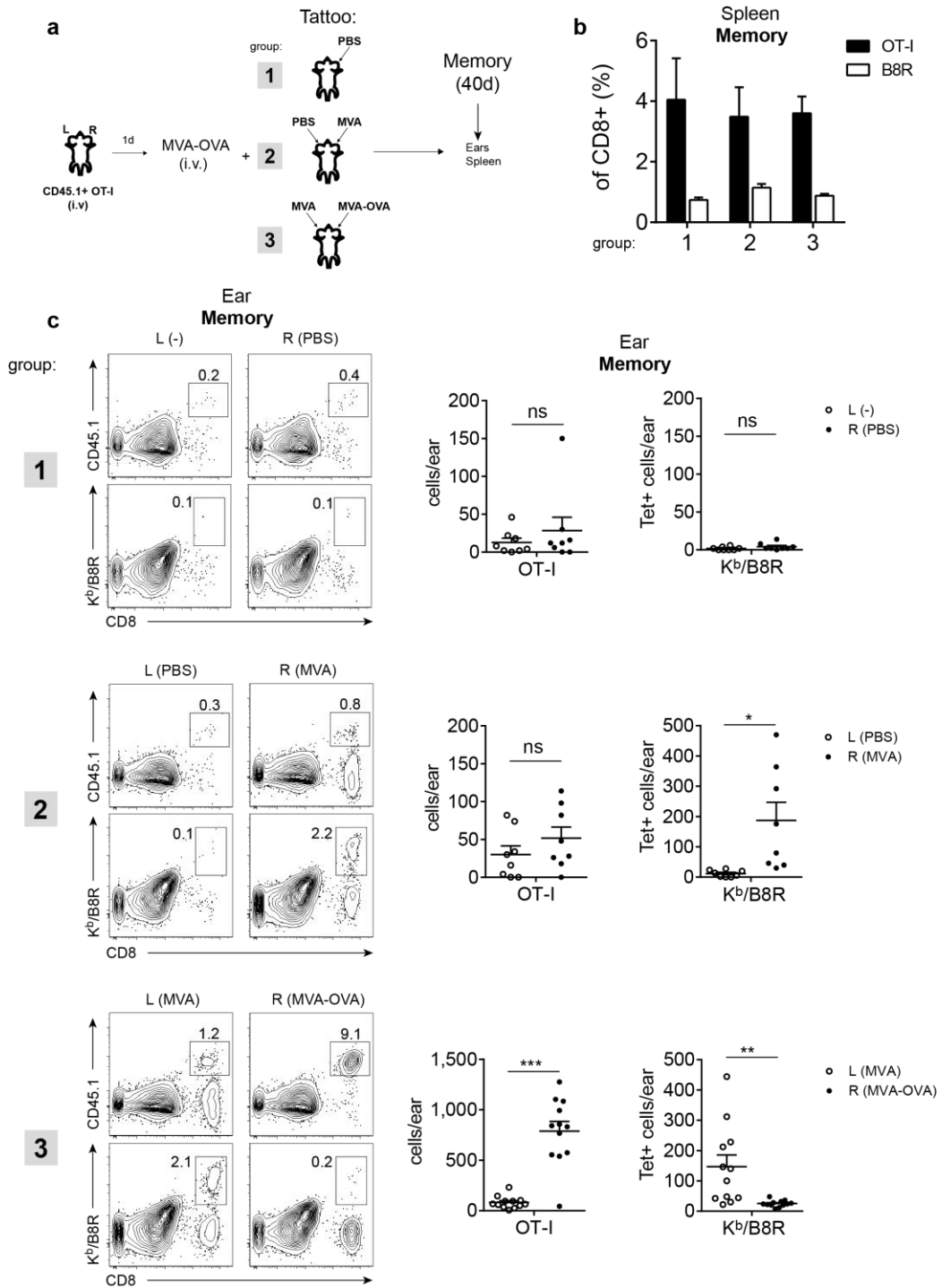


**Figure 20: Local antigen instructs TRM cell formation in MVA-tattooed skin.**

(a) Mice were adoptively transferred (i.v.) with 50,000 naïve CD45.1+ OT-I cells and immunized i.v. with  $2 \times 10^6$  IU MVA-OVA. Shortly after immunization, one group of mice was tattooed on the right (R) ear with PBS (group 1). A second group (group 2) was tattooed on the left (L) and right (R) ear with PBS and  $2 \times 10^6$  IU MVA, respectively. A third group (group 3) was tattooed on the left and right ear with  $2 \times 10^6$  IU MVA and  $2 \times 10^6$  IU MVA-OVA, respectively. During the memory phase after immunization (day 40), ears and spleens of the different groups were analyzed for the presence of OT-I cells as well as B8R-specific CD8+ T cells. (b) Frequency of OT-I cells and B8R-specific CD8+ T cells within the CD8+ T cell population in the spleen of groups 1-3. (c) Representative plots depicting the frequency of OT-I cells (top row) and B8R-specific CD8+ T cells (bottom row) in the CD45+ leukocyte population in left (L) and right (R) ears of group 1-3 (left panel). Absolute number of OT-I cells (top row) and B8R-specific CD8+ T cells (bottom row) isolated from left (L) and right (R) ears (right panel). Dots in graphs represent individual mice. Horizontal bars indicate the mean and error bars represent SEM. Data are pooled from 2-3 independent experiments (n=8-12). Statistical analysis (paired Student's *t*-test). ns, not significant. \*  $P < 0.05$ ; \*\*  $P < 0.001$  \*\*\*  $P < 0.001$

In line with this finding, only very few memory OT-I cells could be isolated from previously PBS-tattooed ears of group 2 (Fig. 20c, group2). Interestingly, MVA-tattooed ears of group 2, which on day 7 post infection were populated by a high number of OT-I effector cells, contained only few OT-I cells after establishment of memory (Fig. 20c, group 2). Although the total number of memory OT-I cells detected in MVA-tattooed ears appeared slightly increased in comparison to contralateral PBS-tattooed ears, this difference was not statistically significant ( $P = 0.1072$ ). Total numbers of memory OT-I cells however were significantly higher in MVA-tattooed ears when compared to untreated ears in group 1 ( $P = 0.0403$ ; unpaired Student's *t*-test; not shown), which suggest that the formation of OT-I TRM cells was to some extent enhanced by the local inflammatory response to the viral skin infection alone. Nevertheless, the marked decline in the absolute number of OT-I cells in MVA-infected ears between day 7 and day 40 indicated a rather poor long-term retention and/or survival of OT-I cells within this site and thus ruled out inflammation as the deciding local factor for the accumulation of TRM cells in MVA-infected skin.

As expected from the previous experiments, B8R-specific TRM cells considerably accumulated in MVA-tattooed ears of group 2, but were nearly absent in previously PBS-tattooed ears (Fig. 20c, group 2). Given the rather poor capacity of cutaneous inflammation alone in supporting the local development of TRM cells, this finding suggested that the accumulation of TRM cells in virus-infected skin might have been instructed by local antigen.

This notion is further supported by the results obtained from group 3, which showed a strong enrichment of OT-I TRM cells only in MVA-OVA-tattooed ears but not in contralateral ears that underwent infection with MVA (Fig. 20c, group 3), Note that a similar number of OT-I cells had infiltrated these differentially tattooed skin regions during the acute phase of the response (day 7 post infection) (Fig. 19c, group 3).

Taken together, these data indicate that antigen expression in virus-infected skin, while being dispensable for the initial recruitment of effector CD8<sup>+</sup> T cells, is critically required for the local development of TRM cells and suggest that antigen recognition in MVA-infected skin can act as a potent local instructive signal for the commitment of skin-infiltrating effector CD8<sup>+</sup> T cells towards a TRM fate.

### **5.14 Local competition between different antiviral CD8<sup>+</sup> T cells influences the composition of the TRM pool in MVA-infected skin**

Given the dominant role of local antigen in promoting the persistence and accumulation of TRM cells in MVA-infected skin, it was rather unexpected that the established pool of B8R-specific TRM cells in group 3 was dramatically different between MVA- and MVA-OVA-infected ears (Fig. 20c, group 3), since the MVA-encoded B8 antigen should have been available at a comparable level in either skin location. While B8R-specific TRM cells formed a sizable local population in MVA-tattooed ears (similar to that found in MVA-infected ears in group 2), B8R-specific TRM cells were only barely detectable in MVA-OVA-tattooed ears (Fig. 20c, group 3). Together with the finding that MVA-OVA-tattooed ears were nearly exclusively populated by OT-I TRM cells, this result suggested that the formation of B8R-specific TRM cells in this site might have been severely impaired by the concomitant local accumulation of OT-I TRM cells.

To rule out the possibility that the reduced formation of B8R-specific TRM cells in MVA-OVA-infected ears was due to an inefficient local recruitment of these cells during the effector phase, ears of doubly MVA/MVA-OVA-tattooed mice (group 3) were again analyzed on day 7 post infection (Fig. 21a).

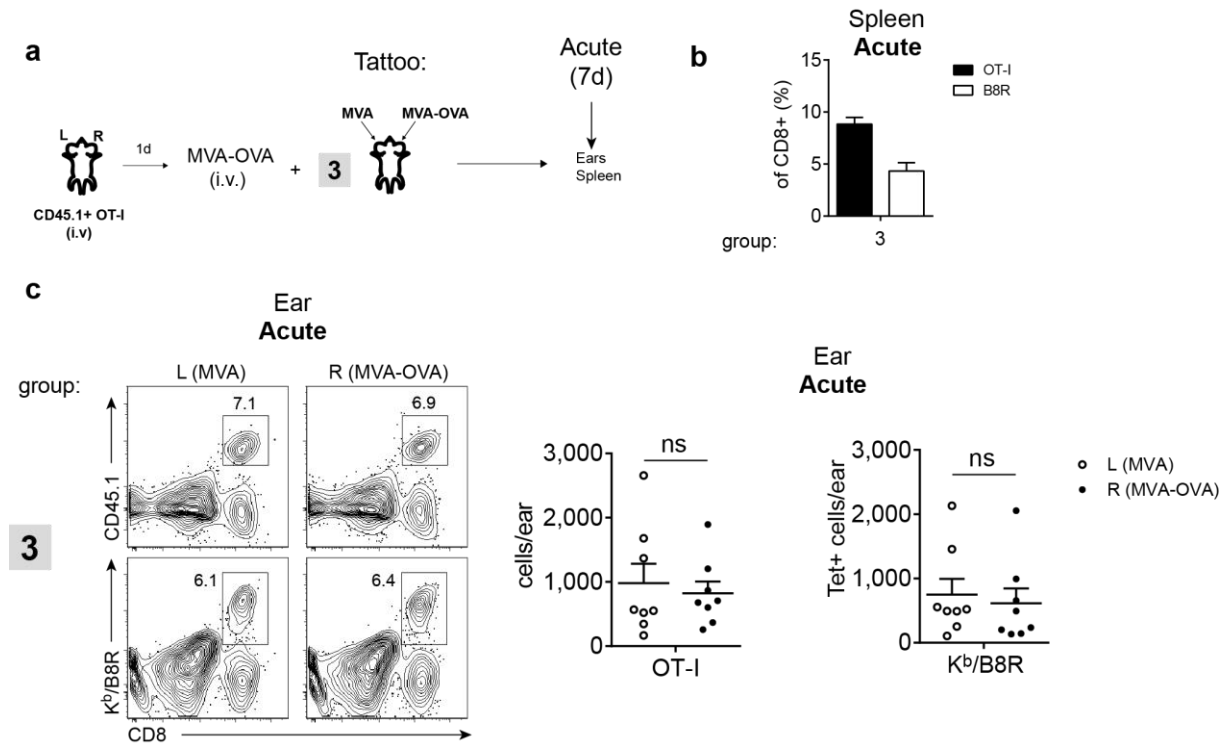


**Figure 21: B8R-specific CD8+ T cells similarly infiltrate into MVA-tattooed and MVA-OVA-tattooed ears.**

(a) Mice were adoptively transferred (i.v.) with 50,000 naïve CD45.1+ OT-I cells and immunized i.v. with  $2 \times 10^6$  IU MVA-OVA. Shortly after immunization, mice were tattooed on the left and right ear with  $2 \times 10^6$  IU MVA and  $2 \times 10^6$  IU MVA-OVA, respectively (analogous to group 3). During the acute phase after immunization (day 7), OT-I cells and B8R-specific CD8+ T cells were identified in ears and spleen. (b) Frequency of OT-I cells and B8R-specific CD8+ T cells within the CD8+ T cell population in the spleen. (c) Representative plots depicting the frequency of OT-I cells (top row) and B8R-specific CD8+ T cells (bottom row) in the CD45+ leukocyte population in left (L) and right (R) ears of group 3 (left panel). Absolute number of OT-I cells (top row) and B8R-specific CD8+ T cells (bottom row) isolated from left (L) and right (R) ears (right panel). Dots in graphs represent individual mice. Horizontal bars indicate the mean and error bars represent SEM. Data are pooled from 2 independent experiments ( $n=8$ ). Statistical analysis (paired Student's *t*-test). ns, not significant.

Similar to the previous experiment (Fig. 19), the analysis revealed comparable amounts of effector OT-I cells between MVA- and MVA-OVA-tattooed ears, further confirming that effector CD8+ T cell recruitment to the site of MVA tattooing is mostly controlled by the local inflammation. Importantly, by day 7 post infection, comparable numbers of B8R-specific CD8+ T cells had infiltrated MVA- and MVA-OVA-tattooed ears (Fig. 21c).

Thus, the failure of B8R-specific CD8+ T cells to establish residency in MVA-OVA-infected ears was not due to an impaired recruitment to the site of infection.

Based on this result, it was hypothesized that the impaired formation of B8R-specific TRM cells in MVA-OVA-infected ears was rather caused by a local competition with OT-I cells (e.g. for limiting TRM-promoting resources, such as local survival factors or possibly antigenic signals) that led to reduced survival and/or retention of recruited B8R-specific CD8+ T cells *in situ*.

To test this hypothesis, it was next investigated whether the establishment of B8R-specific TRM cells in MVA-OVA-infected ears could be restored if the immunodominant OT-I

competitors were absent. Therefore, the above experiment was repeated without adoptive transfer of OT-I cells and spleens and ears of doubly MVA/MVA-OVA-tattooed mice were analyzed after establishment of memory (day 40 post infection) by  $K^b/B8R$  and  $K^b/OVA$  tetramer staining (Fig. 22a).

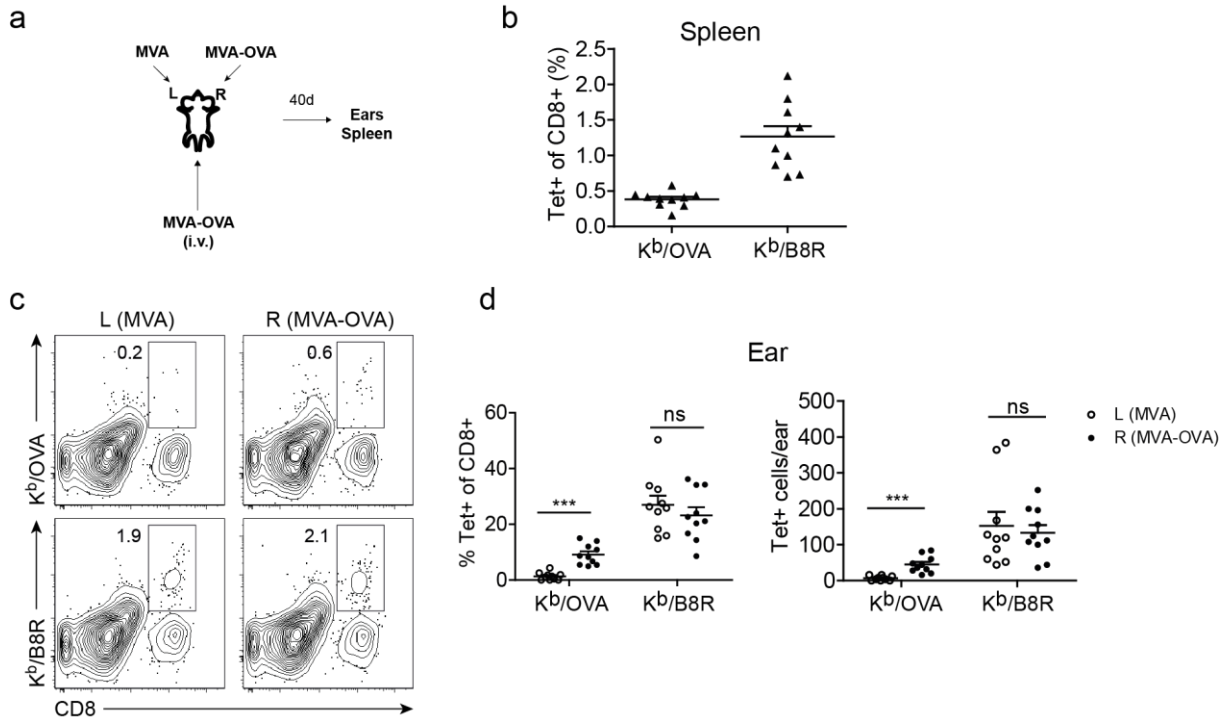


**Figure 22: Formation of B8R-specific TRM cells in MVA-OVA-tattooed skin is restored in the absence of competing OT-I cells.**

(a) Mice were immunized i.v. with  $2 \times 10^6$  IU MVA-OVA and were shortly thereafter tattooed on the left and right ear with  $2 \times 10^6$  IU MVA and  $2 \times 10^6$  IU MVA-OVA, respectively. During the memory phase after immunization (day 40), endogenous OVA-specific and B8R-specific CD8<sup>+</sup> T cells were identified in ears and spleen by  $K^b/OVA$  and  $K^b/B8R$  tetramer staining, respectively. (b) Frequency of OVA-specific and B8R-specific CD8<sup>+</sup> T cells within the CD8<sup>+</sup> T cell population in the spleen. (c) Representative plots depicting the frequency of OVA-specific CD8<sup>+</sup> T cells (top row) and B8R-specific CD8<sup>+</sup> T cells (bottom row) in the CD45<sup>+</sup> leukocyte population in left (L) and right (R) ears. (d) Frequency (in the skin CD8<sup>+</sup> T cell population; left panel) and absolute number (right panel) of OVA-specific CD8<sup>+</sup> T cells and B8R-specific CD8<sup>+</sup> T cells (bottom row) in left (L) and right (R) ears (right panel). Dots in graphs represent individual mice. Horizontal bars indicate the mean and error bars represent SEM. Data are pooled from 2 independent experiments (n=10). Statistical analysis (paired Student's *t*-test). ns, not significant. \*\*\*  $P < 0.001$

In the absence of transferred OT-I cells, B8R-specific CD8<sup>+</sup> T cells represent the dominant fraction of antiviral CD8<sup>+</sup> T cells in the spleen, whereas endogenous OVA-specific CD8<sup>+</sup> T cells are subdominant in the immune dominance hierarchy (Fig. 22b, Fig. 4). It is interesting to note that the absence of OT-I cells appeared to have no considerable impact on the size of the established systemic memory pool of B8R-specific CD8<sup>+</sup> T cells, since similar frequencies of B8R-specific memory CD8<sup>+</sup> T cells were detected in the spleen between experiments with or without OT-I transfer (around 1% versus 1-1.5% of B8R-specific CD8<sup>+</sup> T cells, respectively) (Fig. 22b, Fig. 20b). Consistent with the data obtained in the OT-I transfer model, analysis of ear skin showed that endogenous OVA-specific

CD8<sup>+</sup> T cells significantly accumulated in previously MVA-OVA-infected ears when compared to ears that had been infected with MVA (Fig. 22c, d), strengthening the finding that recognition of antigen in virus-infected skin considerably enhances local TRM formation.

Importantly, in the absence of OT-I cells, comparable amounts of B8R-specific TRM cells were found between MVA-OVA-tattooed ears and MVA-tattooed ears (Fig. 22c, d). This finding confirms that the formation of a B8R-specific TRM cell pool in MVA-OVA-tattooed ears was indeed hindered by the concomitant local lodgment of OT-I TRM cells and therefore suggests that these different virus-specific CD8<sup>+</sup> T cells populations must have competed *in situ* for local factors that were required for their long-term maintenance within the tissue.

Interestingly, the increased lodgment of endogenous OVA-specific TRM cells to MVA-OVA-infected ears appeared to have no influence on the local establishment of B8R-specific TRM cells, as the total number of B8R-specific TRM cells found in this site was similar to that in MVA-infected skin (which hardly contained any OVA-specific TRM cells) (Fig. 22c, d). It thus appears that in contrast to the TCR transgenic OT-I cells, endogenous OVA-specific CD8<sup>+</sup> T cells were largely unable to effectively cross-compete with the immunodominant B8R-specific CD8<sup>+</sup> T cells.



### **5.15 TRM cells generated in MVA-tattooed skin are non-recirculating cells**

In addition to the expression of the surface markers CD103, CD69 and residence within epithelial compartments of non-lymphoid tissues, another defining hallmark of TRM cells is their persistence within a single anatomical site without taking part in the systemic recirculation (Gebhardt & Mackay, 2012; Schenkel & Masopust, 2014).

To demonstrate that TRM cells generated in MVA-infected skin were in fact non-recirculating memory CD8<sup>+</sup> T cells, an adoptive transfer model was used which involved the transfer of male-origin OT-I cells into female recipient mice. In this setting, recirculating male donor T cells are rapidly eliminated by a systemic immune response directed against the male minor histocompatibility antigen, whereas those that do not frequently enter the blood circulation (i.e. tissue-resident cells) are protected from depletion (Gebhardt et al., 2011). In analogy to the previous experiments, mice that had received transfer of male donor OT-I cells were again immunized by i.v. MVA-OVA injection and simultaneously tattooed on the left and right ear with MVA and MVA-OVA, respectively (Fig. 23a).

## Results

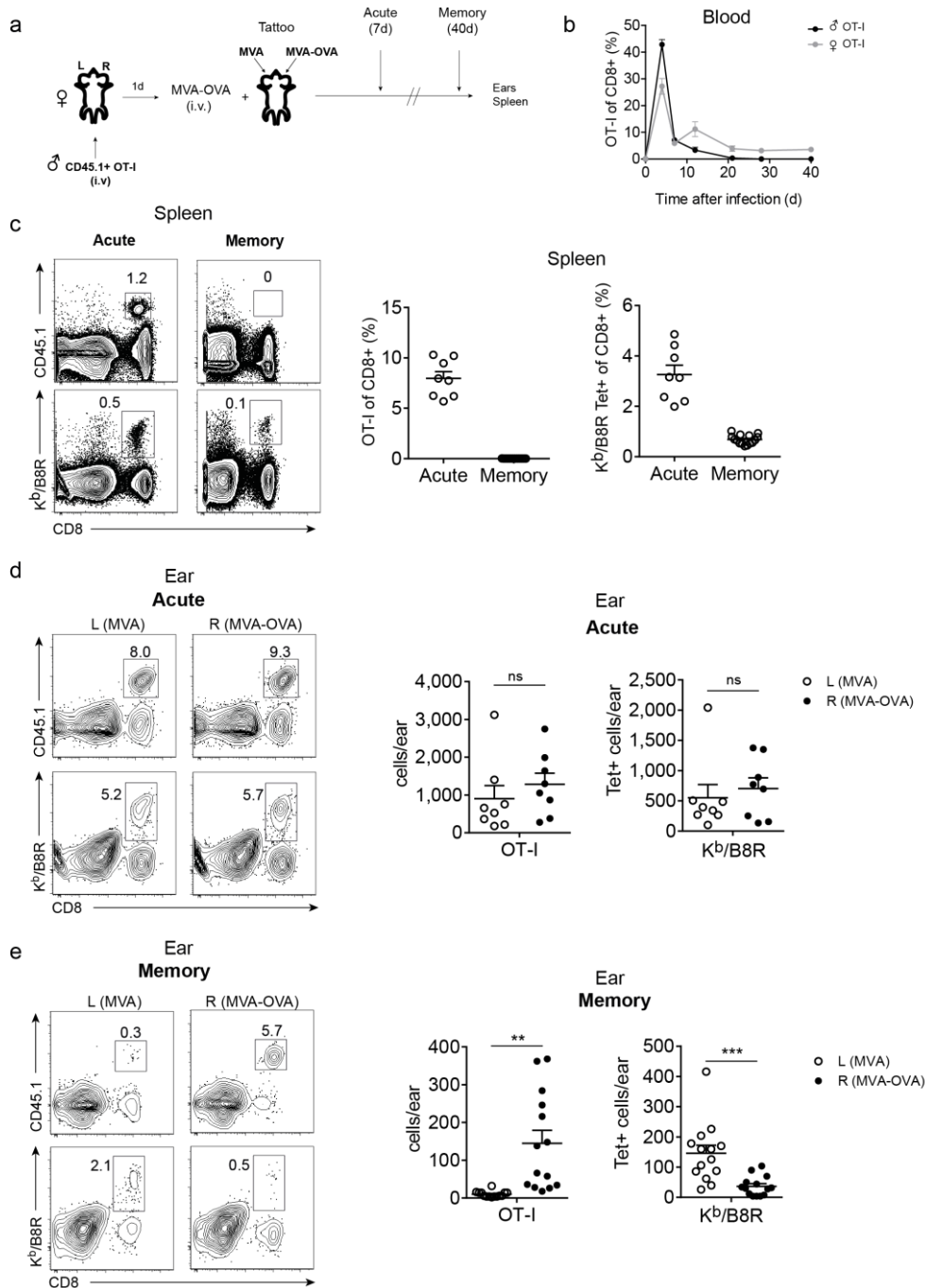


**Figure 23: Virus-specific CD8+ TRM cells generated in MVA-tattooed skin are non-recirculating memory cells.**

(a) Female mice were adoptively transferred (i.v.) with 50,000 naïve male CD45.1+ OT-I cells and immunized i.v. with 2x10<sup>6</sup> IU MVA-OVA. Shortly after immunization, mice were tattooed on the left and right ear with 2x10<sup>6</sup> IU MVA and 2x10<sup>6</sup> IU MVA-OVA, respectively. During the acute phase (Acute, day 7) and the memory phase (Memory, day 40) after immunization, male OT-I donor cells and endogenous B8R-specific CD8+ T cells were identified in ears and spleen. (b) Frequency of male OT-I cells (black line) and female OT-I cells (grey line) in the blood CD8+ T cell population of female recipient mice following infection. (c) Representative plots showing the frequency of male OT-I cells and B8R-specific CD8+ T cells in the CD45+ leukocyte population in the spleen during the acute and memory phase (left panel). Frequency of male OT-I cells and B8R-specific in the CD8+ T cell population in the spleen (right panel). (d, e) Representative plots showing the percentage of male OT-I cells and B8R-specific CD8+ T cells in the CD45+ leukocyte population in left (L) and right (R) ears during the acute (d) and memory phase (e) (left panel). Absolute number of male OT-I cells and B8R-specific CD8+ T cells in the CD45+ leukocyte population in left (L) and right (R) ears during the acute (d) and memory phase (e) (right panel). Dots in graphs represent individual mice. Horizontal bars indicate the mean and error bars represent SEM. Data are pooled from 2 (Acute, n=8) or 3 (Memory, n=14) independent experiments. Statistical analysis (paired Student's *t*-test). ns, not significant. \*\* *P* < 0.001, \*\*\* *P* < 0.001

A time-course analysis of the frequency of male OT-I donor cells in the blood showed that these cells expanded normally in immunized female hosts, but were completely eliminated from the circulation within 3 weeks after immunization (Fig. 23b), in accordance with published data (Ariotti et al., 2014; Gebhardt et al., 2011). In contrast, female recipients of female donor OT-I cells maintained a stable frequency of OT-I cells in the blood after contraction of the T cell response (Fig. 23b). Male-origin donor OT-I cells were also completely rejected from lymphoid tissue, as determined in the spleen 40 days after infection (Fig. 23c). Expectedly, B8R-specific CD8<sup>+</sup> T cells (which are not targeted by the anti-male immune response) were still readily detected in the spleen at this time point and were present at a similar frequency as observed in the previous experiments (Fig. 20b).

Analysis of differentially tattooed ears during the acute phase of the response revealed similar amounts of male-donor OT-I cells between MVA- and MVA-OVA-tattooed ears (Fig. 23d). MVA- and MVA-OVA-tattooed ears also contained similar amounts of endogenous B8R-specific effector CD8<sup>+</sup> T cells (Fig. 23d). Overall, the total number of skin-infiltrating antigen-specific CD8<sup>+</sup> T cells was comparable to that observed in previous experiments involving female OT-I transfer (Fig. 21c), suggesting that the ongoing anti-male immune response did not impair the acute recruitment of the transferred OT-I cells to the skin.

Importantly, despite a complete rejection from the blood or lymphoid tissue, male donor OT-I cells were still readily detected in the skin of immunized mice after establishment of memory and were again found to be strongly enriched in the previous site of MVA-OVA tattoo inoculation (Fig. 23e). In line with the previous data (Fig. 20 c, group 3), MVA-OVA-tattooed ears again harbored significantly lower amounts of B8R-specific TRM cells when compared to MVA-tattooed ears (Fig. 23e), which further supports the finding that the formation of OT-I TRM cells in this site severely impairs the local establishment of B8R-specific TRM cells.

In summary, these data show that skin TRM cells established after MVA tattooing are indeed non-recirculating memory cells that are in disequilibrium with the systemic pool of TCM and TEM cells. However, it should be noted that the total number OT-I TRM cells generated in MVA-OVA-tattooed ears was lower in recipients of male OT-I cells than in recipients of female OT-I cells, suggesting that the ongoing anti-male immune response had some effect on the efficiency in local TRM formation.

### 5.16 TRM cell formation upon MVA delivery by intradermal injection

The above experiments have shown that local antigen recognition in the skin is critical for the development of skin TRM cells after MVA tattooing. As MVA tattooing primarily targets viral antigen expression to the epidermis (Fig. 2), which also represents the anatomical compartment where TRM cells preferentially reside (Fig. 10a), it was interesting to examine whether skin TRM cells are also generated if the viral infection remains localized to the dermis.

In order to restrict MVA-derived antigen expression to the dermis, a model of cutaneous MVA infection was used based on intradermal injection of the virus into the ear pinnae (Tschärke & Smith, 1999). To visualize the site of viral antigen synthesis upon i.d. MVA delivery, mice were injected with  $1 \times 10^8$  IU MVA-lacZ into the ear pinna and sections of infected ears were analyzed 8 hours later by X-Gal staining.



**Figure 24: Intradermal MVA injection restricts infection and viral antigen synthesis to the dermis.** X-Gal staining of virus-infected cells in frozen sections of MVA-lacZ-infected ears 8h post inoculation by either tattooing (Tattoo) or intradermal injection (i.d.). Untreated ears contralateral to the i.d. MVA-lacZ injection site served as negative control. Sections were counterstained with nuclear fast red. 20x magnification; Scale bars, 100  $\mu$ m. Data are representative of a least three independent experiments.

Interestingly, injection of MVA into the ear pinna resulted in a substantially higher number of MVA-infected (lacZ+) cells in the skin when compared to inoculation by tattooing (Fig. 24). Importantly, while upon tattooing virus-infected (lacZ+) cells were predominantly detected within the epidermis, after i.d. MVA injection lacZ+ cells were exclusively found in the underlying dermal compartment (Fig. 24). A similar distribution of virus-infected cells was seen when analyzing MVA-lacZ-injected ears 18 hours post infection (data not shown).

The data therefore show that i.d. injection of MVA into the ear pinna generates a localized infection in the skin, during which viral antigen is produced only within the dermal layer, but not the skin epithelium.

Next, it was investigated i) whether i.d. MVA injection is also capable of eliciting TRM cells in the skin and ii) whether the local establishment of TRM cells might be similarly dependent on *in situ* cognate antigen recognition as in MVA-tattooed skin. To this end, mice harboring CD45.1+ OT-I cells were again immunized i.v. with MVA-OVA and subsequently injected i.d. with MVA and MVA-OVA into the left and right ear, respectively (Fig. 25a).

As expected, this immunization regimen resulted in a robust priming of adoptively transferred OT-I cells as well as endogenous B8R-specific CD8+ T cells and both antigen-specific CD8+ T cell populations were readily detected in the spleens of immunized mice after establishment of T cell memory (Fig. 25b).

Analysis of differentially injected ears on day 7 post infection showed that the two dermal infections with MVA and MVA-OVA promoted a robust local recruitment of virus-specific effector CD8+ T cells. The magnitude of OT-I cell infiltration was found to be roughly similar between MVA- and MVA-OVA-infected ears (Fig. 25c) and also compared to that observed after MVA/MVA-OVA tattooing (Fig. 21c). Unexpectedly, B8R-specific effector CD8+ T cells seemed to be slightly more enriched in both number and frequency in previously MVA-infected ears (Fig. 25c). However, this difference was not statistically significant and could reflect variances in the efficacy of virus inoculation between left and right ears.

In line with the findings obtained after MVA/MVA-OVA tattooing, analysis of i.d. injected ears after establishment of memory revealed that OT-I cells again preferentially resided in previously MVA-OVA-injected ears. B8R-specific CD8+ T cells on the other hand again predominantly occupied MVA-infected ears and were only scarcely found in MVA-OVA-infected ears (Fig. 25c).

A similar regional distribution of memory OT-I and B8R-specific CD8+ T cells was observed in i.d. MVA/MVA-OVA-injected ears of mice which had received transfer of male OT-I cells (data not shown).

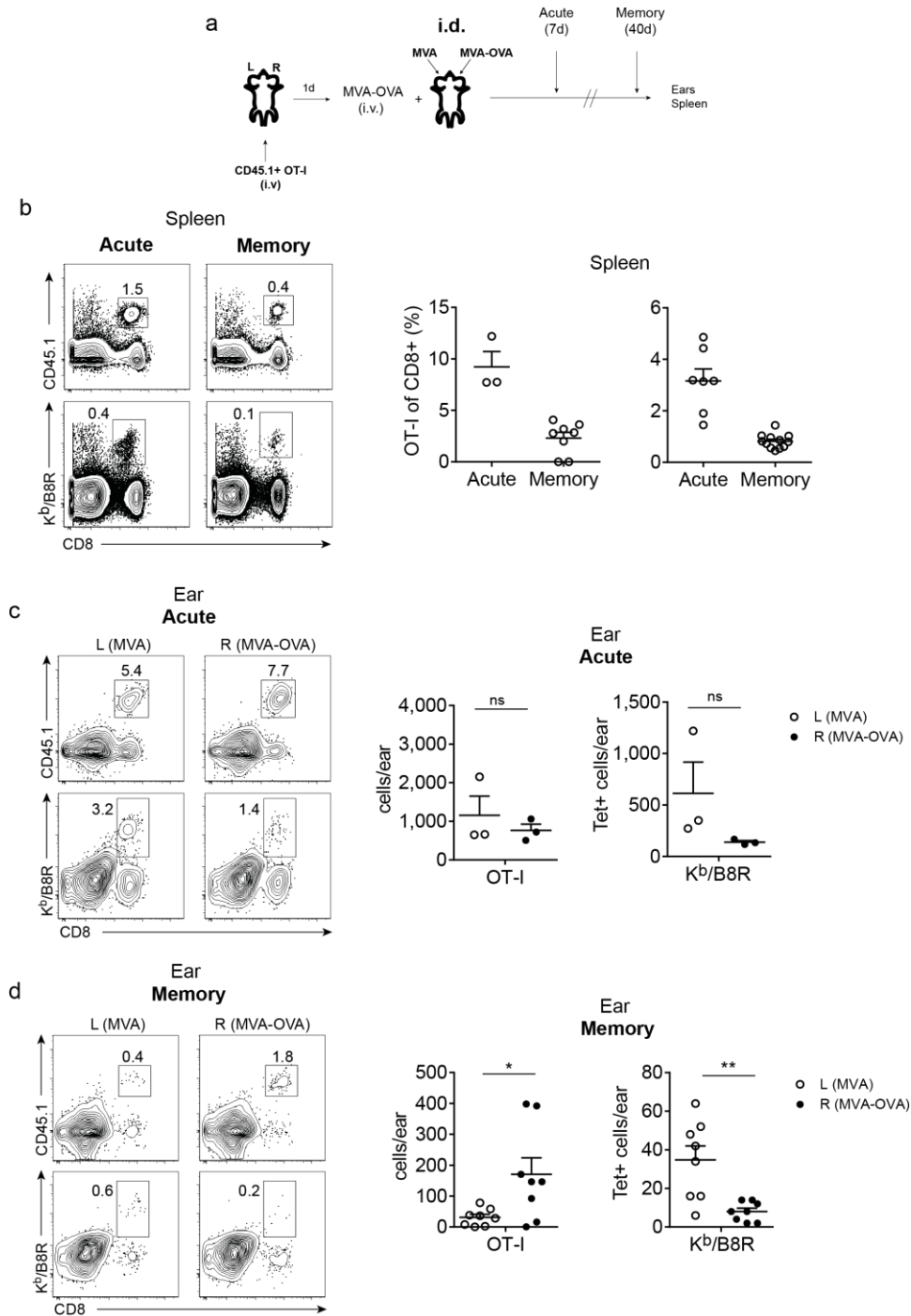


**Figure 25: Virus-specific CD8+ TRM cells are also generated in response to dermal MVA infection.**

(a) Mice were adoptively transferred (i.v.) with 50,000 naïve CD45.1+ OT-I cells and immunized i.v. with  $2 \times 10^6$  IU MVA-OVA. Shortly thereafter, mice were injected i.d. with  $2 \times 10^6$  IU MVA and  $2 \times 10^6$  IU MVA-OVA into the left (L) and right (R) ear pinna, respectively. During the acute phase (Acute, day 7) and the memory phase (Memory, day 40) after immunization, OT-I cells and B8R-specific CD8+ T cells were identified in ears and spleen. (b) Representative plots showing the frequency OT-I cells and B8R-specific CD8+ T cells in the CD45+ leukocyte population in the spleen (left panel). Frequency of OT-I cells and B8R-specific CD8+ T cells in the CD8+ T cell population in spleen (right panel). (c, d) Representative plots depicting the frequency of OT-I cells and B8R-specific CD8+ T cells in the CD45+ leukocyte population in left (L) and right (R) ears during the acute phase (c) and memory phase (d) post infection (left panel). Total number of OT-I cells and B8R-specific CD8+ T cells in left (L) and right (R) ears (right panel) during the acute phase (c) and memory phase (d) (right panel). Horizontal bars indicate the mean and error bars represent SEM. Data are derived from 1 experiment (Acute, n=3) or pooled from 2 independent experiments (n=8). Statistical analysis (paired Student's *t*-test). ns, not significant. \*  $P < 0.05$ , \*\*  $P < 0.01$

In conclusion, these results suggest that skin-resident memory populations of antiviral CD8<sup>+</sup> T cells are also established upon intradermal delivery of MVA and further indicate that local recognition of cognate antigen might be a general prerequisite for the long-term retention and/or survival of TRM cells in MVA-infected skin, regardless of whether the infection is restricted to the epidermis or the underlying dermis. Moreover, the findings show that the composition of the local repertoire of TRM cells generated in previously MVA-injected skin is also shaped by local competition between different virus-specific CD8<sup>+</sup> T cells.

### **5.17 MVA tattooing is superior to i.d. injection of MVA in generating CD103<sup>hi</sup> skin TRM cells**

Interestingly, comparison of the population size of established memory CD8<sup>+</sup> T cell populations in the skin between the two models of cutaneous MVA infection revealed that significantly lower numbers of both OT-I and B8R-specific memory CD8<sup>+</sup> T cells had been generated upon intradermal delivery of the virus (Fig. 26a). Strikingly, phenotypic analysis of OT-I and B8R-specific memory CD8<sup>+</sup> T cells isolated from i.d. MVA-OVA- and MVA-injected ears, respectively, further demonstrated that only around 40-50% of the cells within either population displayed high expression of the TRM cell marker CD103, in contrast to MVA-OVA- or MVA-tattooed ears, in which approximately 80-90% of OT-I and B8R-specific memory CD8<sup>+</sup> T cells were CD103<sup>hi</sup> (Fig. 26b, c).

This difference was even more pronounced when comparing the total number of CD103<sup>hi</sup> cells between i.d. injected and tattooed ear skin (Fig. 26d). Interestingly, i.d. injected and tattooed skin harbored similar total numbers of CD103<sup>hi</sup> OT-I or B8R-specific memory CD8<sup>+</sup> T cells (Fig. 26d).

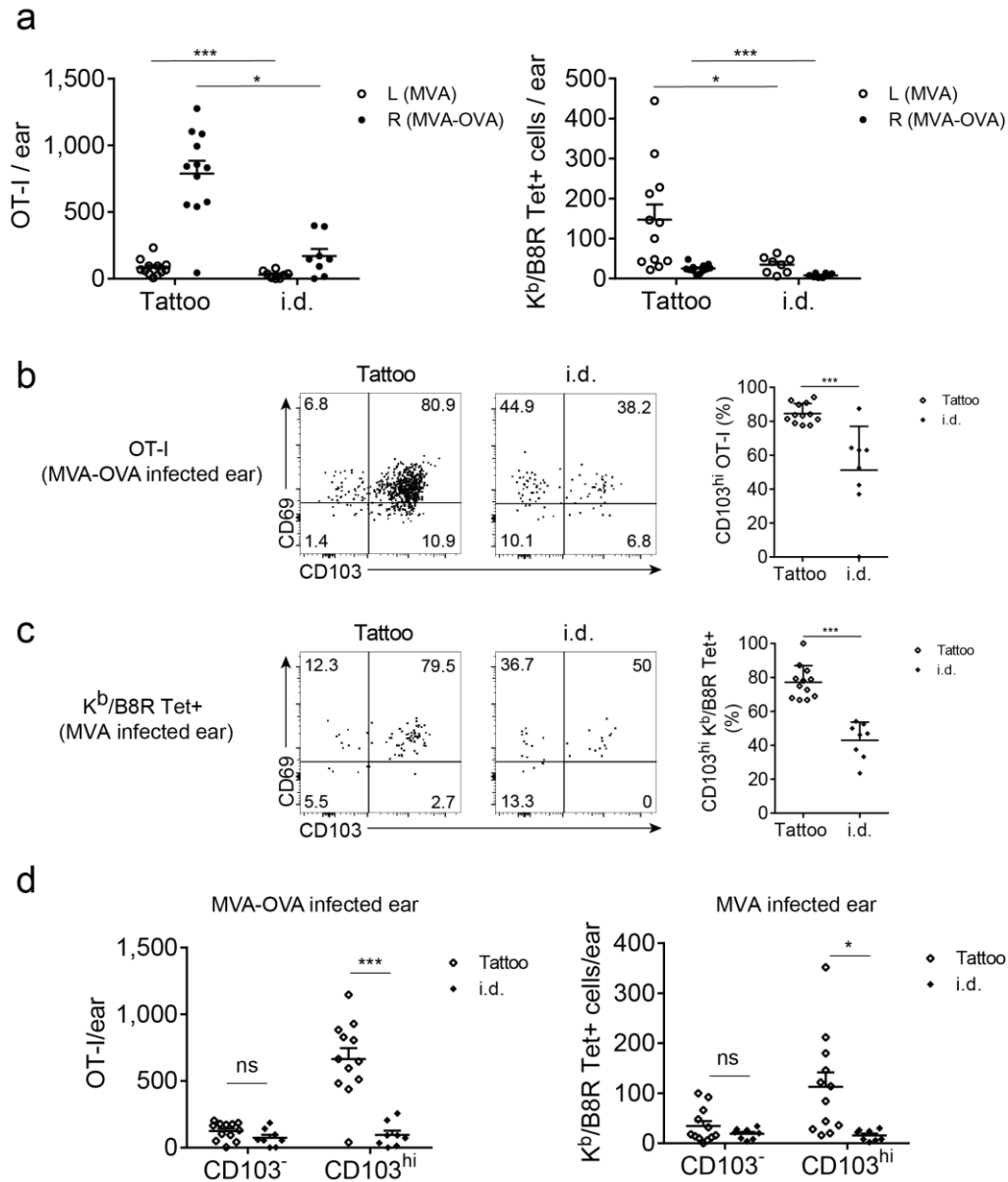


**Figure 26: Intradermal delivery of MVA is inferior to MVA tattooing in generating CD103<sup>hi</sup> TRM cells.**

(a) Comparison of the total number of OT-I (left panel) and B8R-specific CD8<sup>+</sup> T cells (right panel) in MVA-infected ears (L) and MVA-OVA-infected ears (R) of mice (treated as described in Fig. 20a and Fig. 25a) 40 days after local inoculation by tattooing or i.d. injection. (b) CD69 and CD103 expression on skin OT-I cells in previously MVA-OVA-infected ears after tattooing or i.d. injection (left panel) and frequency of CD103<sup>hi</sup> cells in the local OT-I cell population (right panel). (c) CD69 and CD103 expression on B8R-specific CD8<sup>+</sup> T cells in previously MVA-tattooed or MVA-injected ears (left panel) and frequency of CD103<sup>hi</sup> cells within the B8R-specific T cell population. (d) Quantification of CD103<sup>-</sup> and CD103<sup>hi</sup> OT-I cells (left panel) and B8R-specific CD8<sup>+</sup> T cells (right panel) in MVA-OVA- and MVA-infected ears, respectively, upon tattoo or i.d. delivery. Data are based on the experiments shown in Fig. 20 (n=12) and Fig. 25 (n=8). Statistical analysis (unpaired Student's *t*-test). ns, not significant. \* *P* < 0.05, \*\* *P* < 0.01, \*\*\* *P* < 0.001

In line with the lower abundance of CD103<sup>hi</sup> cells in the memory pool of antiviral CD8<sup>+</sup> T cells in previously i.d. injected skin, histological analysis of memory OT-I cells in the memory phase after MVA-OVA injection showed that the cells accumulated mainly within the dermal compartment and only rarely occupied the epidermal layer (Fig. 27). In contrast, memory OT-I cells residing in MVA-OVA-tattooed ears predominantly localized



to the epidermis (Fig. 27), consistent with the markedly increased local frequency of cells expressing CD103 and the role of this integrin in enabling persistence of CD8<sup>+</sup> T cells in this anatomical niche (Mackay et al., 2013).

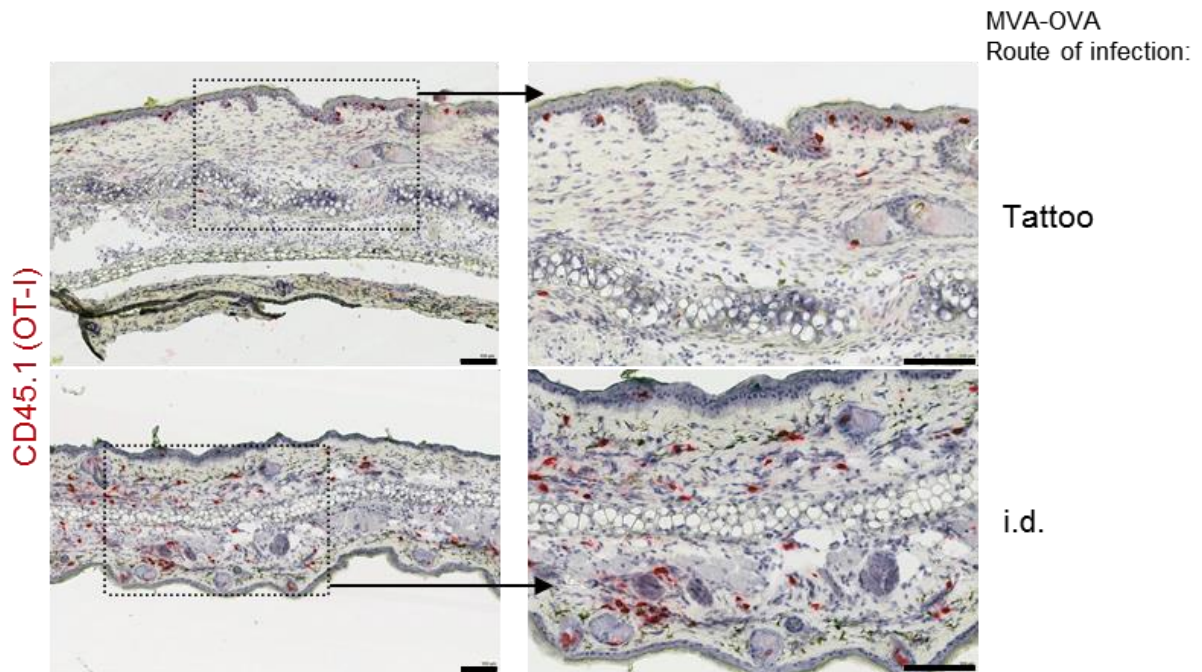


**Figure 27: Differential tissue localization of memory OT-I cells after MVA-OVA tattooing and i.d. MVA-OVA injection.** IHC staining of OT-I cells in frozen ear skin sections obtained >50 day after local MVA-OVA inoculation by tattooing or i.d. injection. OT-I cells (shown in red) were visualized using antibodies against the congenic marker CD45.1. Scale bars, 100  $\mu$ m. Data are representative of at least three independent experiments

In summary, these results indicate that intradermal MVA infection only poorly supports the development of epidermis-resident CD103<sup>hi</sup> TRM cells and suggest that an optimal generation of these cells might require a cutaneous infection which either directly involves the epidermis or takes place in the presence of a local epidermal injury.

## 6 Discussion

Tissue-resident memory (TRM) CD8<sup>+</sup> T cells have been recently identified as non-recirculating memory T cells that reside within non-lymphoid tissues such as the skin, the mucosal epithelia of lung, gut and reproductive tracts as well as the CNS (Casey et al., 2012; Cuburu et al., 2012; Gebhardt et al., 2009; Jiang et al., 2012; Shin & Iwasaki, 2012; Wakim et al., 2013; Wakim et al., 2010). Because CD8<sup>+</sup> TRM cells are typically positioned within epithelial barriers of pathogen entry sites, they are able to mount an immediate response to local reinfection and thereby critically contribute to protective immunity (Gebhardt & Mackay, 2012; Schenkel & Masopust, 2014). Recent data suggest that rapid TRM-mediated pathogen control is not simply based upon a direct elimination of infected cells via contact-dependent cellular cytotoxicity. It has been shown that upon reactivation by their cognate peptide, TRM cells rapidly secrete pro-inflammatory cytokines which not only orchestrate an accelerated recruitment of circulating memory T cells (Schenkel et al., 2013), but also induce a tissue-wide state of pathogen alert that even renders the tissue resistant to infection with antigenically unrelated pathogens (Ariotti et al., 2014; Schenkel et al., 2014).

There is increasing interest to develop novel vaccines or vaccination strategies that optimize TRM cell generation within non-lymphoid barriers, as these memory CD8<sup>+</sup> T cells might be key to provide protection against critical human pathogens, such as HIV, *Mycobacterium tuberculosis* or *Plasmodium falciparum*, which are known to establish infection within mucosal surfaces in non-lymphoid tissues (Seder & Hill, 2000).

In this study, it was investigated whether cutaneous immunization with the modified vaccinia virus Ankara (MVA), a non-replicating poxvirus vector currently evaluated in clinical trials as recombinant vaccine vector against infectious diseases or cancer, is able to induce TRM formation in the skin. To this end, a skin inoculation method was established which was based on the delivery of MVA into superficially injured skin by means of local skin tattooing. In mice, skin tattooing already represents an established technique for the application of DNA vaccines (Bins et al., 2005), however this route of immunization has not been used for MVA vectors yet. Therefore, initial experiments were performed to characterize this novel MVA inoculation method with regard to its efficacy in virus delivery into the skin as well as its immunogenicity.

Using recombinant MVA vectors encoding different reporter genes (*lacZ*, luciferase) it could be shown that a local MVA skin tattoo primarily targets the viral infection into the

epidermal layer of the skin. Expression of MVA-derived recombinant antigen was detectable as early as 6 hours post tattooing and reached its peak at around 10 hours post infection, whereas after 48 hours, only residual recombinant antigen expression was observed. As indicated by histological examination of MVA-lacZ-tattooed skin, MVA-driven antigen synthesis remained strictly confined to the site of initial tattoo inoculation, demonstrating that MVA tattooing induces a highly localized and acute infection of the skin.

Subsequent immunization studies performed with an MVA vector expressing the model antigen ovalbumin (OVA) revealed that MVA delivery by tattooing resulted in a robust induction of both OVA- as well as vector (B8R)-specific CD8<sup>+</sup> T cell responses in the spleens of immunized mice. The primary induction of antigen-specific CTL responses upon MVA tattooing was similar in both quantity and quality to that achieved after intramuscular (i.m.) MVA injection, the current standard mode of MVA administration in clinical studies (Gomez et al., 2007).

Tattoo-immunized mice also demonstrated a similar degree of protection as i.m. immunized animals when challenged in the memory phase post immunization with a lethal intranasal dose of replication-competent vaccinia virus (VV). In summary, these data show that MVA skin tattooing is a highly immunogenic delivery route for MVA vectors, which is in line with recent data showing that inoculation of vaccinia viruses through barrier-disrupted skin represents a potent means to induce long-lasting protective immunity in mice (Liu et al., 2010; Seneschal et al., 2013).

*Cutaneous MVA infection efficiently promotes effector CD8<sup>+</sup> T cell recruitment and local TRM cell development*

Antigen-specific effector CD8<sup>+</sup> T cells primed by MVA tattooing readily infiltrated MVA-infected skin and strongly accumulated in this site by day 7 post infection. In contrast, untreated skin contralateral to the inoculation site harbored only few antigen-specific CD8<sup>+</sup> T cells, indicating that primed effector CD8<sup>+</sup> T cells do not efficiently infiltrate the skin in the absence of infection or inflammation. At this early stage of the immune response, antigen-specific effector CD8<sup>+</sup> T cells predominantly populated the dermal layer of MVA-infected skin, similar to what has been described for antigen-specific effector CD8<sup>+</sup> T cells entering the site of local HSV or VV skin infection (Gebhardt et al., 2009; Liu et al., 2010). Thus, the acute cutaneous MVA infection is sufficient to promote a

robust local recruitment of effector CD8<sup>+</sup> T cells from the circulation. Analyses during the memory stage of the CD8<sup>+</sup> T cell response (more than 40 days p.i.) revealed that previously MVA-tattooed skin was still highly enriched with antigen-specific CD8<sup>+</sup> T cells when compared to contralateral skin or skin regions distant to the original inoculation site. The data provide evidence that a localized and abortive infection with non-replicating MVA was sufficient to generate a long-lived, local memory CD8<sup>+</sup> T cell population in the skin. Interestingly, the total number of antigen-specific memory CD8<sup>+</sup> T cells in the prior MVA inoculation site was remarkably similar when comparing experiments performed during the early (d40 p.i.) or late (> d100 p.i.) memory phase, suggesting that the memory CD8<sup>+</sup> T cell pool established at the site of prior infection does not undergo a substantial contraction over time. Notably, antigen-specific memory CD8<sup>+</sup> T cells remained detectable in MVA-tattooed skin for at least one year after the initial viral application (data not shown), demonstrating that this peripheral memory CD8<sup>+</sup> T cell pool might be maintained throughout the entire life span of the immunized animal.

Previous studies have shown that TRM cells are phenotypically distinct from their effector memory (TEM) and central memory (TCM) CD8<sup>+</sup> T cell counterparts found in the circulation (Gebhardt & Mackay, 2012; Schenkel & Masopust, 2014). In the majority of non-lymphoid compartments, TRM cells express high levels of the  $\alpha$ E subunit (CD103) of  $\alpha$ E $\beta$ 7 integrin and show increased expression of early T cell activation marker CD69. Both molecules have been demonstrated to play a functional role in promoting T cell residence within tissues. CD69 has been suggested to facilitate the initial tissue retention of infiltrating effectors CD8<sup>+</sup> T cells (Mackay et al., 2013; Skon et al., 2013), presumably by antagonizing the function of the sphingosine-1-phosphate receptor (S1P1), which mediates non-lymphoid tissue exit of lymphocytes through lymphatic vessels. CD103 on the other hand has been suggested to be relevant for the long-term retention and/or survival of TRM cells within epithelial barriers (Mackay et al., 2013), possibly by enabling interaction with or anchoring to E-cadherin expressed on epithelial cells. Surface marker analysis of antigen-specific memory CD8<sup>+</sup> T cells isolated from MVA-tattooed skin revealed that the majority of cells exhibited a CD103<sup>hi</sup>, CD69<sup>+</sup> phenotype, whereas memory CD8<sup>+</sup> T cells in lymphoid tissues, such as the spleen, were predominantly CD103<sup>-</sup> and CD69<sup>-</sup>. In contrast to their systemic counterparts, memory CD8<sup>+</sup> T cells retained in MVA skin inoculation sites also expressed high levels of collagen-binding integrin CD49a (VLA-1), consistent with what has been described for TRM cells established upon resolved HSV-1 skin infection (Gebhardt et al., 2009). Also, similar to TRM cells found in skin infection

models using replicating viruses (Gebhardt et al., 2009; Gebhardt et al., 2011; Liu et al., 2010), memory CD8<sup>+</sup> T cells generated upon MVA infection resided mainly in the epidermis, consistent with their high expression of CD103. Another hallmark feature of TRM cells is their persistence within a single non-lymphoid compartment without continuous recirculation through the blood (Gebhardt & Mackay, 2012; Schenkel & Masopust, 2014). To confirm that TRM cells generated in MVA-tattooed skin are indeed part of a non-recirculating memory CD8<sup>+</sup> T cell subset, an adoptive transfer model was used which involved the transfer of male donor CD8<sup>+</sup> T cells into female recipient mice. In this setting, only circulating populations of male origin donor cells are cleared by the resulting immune response directed to the male minor transplantation antigen, whereas cells without access to the circulation (i.e. tissue-resident cells) are spared from depletion (Gebhardt et al., 2011). Using this approach, it could be shown that male-origin donor CD8<sup>+</sup> T cells readily established a long-lived tissue-resident pool of memory CD8<sup>+</sup> T cells in MVA-tattooed skin, despite a complete elimination from the blood or lymphoid tissue within two weeks post infection.

Taken together, these data indicate that antigen-specific memory CD8<sup>+</sup> T cells generated at the site of former MVA skin infection are a long-lived population of bona fide skin TRM cells and suggest that non-replicating MVA might be suitable as a vaccine vector for the establishment of TRM cells in non-lymphoid sites. Furthermore, the finding that skin TRM cells are maintained for extended periods of time after non-replicating skin infection with MVA strongly argues in favor of the notion that the long-term maintenance of this memory CD8<sup>+</sup> T cell subset does not depend on continuous stimulation of the cells by persisting antigen (Casey et al., 2012; Mackay et al., 2012).

The results obtained in this thesis further suggest that local immunization is required to efficiently induce TRM cell lodgment to the skin. This was demonstrated by the finding that the intramuscular route of MVA administration, while similarly effective to the tattoo route in generating circulating populations of antigen-specific effector and memory CD8<sup>+</sup> T cells, did not result in an appreciable formation of TRM cells in the skin. Note that upon priming, the two inoculation routes elicited similar proportions of circulating antigen-specific effector CD8<sup>+</sup> T cells with a memory precursor effector cell (MPEC) phenotype (CD127<sup>+</sup>, KLRG1<sup>lo</sup>), which have previously been identified as the precursors to long-lived TRM cells (Mackay et al., 2013). Thus, the failure of intramuscular route of MVA infection to establish long-lived TRM cells in the skin might be explained by a rather

inefficient skin recruitment of effector T cells due to the absence of cutaneous inflammation.

*Skin TRM cells induced by MVA tattooing provide local immunity*

Previous studies have shown that TRM cells are superior to circulating memory CD8<sup>+</sup> T cells (including TEM and TCM cells) in providing protection against peripheral tissue infections (Jiang et al., 2012; Mackay et al., 2012). The VV skin challenge experiments performed in this study suggest that this is also true for TRM cells generated upon cutaneous immunization with non-replicating MVA. This was demonstrated by the result that MVA-tattooed mice, which harbor both TRM cells at the prior skin inoculation site and circulating systemic memory CD8<sup>+</sup> T cells were able to rapidly clear a secondary local skin infection with VV, whereas i.m. immunized animals which contain mostly circulating populations virus-specific memory CD8<sup>+</sup> T cells, had a clear deficit in eliminating VV from the skin. Interestingly, local viral clearance was similarly impaired in mice that harbored virus-specific TRM cells at a skin location distant to the VV challenge site. Thus, rapid control of a cutaneous VV infection requires TRM cells to be present within the tissue by the time of reinfection. From a practical point of view, however, this means that in case of a large non-lymphoid organ like the skin, efficient TRM-mediated immunity can only be provided if these cells are distributed throughout the entire non-lymphoid organ. Based on the results presented here, however, such wide-spread seeding of TRM cells might not be achieved by a single skin immunization with MVA, as TRM cells were predominantly found at the site of prior virus inoculation. Thus, in order to provide efficient TRM-based immunity by vaccination with MVA, the virus must be targeted directly or in close proximity to potential pathogen entry portals, which dictates that the viral application route should be tailored to the natural location of pathogen transmission.

A recent study has suggested that multiple sequential inoculations of VV performed at different cutaneous locations (i.e. flank, ear and tail) are able to induce protective amounts of TRM cells also in regions remote to the individual VV inoculations sites (Jiang et al., 2012). Although it was not tested here, such a prime/boost regimen could also be a promising strategy to enhance TRM cell lodgment in distant skin locations using MVA vectors.

However, it is known that successive rounds of antigen stimulation increasingly skew the responding memory CD8<sup>+</sup> T cell pool towards a TEM fate, resulting in increased

peripheral homing potential of the cells and possibly also to an enhanced recirculation through non-inflamed non-lymphoid tissues (Jabbari & Harty, 2006; Masopust et al., 2006a). In addition, secondary and tertiary memory CD8<sup>+</sup> T cells were demonstrated to undergo increasingly slower contraction when compared to primary memory CD8<sup>+</sup> T cells. Thus, it remains to be determined whether the sequential skin immunization strategy used by Jiang et al. truly resulted in the establishment of bona fide, non-recirculating (CD103<sup>+</sup> CD69<sup>+</sup>) TRM cells throughout the entire organ, or rather resulted in an increased induction of skin-recirculating TEM cells, which unlike TRM cells might ultimately be lost from the memory cell pool in the absence of antigen (Marzo et al., 2005; Wherry et al., 2003).

#### *Role of regulatory T cells in the establishment of skin-resident CD8<sup>+</sup> T cell memory*

Foxp3<sup>+</sup> regulatory T cells (Tregs) are a specialized subset of CD4<sup>+</sup> T helper cells which have immunosuppressive properties and play an essential role in the maintenance of peripheral tolerance (Kim et al., 2007; Lahl et al., 2007) and the restoration of immune cell homeostasis following inflammation or infection (Belkaid, 2007; Belkaid & Tarbell, 2009). Recent work from our laboratory has demonstrated that upon systemic infection with MVA, Tregs selectively suppress the generation of short-lived effector CD8<sup>+</sup> T cells (SLECs) by reducing the level of expression of the co-stimulatory molecule CD80 and CD86 on DC and also by restricting the availability of IL-2, which is a critical cytokine for SLEC differentiation (Kastenmuller et al., 2011). In line with the selective inhibitory effect on the expansion of SLECs, Treg-mediated suppression was found to have little influence on the development of systemic CD8<sup>+</sup> T cell memory (Kastenmuller et al., 2011). Accumulating data suggest that the microenvironment of non-lymphoid tissues has an instructive role in the formation of CD8<sup>+</sup> TRM cells (Mueller et al., 2014; Schenkel & Masopust, 2014), for example by providing TGF- $\beta$  signals required for the expression of CD103. Notably, Tregs are a known source of TGF- $\beta$  (Nakamura et al., 2001) and are found at a high frequency in various non-lymphoid tissues, including the skin (Dudda et al., 2008; Sather et al., 2007). Given the described role of Tregs in controlling the antiviral CD8<sup>+</sup> T cell response to systemic MVA infection and the high abundance of Tregs in the skin, it was interesting to examine whether this subset also controls the CD8<sup>+</sup> T cell response upon cutaneous MVA infection and might have an influence on the establishment of local tissue-resident CD8<sup>+</sup> T cell memory.

Using DEREK mice (in which Tregs can be depleted by application of diphtheria toxin), it could be shown that in the context of a localized cutaneous infection with MVA, Tregs also dramatically dampen the expansion of virus-specific effector CD8<sup>+</sup> T cells. This was indicated by an approximately 2-fold increase in the frequency of systemic B8R-specific CD8<sup>+</sup> T cells at the peak of expansion in Treg-depleted DEREK mice in comparison to non-depleted littermate controls. After establishment of memory (90 days after MVA-OVA tattooing), however, no difference could be found in the levels of B8R-specific memory CD8<sup>+</sup> T cells in the spleen between Treg-depleted and non-depleted animals.

The depletion of Tregs also resulted in a dramatically increased accumulation of B8R-specific effector CD8<sup>+</sup> T cells within MVA-infected skin on day 7 post MVA tattooing, but appeared to have little impact on the local generation of antiviral TRM cells, as comparable numbers of B8R-specific TRM cells were observed at the site of MVA tattooing between the two experimental groups on day 90 post infection.

Taken together, these results support published data obtained after systemic MVA immunization (Kastenmuller et al., 2011) and further suggest that upon acute MVA infection of the skin, Tregs may not play a significant role in the establishment of localized tissue-resident CD8<sup>+</sup> T cell memory.

Interestingly, a recent study has identified that TRM cells which form in the skin epithelium upon localized HSV-infection originate from KLRG1<sup>lo</sup> memory precursor effector cells (MPECs), which enter the tissue early during the response (Mackay et al., 2013). Given that upon acute MVA infection, Tregs primarily control the pool size of KLRG1<sup>hi</sup> short-lived effector cells (SLECs), but leave the MPEC compartment largely unaltered (Kastenmuller et al., 2011), this finding might explain why despite a more substantial effector CD8<sup>+</sup> T cell accumulation in the tissue, formation of virus-specific skin TRM cells in Treg-depleted mice was not increased.

#### *Relative contribution of skin inflammation and local antigen to TRM formation in MVA-infected skin*

Since the first identification of TRM cells, many studies have sought to elucidate the requirements for TRM cell development, as this knowledge might help in the development of strategies that optimize lodgment of TRM cells within a given tissue.

It has been generally accepted that peripheral pools of CD8<sup>+</sup> TRM cells are established during the effector stage of an immune response, when tissue-homing receptor expression



is at maximum (Klonowski et al., 2004; Mackay et al., 2012; Masopust et al., 2010; Shin & Iwasaki, 2012). Current evidence suggests that TRM cells arise from a subset of tissue-infiltrating effector CD8<sup>+</sup> T cells that still exhibit developmental plasticity (Mackay et al., 2013). Upon tissue entry, these precursor cells (which have been identified as KLRG1<sup>lo</sup> CD127<sup>+</sup> MPECs), are instructed by environmental signals to undergo a local conversion into long-lived CD103<sup>+</sup> CD69<sup>+</sup> TRM cells. In this context, the immunoregulatory cytokine TGF- $\beta$  has been suggested as a major local TRM-promoting factor owing to its capacity to drive expression of CD103 (Casey et al., 2012; Cepek et al., 1993), which is critical for the long-term persistence of lymphocytes within epithelial compartments. In the skin, TRM cell formation seems to further depend upon IL-15 and environmental ligands for the aryl hydrocarbon receptor (Ahr), a ligand-activated cytosolic transcription factor (Mackay et al., 2013; Zaid et al., 2014). Interestingly, responsiveness to IL-15 might be a general requirement for residency within the epidermis, as indicated by the finding that the epidermis-resident DETCs fail to develop in mice deficient in IL-15R $\alpha$  expression (Pantelyushin et al., 2012).

A recent study has demonstrated that in the skin or the mucosa of the female reproductive tract, local inflammation alone can be sufficient to promote a recruitment of circulating effector CD8<sup>+</sup> T cells and to support their differentiation into CD103<sup>+</sup> TRM cells (Mackay et al., 2012). Based on this phenomenon, Shin et al. have developed a ‘prime and pull’ vaccination strategy, which combined a conventional s.c. immunization (‘prime’) with a topical application of the T cell attracting chemokines CXCL9 and CXCL10 (‘pull’) to the vaginal mucosa (Shin & Iwasaki, 2012). By mimicking a local tissue inflammation, this local chemokine treatment was able to recruit (or pull) systemic virus-specific effector CD8<sup>+</sup> T cells into the tissue and was able to establish a long-lived pool of mucosal TRM cells, despite the absence of overt tissue inflammation or viral antigen in the tissue (Shin & Iwasaki, 2012). Thus it appears that in non-lymphoid compartments like the skin or the mucosa, local antigen recognition is dispensable for the differentiation and maturation of long-lived TRM cells. Conversely, in neuronal tissues such as the CNS or the sensory root ganglia *in situ* recognition of cognate antigen was found to be important for the formation and local maintenance of CD103<sup>+</sup> TRM cells (Mackay et al., 2012; Wakim et al., 2010). Considering the finding that local inflammation alone can support TRM development in the skin even in the absence of local antigen (Mackay et al., 2012), it was asked whether the local skin inflammation elicited by the MVA tattoo inoculation might be the determining local factor responsible for the preferential accumulation of TRM cells at the

site of prior skin inoculation. Since local inflammation following an MVA skin tattoo is elicited as a response both to the mechanical skin injury as well as the local virus infection, an experimental model was used to examine the relative roles of these two inflammatory signals as well as *in situ* cognate antigen recognition in mediating TRM cell formation in MVA-infected skin. This model was based on two steps: 1) Generation of a circulating pool of OVA-specific effector CD8<sup>+</sup> T cells by i.v. MVA-OVA immunization of mice seeded with OT-I CD8<sup>+</sup> T cells. 2) Tattoo inoculation on the ear with either PBS alone, wild-type MVA (lacking the relevant antigen for OT-I cells) or MVA-OVA, shortly after i.v. priming.

The model could convincingly show that the acute skin inflammation elicited upon skin injury or MVA infection alone was rather inefficient in supporting the local formation of OT-I TRM cells. Although both inflammatory stimuli were sufficient to recruit circulating effector OT-I cells to the skin, during memory neither PBS- nor MVA-tattooed ears contained significantly increased amounts of OT-I TRM cells when compared to untreated ears, in which only very few OT-I TRM cells were detectable.

Interestingly, *in vivo* primed OT-I cells accumulated to a similar extent in both MVA- and MVA-OVA-infected ears during the acute phase of the response, however, OT-I TRM cells were only efficiently established in previously MVA-OVA-infected ears. A similar bias in OT-I TRM cell lodgment was seen in analogous experiments, in which MVA and MVA-OVA were injected into the ear pinnae, indicating that this phenomenon is not specific to the tattoo route of virus inoculation. Based on these data, it could be concluded that while local antigen expression appeared dispensable for the recruitment of effector CD8<sup>+</sup> T cells to the tissue, it is critically required for long-term retention and/or survival of skin-infiltrating effector CD8<sup>+</sup> T cells *in situ*.

In summary, these experimental data suggest that *in situ* cognate antigen recognition might be a key instructive signal for the development of TRM cells in MVA-infected skin and could explain why TRM cell lodgment in this model of infection is strongly confined to the site of virus inoculation. The insights gained from these studies expand our understanding of how TRM cells are generated after acute viral infection of the skin and provide an important basis for the development of novel MVA-based vaccination strategies aimed to establish resident CD8<sup>+</sup> T cell populations within non-lymphoid tissues.

The findings might also be of interest for already established immunization protocols, such as the ‘prime and pull’ vaccination approach, which could exploit the TRM-promoting capacity of local antigen to enhance TRM cell numbers at the site of chemokine

application (Shin & Iwasaki, 2012). Future work however will be needed to address whether local cognate antigen recognition has a similar role in promoting TRM cell development in non-lymphoid tissues other than the skin. Further work should also go into identifying the cell types involved in the local antigen presentation to tissue-infiltrating CD8<sup>+</sup> T cells, as this knowledge might allow for a rational design of vaccines that efficiently target antigen to relevant antigen-presenting cell population(s).

The finding that local inflammation, either elicited by skin injury alone or MVA tattooing, only poorly supported accumulation of skin OT-I TRM cells in the absence of local antigen is seemingly at odds with the study by Mackay et al. which demonstrated a strong accumulation of CD103<sup>+</sup> skin TRM cells upon local treatment with the contact sensitizer 2,4-dinitrofluorobenzene (DNFB) (Mackay et al., 2012). However, the cutaneous inflammatory response elicited upon MVA tattooing is likely to differ from that induced after topical DNFB application not only in duration but also in the quality of the local cytokine milieu, which makes a direct comparison of these two models difficult. Moreover, the study by Mackay et al. used *in vitro* activated CD8<sup>+</sup> T cells to monitor skin recruitment and local TRM formation, whereas in the experimental model used here *in vivo* primed CD8<sup>+</sup> T cells were analyzed, which are likely to enter the skin with a delayed kinetics.

*Possible mechanism for local antigen-mediated TRM formation in MVA-infected skin*

Although the experimental data have suggested a clear role of local antigen recognition for the establishment of tissue-resident CD8<sup>+</sup> T cell memory in MVA-infected skin, the mechanism by which antigen could facilitate the generation of TRM cells within tissues is still unclear.

It can be speculated however that local encounters with cognate antigen-bearing infected cells could prolong the dwell time of tissue-immigrating effector CD8<sup>+</sup> T cells within the tissue and thus increase the time of exposure to cytokines that mediate TRM differentiation. Antigenic stimulation of the TCR *in situ* could also facilitate local retention and TRM differentiation of infiltrating effector CD8<sup>+</sup> T cell populations by modulating the expression of surface molecules involved in T cell recirculation. For example, previous studies have shown that T cells need to upregulate the expression of chemokine receptor CCR7 in order to leave non-lymphoid compartments, as this molecule is required for T cell entry into the afferent lymphatic vessels (Bromley et al., 2005; Debes et al., 2005). In line with the role of CCR7 in controlling T cell egress from non-lymphoid tissues, Mackay et

al. have demonstrated that upon co-injection into the dermis of mice, CCR7<sup>-/-</sup> CD8<sup>+</sup> T cells more readily established a skin-resident population than wild-type CD8<sup>+</sup> T cells (Mackay et al., 2013). As antigen recognition is known to induce a transient downregulation of CCR7 (Potsch et al., 1999; Unsoeld et al., 2004), it might be expected that skin-infiltrating CD8<sup>+</sup> T cells which receive antigenic signals *in situ* are less likely to exit the tissue than those that do not encounter their cognate antigen.

A recent study has revealed that the loss of the transcription factor KLF2 (Kruppel-like factor 2) represents a critical checkpoint in the commitment of tissue-infiltrating CD8<sup>+</sup> T cells towards a TRM cell fate (Skon et al., 2013). The study demonstrated that KLF2 is lost in tissue-infiltrating effector CD8<sup>+</sup> T cells very soon after their arrival in the tissue and this correlated with a transcriptional downregulation of its target gene *S1pr1*, which encodes for the sphingosine 1-phosphate receptor (S1P1) (Skon et al., 2013). Consistent with these data, it was shown that CD8<sup>+</sup> TRM cells residing in the skin epithelium after local HSV infection contain lower levels of *S1pr1* transcripts than their memory T cell counterparts in lymphoid tissues (Mackay et al., 2013). S1P1 is best known for its role in driving lymphocyte egress from secondary lymphoid organs by mediating their migration towards sphingosine-1-phosphate (S1P) which is present at higher concentrations in blood or lymph than in lymphoid tissue (Matloubian et al., 2004; Schwab et al., 2005). Skon et al. could further demonstrate that forced expression of either KLF2 or S1P1 in CD8<sup>+</sup> T cells dramatically impaired their ability to establish residency in non-lymphoid tissues (Skon et al., 2013), which suggests that S1P1 also has a relevant role in mediating CD8<sup>+</sup> T cell egress from non-lymphoid compartments. Therefore, an early loss of KLF2 and (consequently) S1P1 expression promotes an initial retention of CD8<sup>+</sup> T cells within non-lymphoid tissue and thus might set the course for local tissue residency. KLF2 is expressed at high levels in naïve T cells, but is dramatically downregulated after antigenic stimulation of the TCR (Kuo et al., 1997; Schober et al., 1999). Although the data by Skon et al. suggest that a loss of KLF2 expression in tissue-infiltrating CD8<sup>+</sup> T cells can be induced in the absence of local antigen, most likely by niche-specific cytokines such as TGF- $\beta$  or IL-33 (Skon et al., 2013), it is possible that antigen recognition in MVA-infected skin could further repress the level of KLF2 expression in skin-infiltrating CD8<sup>+</sup> T cells and thus enhance their local retention via downregulation of S1P1 but also CCR7, which represents another major target of this transcription factor (Carlson et al., 2006). In addition, antigenic stimulation of the TCR is known to induce a rapid upregulation of CD69 expression on naïve T cells (van Stipdonk et al., 2001). Given that CD69 has been shown to directly

interfere with the surface expression of S1P1 (Bankovich et al., 2010; Shiow et al., 2006), it is conceivable that a local antigen-driven induction of CD69 could further limit S1P1-mediated tissue egress of recently immigrated virus-specific effector CD8<sup>+</sup> T cells. In fact, Mackay et al. already demonstrated that upon migration into HSV-infected skin, CD69<sup>-/-</sup> HSV-specific CD8<sup>+</sup> T cells were more rapidly lost from the tissue than their wild-type counterparts, indicating that CD69 can indeed facilitate to the retention of T cells in virus-infected skin (Mackay et al., 2013).

In view of these observations, it might be interesting to examine whether KLF2 (including its targets S1P1 and CCR7) or CD69 might be differentially regulated between effector OT-I cell populations in MVA-OVA- versus MVA-infected skin. The dual MVA/MVA-OVA ear inoculation model established here could further be a useful tool to explore whether besides limiting T cells egress from the skin, local antigen signals could have a direct effect on the survival of skin-infiltrating effector CD8<sup>+</sup> T cells, e.g. by inducing the expression of anti-apoptotic proteins such as Bcl-2 or by promoting the expression of cell surface receptors (e.g. IL-15R $\alpha$ ) that increase responsiveness to local survival cytokines.

*MVA delivery through superficially injured epidermis is superior to the intradermal injection route in generating CD103<sup>hi</sup> TRM cells*

The presented data further revealed that the route of skin inoculation is an important factor to consider when aiming at the induction of high densities of CD8<sup>+</sup> TRM cells in the skin. While MVA tattooing resulted in a strong local accumulation of virus-specific memory CD8<sup>+</sup> T cells at the site of prior infection, markedly fewer total numbers of virus-specific memory CD8<sup>+</sup> T cells were found in the skin after i.d. injection of the virus. In addition, the memory CD8<sup>+</sup> T cell pool in previously i.d. MVA-infected skin seemed to contain a substantially lower fraction of CD103<sup>hi</sup> cells (~50%) when compared to that established in tattoo inoculated skin (~90% CD103<sup>hi</sup> cells), which could be indicative of an impaired development of CD103<sup>hi</sup> TRM cells in i.d. MVA-infected skin. This outcome was rather unexpected given that i.d. MVA injection resulted in a higher production of recombinant antigen in the skin when compared to tattooing. Also, the two skin immunization routes promoted a similar recruitment of effector CD8<sup>+</sup> T cells to site of inoculation, suggesting that in addition to local antigen other factors may be needed for an optimal generation of CD103<sup>hi</sup> skin TRM cells.

As recent studies have established that TGF- $\beta$  signals within non-lymphoid compartments are important for the induction of CD103 expression on immigrating effector CD8<sup>+</sup> T cells (Casey et al., 2012; El-Asady et al., 2005; Lee et al., 2011; Mackay et al., 2013; Sheridan et al., 2014; Zhang & Bevan, 2013), a likely explanation for the impaired generation of CD103<sup>hi</sup> TRM cells upon i.d. MVA immunization could be that the levels of TGF- $\beta$  in i.d. injected skin were not sufficient to fully support the differentiation of recruited effector CD8<sup>+</sup> T cells into CD103<sup>hi</sup> TRM cells. TGF- $\beta$  is known to be an important regulatory cytokine during the cutaneous wound healing response and it has been shown that epidermal keratinocytes rapidly upregulate expression of this cytokine in response to epidermal injury (Glick et al., 1993; Yang et al., 2001). Given that injection of MVA into the dermis does not cause any noticeable damage to the skin epithelium, it is likely that the local availability of TGF- $\beta$  in the skin might be considerably lower upon i.d. MVA delivery than after tattooing, which is inherently associated with a disruption of the epithelial barrier. In addition to local injury, it is also possible that MVA infection itself might stimulate keratinocytes to release TGF- $\beta$ . In fact, *in vitro* studies have shown that VV infection can indeed promote an upregulation of TGF- $\beta$  expression in this cell type (Liu et al., 2005). However, given that i.d. injection primarily targets MVA infection to the dermis, it is highly unlikely that keratinocytes become infected and contribute to TGF- $\beta$  production in the skin.

It is interesting to note that most vaccinia virus strains (including MVA) encode a secreted homologue of epidermal growth factor (EGF), called vaccinia virus growth factor (VGF) (Buller et al., 1988), which may in part be responsible for the epidermal thickening typically observed during VV skin infection (Tschärke & Smith, 1999). Given the role of TGF- $\beta$  in suppressing keratinocyte growth (Glick et al., 1993), it is also possible that in the presence of MVA-infected keratinocytes, TGF- $\beta$  expression might be upregulated, e.g. in bystander keratinocytes, in order to counteract VGF-induced epidermal proliferation. In fact, epidermal hyperplasia could only be observed after tattoo application of MVA, but not upon intradermal delivery of MVA (data not shown).

Mackay et al. recently provided evidence that entry into the skin epithelium is a critical step in the development of CD103<sup>hi</sup> TRM cells in HSV-infected epidermis and further showed that this process is facilitated by the chemokine receptor CXCR3 ligands CXCL9 and CXCL10, which are produced during the local infection by epidermal keratinocytes (Mackay et al., 2013). Based on these findings, one could speculate that the poor development of CD103<sup>hi</sup> TRM cells at the site of prior i.d. MVA injection might be the

result of an impaired infiltration of recruited CD8<sup>+</sup> T cells into the epidermal compartment, which might be likely in the absence of epidermal injury or infection of keratinocytes. Indeed, in skin sections of previously i.d. MVA-infected skin, virus-specific memory CD8<sup>+</sup> T cells were only rarely detected in the epidermis and appeared to accumulate mostly in the dermis.

*Local competition between CD8<sup>+</sup> T cells in the skin?*

The dual MVA/MVA-OVA ear inoculation model used in this study could reveal that the generation of CD8<sup>+</sup> TRM cells in MVA-infected skin relies strongly on the presence of *in situ* cognate antigen expression/presentation. While systemically activated OVA-specific effector OT-I cells readily entered MVA-infected skin regardless of whether OVA was expressed *in situ* or not, long-term lodgment of OT-I TRM cells was almost exclusively observed in previously MVA-OVA-infected ears. Considering this strong bias in OT-I TRM cell deposition towards skin that previously contained their cognate antigen, it was surprising that CD8<sup>+</sup> TRM cells specific for the MVA-derived epitope B8R did not accumulate to the same extent in MVA- and MVA-OVA-infected skin. The experiments consistently showed that endogenous B8R-specific CD8<sup>+</sup> T cells were able to form a substantial TRM population in MVA-infected ears, but failed to do so in contralateral MVA-OVA-infected ears, in which high numbers of OT-I TRM cells were established. This disparity was not due to a differential recruitment of B8R-specific effector T cells to MVA- and MVA-OVA-infected ear skin, as both ears contained comparable amounts of B8R-specific CD8<sup>+</sup> T cells during the effector phase. Together these results suggested that these two skin-infiltrating effector CD8<sup>+</sup> T cell subsets might have competed with one another after arrival in the skin, potentially for local resources that promote TRM development. It could further be demonstrated that development of B8R-specific TRM cells in previously MVA-OVA-infected ears was not impaired in mice that did not receive transfer of OT-I cells, indicating that the suppression of local B8R-specific TRM cell lodgment was indeed caused by competing OT-I cells. It is important to note that the systemic B8R-specific memory CD8<sup>+</sup> T cell response (as measured in the spleen) was not dramatically reduced in the presence of OT-I cells, as compared to that seen in the absence of OT-I transfer. Interestingly, in the absence of adoptively transferred OT-I cells, endogenous OVA-specific CD8<sup>+</sup> TRM cells were largely unable to interfere with local establishment of the now immunodominant B8R-specific TRM pool.

Until now, T cell competition has primarily been observed in the context of T cell activation upon primary or secondary infections and has been suggested to contribute to immunodomination. Immunodomination describes the phenomenon that T cell responses to pathogens (even complex pathogens such as VV) typically become skewed towards only a handful of viral epitopes, despite a whole plethora of potential antigenic determinants (Yewdell, 2006).

Especially in experimental systems involving adoptive transfer of high-affinity TCR transgenic CD8<sup>+</sup> T cells (such as OT-I), it has been found that these cells can compete with lower affinity endogenous CD8<sup>+</sup> T cells of the same antigen specificity. For example, it was shown that OT-I cells successfully out-competed endogenous OVA-specific CD8<sup>+</sup> T cells and dramatically suppressed their expansion upon primary immunization with OVA-expressing vaccinia virus or OVA peptide-pulsed DC (Kedl et al., 2000; Kedl et al., 2002). The suppression of the endogenous OVA-specific CD8<sup>+</sup> T cell response by OT-I cells could be overcome by injecting excess amounts of OVA-peptide bearing DCs, suggesting that competition between T cells might occur if their access to antigen-bearing DCs is limited (Kedl et al., 2000). Using immunization with peptide-pulsed DCs, Kedl et al. further demonstrated that adoptively transferred OT-I cells also effectively suppressed the expansion of host-derived CD8<sup>+</sup> T cells specific for a different antigen, provided that the respective epitopes were presented on a shared antigen-presenting cell (APC) (Kedl et al., 2002). These findings suggest that this form of T cell competition (referred to as T cell cross-competition) likely also occurs at the level of the APC, presumably for access to the APC surface or APC-derived factors. Interestingly, a recent study showed that OT-I cells more potently suppressed the response of endogenous VV-specific CD8<sup>+</sup> T cells after i.d. immunization when compared to systemic immunization (Lin et al., 2013). This difference might be explained by the fact that in contrast to systemic immunization, i.d. immunization largely restricts the site of T cell priming to a single lymph node, where resources required for T cell activation might be more limiting (Lin et al., 2013). Studies from our group have revealed that T cell cross-competition is functionally relevant during secondary (but not primary) immune responses to MVA or VV (Kastenmuller et al., 2007). It was demonstrated that upon MVA or VV booster immunization, CD8<sup>+</sup> T cells specific for early viral epitopes successfully out-competed those recognizing late VV epitopes and therefore dominated the antiviral CD8<sup>+</sup> T cell response. Interestingly, the recall expansion of early VV epitope specific CD8<sup>+</sup> T cells was also influenced by competition with CD8<sup>+</sup> T cells recognizing other early VV epitopes (Kastenmuller et al., 2007).



The experimental results obtained in this study show for the first time that T cell cross-competition may not only occur at the level of T cell activation within lymphoid tissue, but might also be a relevant mechanism during the effector-to-TRM transition within non-lymphoid tissues, where local TRM-promoting factors might be limiting.

Since the data provided in this thesis suggest that *in situ* cognate antigen recognition in virus-infected represents a critical signal for local CD8<sup>+</sup> TRM cell establishment, one could speculate that OT-I cells might have prevented B8R-specific CD8<sup>+</sup> T cells from accessing MVA-infected cells and thus blocked their response to their cognate peptide/MHC complex (e.g. by physical exclusion from the cell surface). It is interesting to note that both OVA and the viral B8 protein are expressed early during the MVA life cycle and their antigenic epitopes (OVA<sub>257</sub>, B8R<sub>20</sub>) are presented on the same MHC class I complex (H-2K<sup>b</sup>). Thus, it remains possible that co-expression of OVA (especially when controlled by the strong early/late promoter PH5) might decrease the relative density of K<sup>b</sup>/B8R complexes on infected cells or local APCs and thus could additionally hamper the ability of B8R-specific CD8<sup>+</sup> T cells to compete with the higher affinity OT-I cells. To test this possibility, it might be worthwhile to analyze whether delaying MVA-derived expression of OVA by placing it under the control of a strictly late VV-promoter (P11) might create a less competitive environment for endogenous B8R-specific CD8<sup>+</sup> T cells.

Given that effector CD8<sup>+</sup> T cells should already display cytotoxic activity by the time they enter MVA-infected skin, it might be possible that virus-infected (target) cells are more rapidly eliminated in MVA-OVA-infected skin as opposed to MVA-infected skin, where infected cells are not targeted by the infiltrating OT-I cells. In such a scenario, killing of MVA-OVA-infected cells by OT-I cells would at the same time lower the amount of available local K<sup>b</sup>/B8R complexes and render the local competition for antigen more stringent. To test this hypothesis, it might be interesting to assess whether the local suppression of B8R-specific TRM cells could be overcome by adoptive transfer of perforin-1-deficient OT-I cells, which should be impaired in their ability to kill virus-infected cells *in situ*.

Another important question that needs to be resolved is whether local T cell cross-competition might also take place at the endogenous level. Although it seemed that in experiments without OT-I transfer, endogenous OVA-specific CD8<sup>+</sup> T cells did not impair the formation of B8R-specific TRM cells at the site of prior MVA-OVA skin infection, it cannot be excluded that B8R-specific CD8<sup>+</sup> T cells (which are immunodominant in absence of OT-I) might have interfered with the local development of endogenous OVA-

specific TRM cells. To test this, it might be interesting to compare the capacity of endogenous OVA-specific CD8<sup>+</sup> T cells to establish residency in skin infected with either MVA-OVA or an MVA-OVA deletion mutant that lacks the immunodominant B8R epitope.

Besides competition for local peptide/MHC class I complexes, it is also conceivable that, especially in an anatomical niche like the skin, competition for space within the epidermal compartment or tissue-derived cytokines such as TGF- $\beta$  or IL-15 might further limit the number of TRM cells that can persist at the site of prior local infection. In line with this, Zaid et al. recently suggested that limiting local resources in the skin (survival signals, space) might indeed be responsible for local competition between T cells, as they observed that HSV-specific TRM cells which accumulated in the epidermis at the site of prior HSV skin infection almost completely displaced the local population of DETCs, which normally form a contiguous network throughout the entire epidermis (Zaid et al., 2014).

In conclusion, the finding that different antigen-specific CD8<sup>+</sup> T cell populations can compete with each other for local retention or survival signals within non-lymphoid compartments has important implications for the use of recombinant viral vectors as TRM-inducing vaccines, as the establishment of a local CD8<sup>+</sup> TRM cells specific for a desired Ag-specificity might be confounded by the simultaneous lodgment of potentially more immunodominant but unwanted vector-specific TRM cells. It will therefore be important to explore the basis of local T cell competition within non-lymphoid tissues to enable the rational design of recombinant vectors that can skew the local CD8<sup>+</sup> T cell response towards the desired epitope specificity or allow for a simultaneous induction of a broad repertoire of pathogen-specific CD8<sup>+</sup> TRM cells. The latter might be particularly relevant for a successful control of pathogens which rapidly undergo mutations after establishment of infection within a peripheral non-lymphoid niche and thus escape T cell recognition.

## 7 Reference list

- Allan, R. S., Smith, C. M., Belz, G. T., van Lint, A. L., Wakim, L. M., Heath, W. R., & Carbone, F. R. (2003). Epidermal viral immunity induced by CD8alpha+ dendritic cells but not by Langerhans cells. *Science*, *301*(5641), 1925-1928. doi: 10.1126/science.1087576
- Antoine, G., Scheiflinger, F., Dorner, F., & Falkner, F. G. (1998). The complete genomic sequence of the modified vaccinia Ankara strain: comparison with other orthopoxviruses. *Virology*, *244*(2), 365-396. doi: 10.1006/viro.1998.9123
- Ariotti, S., Beltman, J. B., Chodaczek, G., Hoekstra, M. E., van Beek, A. E., Gomez-Eerland, R., Ritsma, L., van Rheenen, J., Maree, A. F., Zal, T., de Boer, R. J., Haanen, J. B., & Schumacher, T. N. (2012). Tissue-resident memory CD8+ T cells continuously patrol skin epithelia to quickly recognize local antigen. *Proc Natl Acad Sci U S A*, *109*(48), 19739-19744. doi: 10.1073/pnas.1208927109
- Ariotti, S., Hogenbirk, M. A., Dijkgraaf, F. E., Visser, L. L., Hoekstra, M. E., Song, J. Y., Jacobs, H., Haanen, J. B., & Schumacher, T. N. (2014). T cell memory. Skin-resident memory CD8(+) T cells trigger a state of tissue-wide pathogen alert. *Science*, *346*(6205), 101-105. doi: 10.1126/science.1254803
- Badovinac, V. P., Haring, J. S., & Harty, J. T. (2007). Initial T cell receptor transgenic cell precursor frequency dictates critical aspects of the CD8(+) T cell response to infection. *Immunity*, *26*(6), 827-841. doi: 10.1016/j.immuni.2007.04.013
- Bankovich, A. J., Shiow, L. R., & Cyster, J. G. (2010). CD69 suppresses sphingosine 1-phosphate receptor-1 (S1P1) function through interaction with membrane helix 4. *J Biol Chem*, *285*(29), 22328-22337. doi: 10.1074/jbc.M110.123299
- Bedoui, S., Whitney, P. G., Waithman, J., Eidsmo, L., Wakim, L., Caminschi, I., Allan, R. S., Wojtasiak, M., Shortman, K., Carbone, F. R., Brooks, A. G., & Heath, W. R. (2009). Cross-presentation of viral and self antigens by skin-derived CD103+ dendritic cells. *Nat Immunol*, *10*(5), 488-495. doi: 10.1038/ni.1724
- Belkaid, Y. (2007). Regulatory T cells and infection: a dangerous necessity. *Nat Rev Immunol*, *7*(11), 875-888. doi: 10.1038/nri2189
- Belkaid, Y., & Tarbell, K. (2009). Regulatory T cells in the control of host-microorganism interactions (\*). *Annu Rev Immunol*, *27*, 551-589. doi: 10.1146/annurev.immunol.021908.132723
- Belyakov, I. M., Earl, P., Dzutsev, A., Kuznetsov, V. A., Lemon, M., Wyatt, L. S., Snyder, J. T., Ahlers, J. D., Franchini, G., Moss, B., & Berzofsky, J. A. (2003). Shared modes of protection against poxvirus infection by attenuated and conventional smallpox vaccine viruses. *Proc Natl Acad Sci U S A*, *100*(16), 9458-9463. doi: 10.1073/pnas.1233578100
- Belz, G. T., Smith, C. M., Eichner, D., Shortman, K., Karupiah, G., Carbone, F. R., & Heath, W. R. (2004). Cutting edge: conventional CD8 alpha+ dendritic cells are generally involved in priming CTL immunity to viruses. *J Immunol*, *172*(4), 1996-2000.
- Ben-Horin, S., & Bank, I. (2004). The role of very late antigen-1 in immune-mediated inflammation. *Clin Immunol*, *113*(2), 119-129. doi: 10.1016/j.clim.2004.06.007
- Bins, A. D., Jorritsma, A., Wolkers, M. C., Hung, C. F., Wu, T. C., Schumacher, T. N., & Haanen, J. B. (2005). A rapid and potent DNA vaccination strategy defined by in vivo monitoring of antigen expression. *Nat Med*, *11*(8), 899-904. doi: 10.1038/nm1264

- Blanchard, T. J., Alcamí, A., Andrea, P., & Smith, G. L. (1998). Modified vaccinia virus Ankara undergoes limited replication in human cells and lacks several immunomodulatory proteins: implications for use as a human vaccine. *J Gen Virol*, *79* ( Pt 5), 1159-1167.
- Blattman, J. N., Antia, R., Sourdive, D. J., Wang, X., Kaech, S. M., Murali-Krishna, K., Altman, J. D., & Ahmed, R. (2002). Estimating the precursor frequency of naive antigen-specific CD8 T cells. *J Exp Med*, *195*(5), 657-664.
- Bromley, S. K., Thomas, S. Y., & Luster, A. D. (2005). Chemokine receptor CCR7 guides T cell exit from peripheral tissues and entry into afferent lymphatics. *Nat Immunol*, *6*(9), 895-901. doi: 10.1038/ni1240
- Buller, R. M., Chakrabarti, S., Moss, B., & Fredrickson, T. (1988). Cell proliferative response to vaccinia virus is mediated by VGF. *Virology*, *164*(1), 182-192.
- Bursch, L. S., Wang, L., Igyarto, B., Kissenpfennig, A., Malissen, B., Kaplan, D. H., & Hogquist, K. A. (2007). Identification of a novel population of Langerin+ dendritic cells. *J Exp Med*, *204*(13), 3147-3156. doi: 10.1084/jem.20071966
- Campbell, D. J., & Butcher, E. C. (2002). Rapid acquisition of tissue-specific homing phenotypes by CD4(+) T cells activated in cutaneous or mucosal lymphoid tissues. *J Exp Med*, *195*(1), 135-141.
- Carlson, C. M., Endrizzi, B. T., Wu, J., Ding, X., Weinreich, M. A., Walsh, E. R., Wani, M. A., Lingrel, J. B., Hogquist, K. A., & Jameson, S. C. (2006). Kruppel-like factor 2 regulates thymocyte and T-cell migration. *Nature*, *442*(7100), 299-302. doi: 10.1038/nature04882
- Carroll, M. W., & Moss, B. (1997). Host range and cytopathogenicity of the highly attenuated MVA strain of vaccinia virus: propagation and generation of recombinant viruses in a nonhuman mammalian cell line. *Virology*, *238*(2), 198-211. doi: 10.1006/viro.1997.8845
- Casey, K. A., Fraser, K. A., Schenkel, J. M., Moran, A., Abt, M. C., Beura, L. K., Lucas, P. J., Artis, D., Wherry, E. J., Hogquist, K., Vezys, V., & Masopust, D. (2012). Antigen-independent differentiation and maintenance of effector-like resident memory T cells in tissues. *J Immunol*, *188*(10), 4866-4875. doi: 10.4049/jimmunol.1200402
- Cepek, K. L., Parker, C. M., Madara, J. L., & Brenner, M. B. (1993). Integrin alpha E beta 7 mediates adhesion of T lymphocytes to epithelial cells. *J Immunol*, *150*(8 Pt 1), 3459-3470.
- Cepek, K. L., Shaw, S. K., Parker, C. M., Russell, G. J., Morrow, J. S., Rimm, D. L., & Brenner, M. B. (1994). Adhesion between epithelial cells and T lymphocytes mediated by E-cadherin and the alpha E beta 7 integrin. *Nature*, *372*(6502), 190-193. doi: 10.1038/372190a0
- Combadiere, B., Boissonnas, A., Carcelain, G., Lefranc, E., Samri, A., Bricaire, F., Debre, P., & Autran, B. (2004). Distinct time effects of vaccination on long-term proliferative and IFN-gamma-producing T cell memory to smallpox in humans. *J Exp Med*, *199*(11), 1585-1593. doi: 10.1084/jem.20032083
- Cosma, A., Nagaraj, R., Buhler, S., Hinkula, J., Busch, D. H., Sutter, G., Goebel, F. D., & Erfle, V. (2003). Therapeutic vaccination with MVA-HIV-1 nef elicits Nef-specific T-helper cell responses in chronically HIV-1 infected individuals. *Vaccine*, *22*(1), 21-29.
- Cuburu, N., Graham, B. S., Buck, C. B., Kines, R. C., Pang, Y. Y., Day, P. M., Lowy, D. R., & Schiller, J. T. (2012). Intravaginal immunization with HPV vectors induces tissue-resident CD8+ T cell responses. *J Clin Invest*, *122*(12), 4606-4620. doi: 10.1172/JCI63287

- Debes, G. F., Arnold, C. N., Young, A. J., Krautwald, S., Lipp, M., Hay, J. B., & Butcher, E. C. (2005). Chemokine receptor CCR7 required for T lymphocyte exit from peripheral tissues. *Nat Immunol*, *6*(9), 889-894. doi: 10.1038/ni1238
- Di Giulio, D. B., & Eckburg, P. B. (2004). Human monkeypox: an emerging zoonosis. *Lancet Infect Dis*, *4*(1), 15-25.
- Di Meglio, P., Perera, G. K., & Nestle, F. O. (2011). The multitasking organ: recent insights into skin immune function. *Immunity*, *35*(6), 857-869. doi: 10.1016/j.immuni.2011.12.003
- Drexler, I., Heller, K., Wahren, B., Erfle, V., & Sutter, G. (1998). Highly attenuated modified vaccinia virus Ankara replicates in baby hamster kidney cells, a potential host for virus propagation, but not in various human transformed and primary cells. *J Gen Virol*, *79* ( Pt 2), 347-352.
- Drexler, I., Staib, C., Kastenmuller, W., Stevanovic, S., Schmidt, B., Lemonnier, F. A., Rammensee, H. G., Busch, D. H., Bernhard, H., Erfle, V., & Sutter, G. (2003). Identification of vaccinia virus epitope-specific HLA-A\*0201-restricted T cells and comparative analysis of smallpox vaccines. *Proc Natl Acad Sci U S A*, *100*(1), 217-222. doi: 10.1073/pnas.262668999
- Drexler, I., Staib, C., & Sutter, G. (2004). Modified vaccinia virus Ankara as antigen delivery system: how can we best use its potential? *Curr Opin Biotechnol*, *15*(6), 506-512. doi: 10.1016/j.copbio.2004.09.001
- Dudda, J. C., Perdue, N., Bachtanian, E., & Campbell, D. J. (2008). Foxp3+ regulatory T cells maintain immune homeostasis in the skin. *J Exp Med*, *205*(7), 1559-1565. doi: 10.1084/jem.20072594
- Earl, P. L., Americo, J. L., Wyatt, L. S., Eller, L. A., Whitbeck, J. C., Cohen, G. H., Eisenberg, R. J., Hartmann, C. J., Jackson, D. L., Kulesh, D. A., Martinez, M. J., Miller, D. M., Mucker, E. M., Shamblin, J. D., Zwiers, S. H., Huggins, J. W., Jahrling, P. B., & Moss, B. (2004). Immunogenicity of a highly attenuated MVA smallpox vaccine and protection against monkeypox. *Nature*, *428*(6979), 182-185. doi: 10.1038/nature02331
- El-Asady, R., Yuan, R., Liu, K., Wang, D., Gress, R. E., Lucas, P. J., Drachenberg, C. B., & Hadley, G. A. (2005). TGF- $\beta$ -dependent CD103 expression by CD8(+) T cells promotes selective destruction of the host intestinal epithelium during graft-versus-host disease. *J Exp Med*, *201*(10), 1647-1657. doi: 10.1084/jem.20041044
- Fenner, F., Henderson, D. A., Arita, I., Jezek, Z., & and Ladnyi, I. (1988). Smallpox and Its Eradication. (*Geneva, Switzerland: World Health Organization*).
- Gebhardt, T., & Mackay, L. K. (2012). Local immunity by tissue-resident CD8(+) memory T cells. *Front Immunol*, *3*, 340. doi: 10.3389/fimmu.2012.00340
- Gebhardt, T., Wakim, L. M., Eidsmo, L., Reading, P. C., Heath, W. R., & Carbone, F. R. (2009). Memory T cells in nonlymphoid tissue that provide enhanced local immunity during infection with herpes simplex virus. *Nat Immunol*, *10*(5), 524-530. doi: 10.1038/ni.1718
- Gebhardt, T., Whitney, P. G., Zaid, A., Mackay, L. K., Brooks, A. G., Heath, W. R., Carbone, F. R., & Mueller, S. N. (2011). Different patterns of peripheral migration by memory CD4+ and CD8+ T cells. *Nature*, *477*(7363), 216-219. doi: 10.1038/nature10339
- Gilbert, S. C. (2013). Clinical development of Modified Vaccinia virus Ankara vaccines. *Vaccine*, *31*(39), 4241-4246. doi: 10.1016/j.vaccine.2013.03.020
- Ginhoux, F., Collin, M. P., Bogunovic, M., Abel, M., Leboeuf, M., Helft, J., Ochando, J., Kissenpfennig, A., Malissen, B., Grisotto, M., Snoeck, H., Randolph, G., & Merad,

- M. (2007). Blood-derived dermal langerin+ dendritic cells survey the skin in the steady state. *J Exp Med*, 204(13), 3133-3146. doi: 10.1084/jem.20071733
- Girardi, M., Oppenheim, D. E., Steele, C. R., Lewis, J. M., Glusac, E., Filler, R., Hobby, P., Sutton, B., Tigelaar, R. E., & Hayday, A. C. (2001). Regulation of cutaneous malignancy by gammadelta T cells. *Science*, 294(5542), 605-609. doi: 10.1126/science.1063916
- Glick, A. B., Kulkarni, A. B., Tennenbaum, T., Hennings, H., Flanders, K. C., O'Reilly, M., Sporn, M. B., Karlsson, S., & Yuspa, S. H. (1993). Loss of expression of transforming growth factor beta in skin and skin tumors is associated with hyperproliferation and a high risk for malignant conversion. *Proc Natl Acad Sci U S A*, 90(13), 6076-6080.
- Gomez, C. E., Najera, J. L., Domingo-Gil, E., Ochoa-Callejero, L., Gonzalez-Asequinolaza, G., & Esteban, M. (2007). Virus distribution of the attenuated MVA and NYVAC poxvirus strains in mice. *J Gen Virol*, 88(Pt 9), 2473-2478. doi: 10.1099/vir.0.83018-0
- Gutowska-Owsiak, D., & Ogg, G. S. (2012). The epidermis as an adjuvant. *J Invest Dermatol*, 132(3 Pt 2), 940-948. doi: 10.1038/jid.2011.398
- Haluszczak, C., Akue, A. D., Hamilton, S. E., Johnson, L. D., Pujanauski, L., Teodorovic, L., Jameson, S. C., & Kedl, R. M. (2009). The antigen-specific CD8+ T cell repertoire in unimmunized mice includes memory phenotype cells bearing markers of homeostatic expansion. *J Exp Med*, 206(2), 435-448. doi: 10.1084/jem.20081829
- Hammarlund, E., Lewis, M. W., Hansen, S. G., Strelow, L. I., Nelson, J. A., Sexton, G. J., Hanifin, J. M., & Slifka, M. K. (2003). Duration of antiviral immunity after smallpox vaccination. *Nat Med*, 9(9), 1131-1137. doi: 10.1038/nm917
- Havran, W. L., & Jameson, J. M. (2010). Epidermal T cells and wound healing. *J Immunol*, 184(10), 5423-5428. doi: 10.4049/jimmunol.0902733
- He, Y., Zhang, J., Donahue, C., & Falo, L. D., Jr. (2006). Skin-derived dendritic cells induce potent CD8(+) T cell immunity in recombinant lentivector-mediated genetic immunization. *Immunity*, 24(5), 643-656. doi: 10.1016/j.immuni.2006.03.014
- Heath, W. R., & Carbone, F. R. (2013). The skin-resident and migratory immune system in steady state and memory: innate lymphocytes, dendritic cells and T cells. *Nat Immunol*, 14(10), 978-985. doi: 10.1038/ni.2680
- Hofmann, M., & Pircher, H. (2011). E-cadherin promotes accumulation of a unique memory CD8 T-cell population in murine salivary glands. *Proc Natl Acad Sci U S A*, 108(40), 16741-16746. doi: 10.1073/pnas.1107200108
- Huster, K. M., Busch, V., Schiemann, M., Linkemann, K., Kerksiek, K. M., Wagner, H., & Busch, D. H. (2004). Selective expression of IL-7 receptor on memory T cells identifies early CD40L-dependent generation of distinct CD8+ memory T cell subsets. *Proc Natl Acad Sci U S A*, 101(15), 5610-5615. doi: 10.1073/pnas.0308054101
- Jabbari, A., & Harty, J. T. (2006). Secondary memory CD8+ T cells are more protective but slower to acquire a central-memory phenotype. *J Exp Med*, 203(4), 919-932. doi: 10.1084/jem.20052237
- Jiang, X., Clark, R. A., Liu, L., Wagers, A. J., Fuhlbrigge, R. C., & Kupper, T. S. (2012). Skin infection generates non-migratory memory CD8+ T(RM) cells providing global skin immunity. *Nature*, 483(7388), 227-231. doi: 10.1038/nature10851
- Joshi, N. S., Cui, W., Chandele, A., Lee, H. K., Urso, D. R., Hagman, J., Gapin, L., & Kaech, S. M. (2007). Inflammation directs memory precursor and short-lived

- effector CD8(+) T cell fates via the graded expression of T-bet transcription factor. *Immunity*, 27(2), 281-295. doi: 10.1016/j.immuni.2007.07.010
- Kaech, S. M., & Cui, W. (2012). Transcriptional control of effector and memory CD8+ T cell differentiation. *Nat Rev Immunol*, 12(11), 749-761. doi: 10.1038/nri3307
- Kaech, S. M., Tan, J. T., Wherry, E. J., Konieczny, B. T., Surh, C. D., & Ahmed, R. (2003). Selective expression of the interleukin 7 receptor identifies effector CD8 T cells that give rise to long-lived memory cells. *Nat Immunol*, 4(12), 1191-1198. doi: 10.1038/ni1009
- Kaech, S. M., Wherry, E. J., & Ahmed, R. (2002). Effector and memory T-cell differentiation: implications for vaccine development. *Nat Rev Immunol*, 2(4), 251-262. doi: 10.1038/nri778
- Kane, C. J., Knapp, A. M., Mansbridge, J. N., & Hanawalt, P. C. (1990). Transforming growth factor-beta 1 localization in normal and psoriatic epidermal keratinocytes in situ. *J Cell Physiol*, 144(1), 144-150. doi: 10.1002/jcp.1041440119
- Kastenmuller, W., Gasteiger, G., Gronau, J. H., Baier, R., Ljapoci, R., Busch, D. H., & Drexler, I. (2007). Cross-competition of CD8+ T cells shapes the immunodominance hierarchy during boost vaccination. *J Exp Med*, 204(9), 2187-2198. doi: 10.1084/jem.20070489
- Kastenmuller, W., Gasteiger, G., Stross, L., Busch, D. H., & Drexler, I. (2009). Cutting edge: mucosal application of a lyophilized viral vector vaccine confers systemic and protective immunity toward intracellular pathogens. *J Immunol*, 182(5), 2573-2577. doi: 10.4049/jimmunol.0803871
- Kastenmuller, W., Gasteiger, G., Subramanian, N., Sparwasser, T., Busch, D. H., Belkaid, Y., Drexler, I., & Germain, R. N. (2011). Regulatory T cells selectively control CD8+ T cell effector pool size via IL-2 restriction. *J Immunol*, 187(6), 3186-3197. doi: 10.4049/jimmunol.1101649
- Kedl, R. M., Rees, W. A., Hildeman, D. A., Schaefer, B., Mitchell, T., Kappler, J., & Marrack, P. (2000). T cells compete for access to antigen-bearing antigen-presenting cells. *J Exp Med*, 192(8), 1105-1113.
- Kedl, R. M., Schaefer, B. C., Kappler, J. W., & Marrack, P. (2002). T cells down-modulate peptide-MHC complexes on APCs in vivo. *Nat Immunol*, 3(1), 27-32. doi: 10.1038/ni742
- Kim, J. M., Rasmussen, J. P., & Rudensky, A. Y. (2007). Regulatory T cells prevent catastrophic autoimmunity throughout the lifespan of mice. *Nat Immunol*, 8(2), 191-197. doi: 10.1038/ni1428
- Kim, S. K., Schluns, K. S., & Lefrancois, L. (1999). Induction and visualization of mucosal memory CD8 T cells following systemic virus infection. *J Immunol*, 163(8), 4125-4132.
- Klonowski, K. D., Williams, K. J., Marzo, A. L., Blair, D. A., Lingenheld, E. G., & Lefrancois, L. (2004). Dynamics of blood-borne CD8 memory T cell migration in vivo. *Immunity*, 20(5), 551-562.
- Koyama, S. Y., & Podolsky, D. K. (1989). Differential expression of transforming growth factors alpha and beta in rat intestinal epithelial cells. *J Clin Invest*, 83(5), 1768-1773. doi: 10.1172/JCI114080
- Kuo, C. T., Veselits, M. L., & Leiden, J. M. (1997). LKLF: A transcriptional regulator of single-positive T cell quiescence and survival. *Science*, 277(5334), 1986-1990.
- Lahl, K., Loddenkemper, C., Drouin, C., Freyer, J., Arnason, J., Eberl, G., Hamann, A., Wagner, H., Huehn, J., & Sparwasser, T. (2007). Selective depletion of Foxp3+ regulatory T cells induces a scurfy-like disease. *J Exp Med*, 204(1), 57-63. doi: 10.1084/jem.20061852

- Lai, Y., Di Nardo, A., Nakatsuji, T., Leichtle, A., Yang, Y., Cogen, A. L., Wu, Z. R., Hooper, L. V., Schmidt, R. R., von Aulock, S., Radek, K. A., Huang, C. M., Ryan, A. F., & Gallo, R. L. (2009). Commensal bacteria regulate Toll-like receptor 3-dependent inflammation after skin injury. *Nat Med*, *15*(12), 1377-1382. doi: 10.1038/nm.2062
- Lauterbach, H., Patzold, J., Kassub, R., Bathke, B., Brinkmann, K., Chaplin, P., Suter, M., & Hochrein, H. (2013). Genetic Adjuvantation of Recombinant MVA with CD40L Potentiates CD8 T Cell Mediated Immunity. *Front Immunol*, *4*, 251. doi: 10.3389/fimmu.2013.00251
- Lee, Y. T., Suarez-Ramirez, J. E., Wu, T., Redman, J. M., Bouchard, K., Hadley, G. A., & Cauley, L. S. (2011). Environmental and antigen receptor-derived signals support sustained surveillance of the lungs by pathogen-specific cytotoxic T lymphocytes. *J Virol*, *85*(9), 4085-4094. doi: 10.1128/JVI.02493-10
- Liard, C., Munier, S., Joulin-Giet, A., Bonduelle, O., Hadam, S., Duffy, D., Vogt, A., Verrier, B., & Combadiere, B. (2012). Intradermal immunization triggers epidermal Langerhans cell mobilization required for CD8 T-cell immune responses. *J Invest Dermatol*, *132*(3 Pt 1), 615-625. doi: 10.1038/jid.2011.346
- Lin, L. C., Flesch, I. E., & Tschärke, D. C. (2013). Immunodomination during peripheral vaccinia virus infection. *PLoS Pathog*, *9*(4), e1003329. doi: 10.1371/journal.ppat.1003329
- Liu, L., Xu, Z., Fuhlbrigge, R. C., Pena-Cruz, V., Lieberman, J., & Kupper, T. S. (2005). Vaccinia virus induces strong immunoregulatory cytokine production in healthy human epidermal keratinocytes: a novel strategy for immune evasion. *J Virol*, *79*(12), 7363-7370. doi: 10.1128/JVI.79.12.7363-7370.2005
- Liu, L., Zhong, Q., Tian, T., Dubin, K., Athale, S. K., & Kupper, T. S. (2010). Epidermal injury and infection during poxvirus immunization is crucial for the generation of highly protective T cell-mediated immunity. *Nat Med*, *16*(2), 224-227. doi: 10.1038/nm.2078
- Mackay, L. K., Rahimpour, A., Ma, J. Z., Collins, N., Stock, A. T., Hafon, M. L., Vega-Ramos, J., Lauzurica, P., Mueller, S. N., Stefanovic, T., Tschärke, D. C., Heath, W. R., Inouye, M., Carbone, F. R., & Gebhardt, T. (2013). The developmental pathway for CD103(+)CD8+ tissue-resident memory T cells of skin. *Nat Immunol*, *14*(12), 1294-1301. doi: 10.1038/ni.2744
- Mackay, L. K., Stock, A. T., Ma, J. Z., Jones, C. M., Kent, S. J., Mueller, S. N., Heath, W. R., Carbone, F. R., & Gebhardt, T. (2012). Long-lived epithelial immunity by tissue-resident memory T (TRM) cells in the absence of persisting local antigen presentation. *Proc Natl Acad Sci U S A*, *109*(18), 7037-7042. doi: 10.1073/pnas.1202288109
- Macleod, A. S., & Havran, W. L. (2011). Functions of skin-resident gammadelta T cells. *Cell Mol Life Sci*, *68*(14), 2399-2408. doi: 10.1007/s00018-011-0702-x
- Marzo, A. L., Klonowski, K. D., Le Bon, A., Borrow, P., Tough, D. F., & Lefrançois, L. (2005). Initial T cell frequency dictates memory CD8+ T cell lineage commitment. *Nat Immunol*, *6*(8), 793-799. doi: 10.1038/ni1227
- Masopust, D., Choo, D., Vezys, V., Wherry, E. J., Duraiswamy, J., Akondy, R., Wang, J., Casey, K. A., Barber, D. L., Kawamura, K. S., Fraser, K. A., Webby, R. J., Brinkmann, V., Butcher, E. C., Newell, K. A., & Ahmed, R. (2010). Dynamic T cell migration program provides resident memory within intestinal epithelium. *J Exp Med*, *207*(3), 553-564. doi: 10.1084/jem.20090858



- Masopust, D., Ha, S. J., Vezys, V., & Ahmed, R. (2006a). Stimulation history dictates memory CD8 T cell phenotype: implications for prime-boost vaccination. *J Immunol*, *177*(2), 831-839.
- Masopust, D., Vezys, V., Marzo, A. L., & Lefrancois, L. (2001). Preferential localization of effector memory cells in nonlymphoid tissue. *Science*, *291*(5512), 2413-2417. doi: 10.1126/science.1058867
- Masopust, D., Vezys, V., Usherwood, E. J., Cauley, L. S., Olson, S., Marzo, A. L., Ward, R. L., Woodland, D. L., & Lefrancois, L. (2004). Activated primary and memory CD8 T cells migrate to nonlymphoid tissues regardless of site of activation or tissue of origin. *J Immunol*, *172*(8), 4875-4882.
- Masopust, D., Vezys, V., Wherry, E. J., Barber, D. L., & Ahmed, R. (2006b). Cutting edge: gut microenvironment promotes differentiation of a unique memory CD8 T cell population. *J Immunol*, *176*(4), 2079-2083.
- Matloubian, M., Lo, C. G., Cinamon, G., Lesneski, M. J., Xu, Y., Brinkmann, V., Allende, M. L., Proia, R. L., & Cyster, J. G. (2004). Lymphocyte egress from thymus and peripheral lymphoid organs is dependent on S1P receptor 1. *Nature*, *427*(6972), 355-360. doi: 10.1038/nature02284
- Mayr, A., Stickl, H., Muller, H. K., Danner, K., & Singer, H. (1978). [The smallpox vaccination strain MVA: marker, genetic structure, experience gained with the parenteral vaccination and behavior in organisms with a debilitated defence mechanism (author's transl)]. *Zentralbl Bakteriolog B*, *167*(5-6), 375-390.
- McConkey, S. J., Reece, W. H., Moorthy, V. S., Webster, D., Dunachie, S., Butcher, G., Vuola, J. M., Blanchard, T. J., Gothard, P., Watkins, K., Hannan, C. M., Everaere, S., Brown, K., Kester, K. E., Cummings, J., Williams, J., Heppner, D. G., Pathan, A., Flanagan, K., Arulanantham, N., Roberts, M. T., Roy, M., Smith, G. L., Schneider, J., Peto, T., Sinden, R. E., Gilbert, S. C., & Hill, A. V. (2003). Enhanced T-cell immunogenicity of plasmid DNA vaccines boosted by recombinant modified vaccinia virus Ankara in humans. *Nat Med*, *9*(6), 729-735. doi: 10.1038/nm881
- McLachlan, J. B., Catron, D. M., Moon, J. J., & Jenkins, M. K. (2009). Dendritic cell antigen presentation drives simultaneous cytokine production by effector and regulatory T cells in inflamed skin. *Immunity*, *30*(2), 277-288. doi: 10.1016/j.immuni.2008.11.013
- McShane, H., Pathan, A. A., Sander, C. R., Keating, S. M., Gilbert, S. C., Huygen, K., Fletcher, H. A., & Hill, A. V. (2004). Recombinant modified vaccinia virus Ankara expressing antigen 85A boosts BCG-primed and naturally acquired antimycobacterial immunity in humans. *Nat Med*, *10*(11), 1240-1244. doi: 10.1038/nm1128
- Merad, M., Ginhoux, F., & Collin, M. (2008). Origin, homeostasis and function of Langerhans cells and other langerin-expressing dendritic cells. *Nat Rev Immunol*, *8*(12), 935-947. doi: 10.1038/nri2455
- Meyer, H., Sutter, G., & Mayr, A. (1991). Mapping of deletions in the genome of the highly attenuated vaccinia virus MVA and their influence on virulence. *J Gen Virol*, *72* ( Pt 5), 1031-1038.
- Moorthy, V. S., Pinder, M., Reece, W. H., Watkins, K., Atabani, S., Hannan, C., Bojang, K., McAdam, K. P., Schneider, J., Gilbert, S., & Hill, A. V. (2003). Safety and immunogenicity of DNA/modified vaccinia virus ankara malaria vaccination in African adults. *J Infect Dis*, *188*(8), 1239-1244. doi: 10.1086/378515

- Mora, J. R., Bono, M. R., Manjunath, N., Weninger, W., Cavanagh, L. L., Roseblatt, M., & Von Andrian, U. H. (2003). Selective imprinting of gut-homing T cells by Peyer's patch dendritic cells. *Nature*, *424*(6944), 88-93. doi: 10.1038/nature01726
- Mora, J. R., Cheng, G., Picarella, D., Briskin, M., Buchanan, N., & von Andrian, U. H. (2005). Reciprocal and dynamic control of CD8 T cell homing by dendritic cells from skin- and gut-associated lymphoid tissues. *J Exp Med*, *201*(2), 303-316. doi: 10.1084/jem.20041645
- Moss, B. (2001). Poxviridae: the viruses and their replication. *Fields Virology, fourth edition*, D.M. Knipe and P.M. Howley, eds. (Philadelphia: Lippincott, Williams, and Wilkins), 2849-2884.
- Moutaftsi, M., Peters, B., Pasquetto, V., Tschärke, D. C., Sidney, J., Bui, H. H., Grey, H., & Sette, A. (2006). A consensus epitope prediction approach identifies the breadth of murine T(CD8+)-cell responses to vaccinia virus. *Nat Biotechnol*, *24*(7), 817-819. doi: 10.1038/nbt1215
- Mueller, S. N., Zaid, A., & Carbone, F. R. (2014). Tissue-resident T cells: dynamic players in skin immunity. *Front Immunol*, *5*, 332. doi: 10.3389/fimmu.2014.00332
- Nakamura, K., Kitani, A., & Strober, W. (2001). Cell contact-dependent immunosuppression by CD4(+)CD25(+) regulatory T cells is mediated by cell surface-bound transforming growth factor beta. *J Exp Med*, *194*(5), 629-644.
- Nakanishi, Y., Lu, B., Gerard, C., & Iwasaki, A. (2009). CD8(+) T lymphocyte mobilization to virus-infected tissue requires CD4(+) T-cell help. *Nature*, *462*(7272), 510-513. doi: 10.1038/nature08511
- Nestle, F. O., Di Meglio, P., Qin, J. Z., & Nickoloff, B. J. (2009). Skin immune sentinels in health and disease. *Nat Rev Immunol*, *9*(10), 679-691. doi: 10.1038/nri2622
- Obar, J. J., & Lefrançois, L. (2010). Early signals during CD8 T cell priming regulate the generation of central memory cells. *J Immunol*, *185*(1), 263-272. doi: 10.4049/jimmunol.1000492
- Overwijk, W. W., Surman, D. R., Tsung, K., & Restifo, N. P. (1997). Identification of a Kb-restricted CTL epitope of beta-galactosidase: potential use in development of immunization protocols for "self" antigens. *Methods*, *12*(2), 117-123. doi: 10.1006/meth.1997.0461
- Pantelyushin, S., Haak, S., Ingold, B., Kulig, P., Heppner, F. L., Navarini, A. A., & Becher, B. (2012). Rorγ<sup>+</sup> innate lymphocytes and γδ T cells initiate psoriasiform plaque formation in mice. *J Clin Invest*, *122*(6), 2252-2256. doi: 10.1172/JCI61862
- Pastoret, P. P., & Vanderplassen, A. (2003). Poxviruses as vaccine vectors. *Comp Immunol Microbiol Infect Dis*, *26*(5-6), 343-355. doi: 10.1016/S0147-9571(03)00019-5
- Potsch, C., Vohringer, D., & Pircher, H. (1999). Distinct migration patterns of naive and effector CD8 T cells in the spleen: correlation with CCR7 receptor expression and chemokine reactivity. *Eur J Immunol*, *29*(11), 3562-3570. doi: 10.1002/(SICI)1521-4141(199911)29:11<3562::AID-IMMU3562>3.0.CO;2-R
- Poulin, L. F., Henri, S., de Bovis, B., Devilard, E., Kissenpfennig, A., & Malissen, B. (2007). The dermis contains langerin<sup>+</sup> dendritic cells that develop and function independently of epidermal Langerhans cells. *J Exp Med*, *204*(13), 3119-3131. doi: 10.1084/jem.20071724
- Ray, S. J., Franki, S. N., Pierce, R. H., Dimitrova, S., Kotliansky, V., Sprague, A. G., Doherty, P. C., de Fougères, A. R., & Topham, D. J. (2004). The collagen

- binding alpha1beta1 integrin VLA-1 regulates CD8 T cell-mediated immune protection against heterologous influenza infection. *Immunity*, 20(2), 167-179.
- Reinhardt, R. L., Khoruts, A., Merica, R., Zell, T., & Jenkins, M. K. (2001). Visualizing the generation of memory CD4 T cells in the whole body. *Nature*, 410(6824), 101-105. doi: 10.1038/35065111
- Romani, N., Flacher, V., Tripp, C. H., Sparber, F., Ebner, S., & Stoitzner, P. (2012a). Targeting skin dendritic cells to improve intradermal vaccination. *Curr Top Microbiol Immunol*, 351, 113-138. doi: 10.1007/82\_2010\_118
- Romani, N., Tripp, C. H., & Stoitzner, P. (2012b). Langerhans cells come in waves. *Immunity*, 37(5), 766-768. doi: 10.1016/j.immuni.2012.10.013
- Roos, K. L., & Eckerman, N. L. (2002). The smallpox vaccine and postvaccinal encephalitis. *Semin Neurol*, 22(1), 95-98. doi: 10.1055/s-2002-33052
- Rotzschke, O., Falk, K., Stevanovic, S., Jung, G., Walden, P., & Rammensee, H. G. (1991). Exact prediction of a natural T cell epitope. *Eur J Immunol*, 21(11), 2891-2894. doi: 10.1002/eji.1830211136
- Russell, J. H., & Ley, T. J. (2002). Lymphocyte-mediated cytotoxicity. *Annu Rev Immunol*, 20, 323-370. doi: 10.1146/annurev.immunol.20.100201.131730
- Sallusto, F., Geginat, J., & Lanzavecchia, A. (2004). Central memory and effector memory T cell subsets: function, generation, and maintenance. *Annu Rev Immunol*, 22, 745-763. doi: 10.1146/annurev.immunol.22.012703.104702
- Sallusto, F., Lenig, D., Forster, R., Lipp, M., & Lanzavecchia, A. (1999). Two subsets of memory T lymphocytes with distinct homing potentials and effector functions. *Nature*, 401(6754), 708-712. doi: 10.1038/44385
- Sarkar, S., Kalia, V., Haining, W. N., Konieczny, B. T., Subramaniam, S., & Ahmed, R. (2008). Functional and genomic profiling of effector CD8 T cell subsets with distinct memory fates. *J Exp Med*, 205(3), 625-640. doi: 10.1084/jem.20071641
- Sather, B. D., Treuting, P., Perdue, N., Miazgowicz, M., Fontenot, J. D., Rudensky, A. Y., & Campbell, D. J. (2007). Altering the distribution of Foxp3(+) regulatory T cells results in tissue-specific inflammatory disease. *J Exp Med*, 204(6), 1335-1347. doi: 10.1084/jem.20070081
- Schenkel, J. M., Fraser, K. A., Beura, L. K., Pauken, K. E., Vezys, V., & Masopust, D. (2014). T cell memory. Resident memory CD8 T cells trigger protective innate and adaptive immune responses. *Science*, 346(6205), 98-101. doi: 10.1126/science.1254536
- Schenkel, J. M., Fraser, K. A., Vezys, V., & Masopust, D. (2013). Sensing and alarm function of resident memory CD8(+) T cells. *Nat Immunol*, 14(8), 876. doi: 10.1038/ni0813-876c
- Schenkel, J. M., & Masopust, D. (2014). Tissue-resident memory T cells. *Immunity*, 41(6), 886-897. doi: 10.1016/j.immuni.2014.12.007
- Schepers, K., Arens, R., & Schumacher, T. N. (2005). Dissection of cytotoxic and helper T cell responses. *Cell Mol Life Sci*, 62(23), 2695-2710. doi: 10.1007/s00018-005-5266-1
- Schober, S. L., Kuo, C. T., Schluns, K. S., Lefrancois, L., Leiden, J. M., & Jameson, S. C. (1999). Expression of the transcription factor lung Kruppel-like factor is regulated by cytokines and correlates with survival of memory T cells in vitro and in vivo. *J Immunol*, 163(7), 3662-3667.
- Schon, M. P., Schon, M., Parker, C. M., & Williams, I. R. (2002). Dendritic epidermal T cells (DETC) are diminished in integrin alphaE(CD103)-deficient mice. *J Invest Dermatol*, 119(1), 190-193. doi: 10.1046/j.1523-1747.2002.17973.x

- Schuler, G., & Steinman, R. M. (1985). Murine epidermal Langerhans cells mature into potent immunostimulatory dendritic cells in vitro. *J Exp Med*, *161*(3), 526-546.
- Schwab, S. R., Pereira, J. P., Matloubian, M., Xu, Y., Huang, Y., & Cyster, J. G. (2005). Lymphocyte sequestration through S1P lyase inhibition and disruption of S1P gradients. *Science*, *309*(5741), 1735-1739. doi: 10.1126/science.1113640
- Seder, R. A., & Hill, A. V. (2000). Vaccines against intracellular infections requiring cellular immunity. *Nature*, *406*(6797), 793-798. doi: 10.1038/35021239
- Seneschal, J., Jiang, X., & Kupper, T. S. (2013). Langerin Dermal DC, but Not Langerhans Cells, Are Required for Effective CD8-Mediated Immune Responses after Skin Scarification with Vaccinia Virus. *J Invest Dermatol*. doi: 10.1038/jid.2013.418
- Sheridan, B. S., Pham, Q. M., Lee, Y. T., Cauley, L. S., Puddington, L., & Lefrancois, L. (2014). Oral infection drives a distinct population of intestinal resident memory CD8(+) T cells with enhanced protective function. *Immunity*, *40*(5), 747-757. doi: 10.1016/j.immuni.2014.03.007
- Shin, H., & Iwasaki, A. (2012). A vaccine strategy that protects against genital herpes by establishing local memory T cells. *Nature*, *491*(7424), 463-467. doi: 10.1038/nature11522
- Shiow, L. R., Rosen, D. B., Brdickova, N., Xu, Y., An, J., Lanier, L. L., Cyster, J. G., & Matloubian, M. (2006). CD69 acts downstream of interferon-alpha/beta to inhibit S1P1 and lymphocyte egress from lymphoid organs. *Nature*, *440*(7083), 540-544. doi: 10.1038/nature04606
- Skon, C. N., Lee, J. Y., Anderson, K. G., Masopust, D., Hogquist, K. A., & Jameson, S. C. (2013). Transcriptional downregulation of S1pr1 is required for the establishment of resident memory CD8+ T cells. *Nat Immunol*, *14*(12), 1285-1293. doi: 10.1038/ni.2745
- Stemberger, C., Huster, K. M., Koffler, M., Anderl, F., Schiemann, M., Wagner, H., & Busch, D. H. (2007). A single naive CD8+ T cell precursor can develop into diverse effector and memory subsets. *Immunity*, *27*(6), 985-997. doi: 10.1016/j.immuni.2007.10.012
- Stickl, H., Hochstein-Mintzel, V., Mayr, A., Huber, H. C., Schafer, H., & Holzner, A. (1974). [MVA vaccination against smallpox: clinical tests with an attenuated live vaccinia virus strain (MVA) (author's transl)]. *Dtsch Med Wochenschr*, *99*(47), 2386-2392. doi: 10.1055/s-0028-1108143
- Stittelaar, K. J., Kuiken, T., de Swart, R. L., van Amerongen, G., Vos, H. W., Niesters, H. G., van Schalkwijk, P., van der Kwast, T., Wyatt, L. S., Moss, B., & Osterhaus, A. D. (2001). Safety of modified vaccinia virus Ankara (MVA) in immune-suppressed macaques. *Vaccine*, *19*(27), 3700-3709.
- Stoitzner, P., Tripp, C. H., Eberhart, A., Price, K. M., Jung, J. Y., Bursch, L., Ronchese, F., & Romani, N. (2006). Langerhans cells cross-present antigen derived from skin. *Proc Natl Acad Sci U S A*, *103*(20), 7783-7788. doi: 10.1073/pnas.0509307103
- Sutter, G., & Moss, B. (1992). Nonreplicating vaccinia vector efficiently expresses recombinant genes. *Proc Natl Acad Sci U S A*, *89*(22), 10847-10851.
- Sutter, G., & Staib, C. (2003). Vaccinia vectors as candidate vaccines: the development of modified vaccinia virus Ankara for antigen delivery. *Curr Drug Targets Infect Disord*, *3*(3), 263-271.
- Tscharke, D. C., Karupiah, G., Zhou, J., Palmore, T., Irvine, K. R., Haeryfar, S. M., Williams, S., Sidney, J., Sette, A., Bennink, J. R., & Yewdell, J. W. (2005). Identification of poxvirus CD8+ T cell determinants to enable rational design and

- characterization of smallpox vaccines. *J Exp Med*, 201(1), 95-104. doi: 10.1084/jem.20041912
- Tscharke, D. C., & Smith, G. L. (1999). A model for vaccinia virus pathogenesis and immunity based on intradermal injection of mouse ear pinnae. *J Gen Virol*, 80 ( Pt 10), 2751-2755.
- Unsoeld, H., Voehringer, D., Krautwald, S., & Pircher, H. (2004). Constitutive expression of CCR7 directs effector CD8 T cells into the splenic white pulp and impairs functional activity. *J Immunol*, 173(5), 3013-3019.
- van Stipdonk, M. J., Lemmens, E. E., & Schoenberger, S. P. (2001). Naive CTLs require a single brief period of antigenic stimulation for clonal expansion and differentiation. *Nat Immunol*, 2(5), 423-429. doi: 10.1038/87730
- Wakim, L. M., Gupta, N., Mintern, J. D., & Villadangos, J. A. (2013). Enhanced survival of lung tissue-resident memory CD8(+) T cells during infection with influenza virus due to selective expression of IFITM3. *Nat Immunol*, 14(3), 238-245. doi: 10.1038/ni.2525
- Wakim, L. M., Woodward-Davis, A., & Bevan, M. J. (2010). Memory T cells persisting within the brain after local infection show functional adaptations to their tissue of residence. *Proc Natl Acad Sci U S A*, 107(42), 17872-17879. doi: 10.1073/pnas.1010201107
- Whang, M. I., Guerra, N., & Raulat, D. H. (2009). Costimulation of dendritic epidermal gammadelta T cells by a new NKG2D ligand expressed specifically in the skin. *J Immunol*, 182(8), 4557-4564. doi: 10.4049/jimmunol.0802439
- Wherry, E. J., Teichgraber, V., Becker, T. C., Masopust, D., Kaech, S. M., Antia, R., von Andrian, U. H., & Ahmed, R. (2003). Lineage relationship and protective immunity of memory CD8 T cell subsets. *Nat Immunol*, 4(3), 225-234. doi: 10.1038/ni889
- Whitley, R. J. (2003). Smallpox: a potential agent of bioterrorism. *Antiviral Res*, 57(1-2), 7-12.
- Williams, M. A., & Bevan, M. J. (2007). Effector and memory CTL differentiation. *Annu Rev Immunol*, 25, 171-192. doi: 10.1146/annurev.immunol.25.022106.141548
- Witherden, D. A., Verdino, P., Rieder, S. E., Garijo, O., Mills, R. E., Teyton, L., Fischer, W. H., Wilson, I. A., & Havran, W. L. (2010). The junctional adhesion molecule JAML is a costimulatory receptor for epithelial gammadelta T cell activation. *Science*, 329(5996), 1205-1210. doi: 10.1126/science.1192698
- Witherden, D. A., Watanabe, M., Garijo, O., Rieder, S. E., Sarkisyan, G., Cronin, S. J., Verdino, P., Wilson, I. A., Kumanogoh, A., Kikutani, H., Teyton, L., Fischer, W. H., & Havran, W. L. (2012). The CD100 receptor interacts with its plexin B2 ligand to regulate epidermal gammadelta T cell function. *Immunity*, 37(2), 314-325. doi: 10.1016/j.immuni.2012.05.026
- Wyatt, L. S., Earl, P. L., Eller, L. A., & Moss, B. (2004). Highly attenuated smallpox vaccine protects mice with and without immune deficiencies against pathogenic vaccinia virus challenge. *Proc Natl Acad Sci U S A*, 101(13), 4590-4595. doi: 10.1073/pnas.0401165101
- Yang, L., Chan, T., Demare, J., Iwashina, T., Ghahary, A., Scott, P. G., & Tredget, E. E. (2001). Healing of burn wounds in transgenic mice overexpressing transforming growth factor-beta 1 in the epidermis. *Am J Pathol*, 159(6), 2147-2157.
- Yewdell, J. W. (2006). Confronting complexity: real-world immunodominance in antiviral CD8+ T cell responses. *Immunity*, 25(4), 533-543. doi: 10.1016/j.immuni.2006.09.005

- Zaid, A., Mackay, L. K., Rahimpour, A., Braun, A., Veldhoen, M., Carbone, F. R., Manton, J. H., Heath, W. R., & Mueller, S. N. (2014). Persistence of skin-resident memory T cells within an epidermal niche. *Proc Natl Acad Sci U S A*, *111*(14), 5307-5312. doi: 10.1073/pnas.1322292111
- Zhang, N., & Bevan, M. J. (2013). Transforming growth factor-beta signaling controls the formation and maintenance of gut-resident memory T cells by regulating migration and retention. *Immunity*, *39*(4), 687-696. doi: 10.1016/j.immuni.2013.08.019
- Zhu, J., Peng, T., Johnston, C., Phasouk, K., Kask, A. S., Klock, A., Jin, L., Diem, K., Koelle, D. M., Wald, A., Robins, H., & Corey, L. (2013). Immune surveillance by CD8alpha<sup>+</sup> skin-resident T cells in human herpes virus infection. *Nature*, *497*(7450), 494-497. doi: 10.1038/nature12110

## 8 Danksagung

Ich möchte mich an dieser Stelle bei allen Personen bedanken, die zum Gelingen dieser Arbeit beigetragen haben.

Zuallererst möchte ich mich bei meinem Betreuer Herrn Prof. Dr. Ingo Drexler bedanken, der mir die Möglichkeit gegeben hat, diese Arbeit in seiner Arbeitsgruppe anzufertigen. Er hatte immer ein offenes Ohr für meine Ideen und hat mir alle Freiheiten gegeben, mich in diesem hochinteressanten Forschungsprojekt zu verwirklichen. Ich danke ihm außerdem für das Vertrauen, das er mir in letzten Jahren - insbesondere seit dem Umzug der Arbeitsgruppe nach Düsseldorf - entgegengebracht hat, sowie für seine Unterstützung und Mühe bei der Betreuung über die doch relativ große Distanz.

Herrn Prof. Dr. Jörg Durner danke ich ganz herzlich für die offizielle Betreuung meiner Dissertation und die hilfreichen Diskussionen und Anregungen bei meinen Thesis Committee Meetings.

Ein spezieller Dank gilt auch Dr. Georg Gasteiger, der mich schon zu meiner Zeit als Bachelor im Labor betreut hat und mich schon damals mit seinem großen wissenschaftlichen Enthusiasmus angesteckt hat und für die T-Zell-Immunologie begeistern konnte. Ich danke ihm für die ausgiebigen fachlichen Diskussionen sowohl vor Ort als auch später über Skype, die meinem Projekt (und mir) immer wieder einen neuen Impuls verliehen haben. Danke dir Georg!

Ein herzliches Dankeschön geht auch an alle restlichen Mitglieder meiner Arbeitsgruppe: Dr. Yi "Annie" Zhang, Dr. Frank Thiele, Dr. Lianpan "David" Dai, Dr. Sha Tao, Ronny Ljapoci und Robert Baier für ihre Unterstützung, die hilfreichen Diskussionen und die überaus angenehme und freundschaftliche Arbeitsatmosphäre im Labor. Ein besonderer Dank geht an Annie für ihre Freundschaft und mentale Unterstützung beim Erstellen dieser Arbeit.

Ein Dankeschön möchte ich auch an Dr. Veit Buchholz richten für die vielen anregenden Diskussionen und Ideen.

Danke auch an meine anderen Kollegen aus der Schneckenburger Str. 8: Dr. Florian Reisinger, Judith Bauer, Sukumar Namineni, Clemens Jäger, Dr. Claudia Dembek, Dr. Carolina Russo, Dr. Sarah Kutscher, Dr. Simone Backes, Andrea Schmidbauer für die vielen gemeinsamen Stunden im Laborcontainer. Besonders möchte ich hier Flo und Clemens hervorheben, zu denen sich über die Jahre auch privat eine sehr gute Freundschaft entwickelt hat. Danke euch für die aufmunternden Gespräche während der Kaffeepausen oder den abendlichen Grillaktionen sowie für die zahlreichen sportlichen und anderweitigen Aktivitäten außerhalb des Containers. Außerdem möchte ich Clemens für seine tatkräftige Mithilfe bei einigen meiner spätabendlichen Experimente, für das Organisieren der Instituts-Fußballmannschaft „Virogoal“ sowie für das Korrekturlesen dieser Arbeit danken. Daniel Kull und Ruth Hillermann danke ich für die exzellente technische Hilfestellung beim Schneiden der Cryoblöcke und den immunhistochemischen Färbungen. Ich möchte auch Hr. Mahmoudi für seine herzliche Art danken, die netten Gespräche und dafür, dass immer genug Präparierbesteck für mich reserviert wurde.

Meiner Freundin Jessica danke ich von ganzen Herzen dafür, dass sie mir während sämtlicher Höhen und Tiefen dieser Promotion zur Seite gestanden ist. Gerade wenn es einmal nicht so rund lief hat sie stets an mich geglaubt und mich motiviert. Ohne ihr Verständnis und ihre unglaubliche Geduld wäre diese Arbeit undenkbar gewesen.

Nicht zuletzt danke meinen Eltern Renate und Werner, sowie meinem Bruder Florian für ihre bedingungslose Unterstützung und Geduld in diesem Abschnitt meines Lebens. Ohne euch würde ich sicherlich nicht dort stehen, wo ich jetzt stehe. Danke!



# Curriculum vitae

## Persönliche Daten

Name Andreas Muschaweckh  
Geburtsdatum 26. September 1982  
Geburtsort München  
Adresse Blumenstraße 58, 85774 Unterföhring  
E-mail muschaweckh@lrz.tum.de  
Telefon +49 (0)176-84259073

## Ausbildungsweg

08/2013-heute wissenschaftlicher Mitarbeiter  
  
Klinikum rechts der Isar der Technischen Universität München (TUM)  
Klinik und Poliklinik für Neurologie  
AG Experimentelle Neuroimmunologie  
(Prof. Dr. Thomas Korn)

05/2009-07/2013 Doktorarbeit  
  
Institut für Virologie, TUM/Helmholtz Zentrum München  
Thesis: “Characterization of tissue-resident CD8+ T cell memory  
formation upon skin infection with the viral vector MVA”  
Supervision: Prof. Dr. Ingo Drexler

2006-2008 Masterstudium Molekulare Biotechnologie (M. Sc.)  
  
TUM  
Thesis: “Impact of induced apoptotic and necrotic cell death on the  
antitumor immunity to B16 melanoma”  
Supervision: Prof. Dr. Georg Häcker  
Institut für Mikrobiologie, Immunologie und Hygiene, TUM

2003-2006 Bachelorstudium Biochemie (B. Sc.)  
  
TUM  
Thesis: “Immunogenicity of modified vaccinia virus Ankara expressing  
different formulations of the melanoma-associated antigen human  
tyrosinase“  
Supervision: Prof. Dr. Ingo Drexler  
Institut für Virologie, TUM/Helmholtz Zentrum München

2002-2003 Zivildienst, Bayerisches Rotes Kreuz München

1993-2002 Wilhelm-Hausenstein-Gymnasium München

## Publikationsliste

- Thiele, F., Tao, S., Zhang, Y., **Muschaweckh, A.**, Zollmann, T., Protzer, U., Abele, R., & Drexler, I. (2015). Modified vaccinia virus Ankara-infected dendritic cells present CD4+ T cell epitopes by endogenous major histocompatibility complex class II presentation pathways. *J Virol*, 89(5), 2698-2709.
- Roth, S. Rottach, A., Lotz-Havla, A. S., Laux, V., **Muschaweckh, A.**, Gersting, S. W., Muntau, A. C., Hopfner, K. P., Jin, L., Vaness, K., Petrini, J. H., Drexler, I., Leonhardt, H., & Ruland, J. (2014). Rad50-CARD9 interactions link cytosolic DNA sensing to IL-1beta production. *Nat Immunol*, 15(6), 538-545.
- Rothhammer, V.\*, **Muschaweckh, A.\***, Gasteiger, G., Petermann, F., Heink, S., Busch, D. H., Heikenwalder, M., Hemmer, B., Drexler, I., & Korn, T. (2014). Alpha4-integrins control viral meningoencephalitis through differential recruitment of T helper cell subsets. *Acta Neuropathol Commun*, 2, 27. (\* equal contribution)
- Lohmann, C.\*, **Muschaweckh, A.\***, Kirschnek, S.\*, Jennen, L., Wagner, H., & Hacker, G. (2009). Induction of tumor cell apoptosis or necrosis by conditional expression of cell death proteins: analysis of cell death pathways and in vitro immune stimulatory potential. *J Immunol*, 182(8), 4538-4546. (\* equal contribution)